



Department of
Primary Industries
Office of Water

Upper Lachlan Groundwater Flow Model



Leading policy and reform in sustainable water management

Publisher

NSW Department of Primary Industries, Office of Water.

Level 18, 227 Elizabeth Street

GPO Box 3889

Sydney NSW 2001

T 02 8281 7777 F 02 8281 7799

information@water.nsw.gov.au

www.water.nsw.gov.au

The NSW Office of Water manages the policy and regulatory frameworks for the state's surface water and groundwater resources, to provide a secure and sustainable water supply for all users. It also supports water utilities in the provision of water and sewerage services throughout New South Wales.

Upper Lachlan Groundwater Flow Model

February 2012

ISBN 978 0 7313 3503 9

This publication may be cited as:

Bilge, H., (2012), *Upper Lachlan Groundwater Flow Model*, NSW Office of Water, Sydney



Australian Government
National Water Commission

Funding for this project has been provided by a National Water Commission grant to the NSW Office of Water under the Raising National Water Standards Program

© State of New South Wales through the Department of Trade and Investment, Regional Infrastructure and Services, 2012

This material may be reproduced in whole or in part for educational and non-commercial use, providing the meaning is unchanged and its source, publisher and authorship are clearly and correctly acknowledged.

Disclaimer: While every reasonable effort has been made to ensure that this document is correct at the time of publication, the State of New South Wales, its agents and employees, disclaim any and all liability to any person in respect of anything or the consequences of anything done or omitted to be done in reliance upon the whole or any part of this document.

NOW 11_281

Contents

Abstract.....	iv
1. Introduction.....	1
2. Description of the model area	2
2.1 Rainfall and evaporation	4
2.1.1 Rainfall.....	4
2.1.2 Evaporation.....	8
2.2 Geology.....	8
2.3 Hydrogeology.....	9
2.4 Surface water.....	11
2.5 Groundwater usage	12
3. Model development.....	14
3.1 Conceptual model	14
3.2 Model discretisation	16
3.3 Initial heads.....	18
3.4 Aquifer parameters.....	18
3.5 Boundary conditions	20
3.6 Well package.....	20
3.7 Recharge.....	21
3.7.1 Rainfall Recharge	21
3.7.2 Irrigation Recharge	22
3.7.3 Flood Recharge	23
3.8 River aquifer interaction	25
3.9 Evaporation	28
3.10 Solver	28
4. Model calibration	29
4.1 Automatic calibration.....	29
4.2 Final estimates of aquifer parameters	31
4.3 Head response.....	39
4.4 Calibration assesment	39
4.5 Sensitivity analysis.....	44
4.6 Water balance	46
5. Scenario runs	48
5.1 Scenario water balance	48

6. Conclusions and recommendations	56
7. References	58
APPENDIX 1: Model geometry	59
APPENDIX 2: Initial head	63
APPENDIX 3: Production bore locations.....	66
Table List of Usage Bores	66
APPENDIX 4: River details.....	67
APPENDIX 5: Monitoring bore locations and model layer boundaries	69
APPENDIX 6: Observed and simulated water level hydrographs.....	72

Tables

Table 3-1 Model Grid Specifications	16
Table 3-2 Model Time-Discretisation Parameters.....	16
Table 3-3 Parameter settings in GMG solver package	28
Table 4-1 Model Parameters.....	30
Table 4-2 Calibrated Model Parameters.....	38

Figures

Figure 2-1 Location of the Upper Lachlan Valley	3
Figure 2-2 Rainfall stations and contours of average annual rainfall (1986-2008) in the model area ..	4
Figure 2-3 Average monthly Rainfall (mm) registered by eight Meteorological Stations in the model area	5
Figure 2-4 Residual Mass Curve of Rainfall for the period in the model area 1889-2007	6
Figure 2-5 Residual Mass Curve of Rainfall (65016) against water levels in monitoring bores of 36064_1, 36085_1, 36086_1, 36552_1 and 26554_1.....	7
Figure 2-6 Monthly average evaporation data between 1986 and 2008.....	8
Figure 2-7 Location of model cross-sections	9
Figure 2-8 Cross section of the model area	10
Figure 2-9 The rivers and creeks in the model area	11
Figure 2-10 Groundwater usage pattern for each water year in the Upper Lachlan GWMA (1986-2008).....	12
Figure 2-11 Groundwater usage bores in the model area	13
Figure 3-1 Conceptual Model	15
Figure 3-2 Conceptual Model – Plan View	15
Figure 3-3 Grid details	17

Figure 3-4 Definition of Vertical Leakage Parameter (VCONT) (from Chiang & Kinzelbach, 1996) .	19
Figure 3-5 Assumed monthly pumping and irrigation schedule	20
Figure 3-6 Rainfall Recharge & Evaporation Distribution.....	21
Figure 3-7 Irrigation recharge areas.....	22
Figure 3-8 Assumed yearly irrigation recharge rates	23
Figure 3-9 Flood recharge areas.....	24
Figure 3-10 MODFLOW conceptualisation of river/aquifer interaction	26
Figure 3-11 Schematic diagram of the river sections and gauging stations	27
Figure 4-1 Location of pilot points in the Lower Cowra Formation.....	31
Figure 4-2 Hydraulic Conductivity (m/d) distributions in Upper Cowra (Layer 1).....	33
Figure 4-3 Hydraulic Conductivity (m/d) distributions in Lower Cowra (Layer 2).....	33
Figure 4-4 Hydraulic Conductivity (m/d) distributions in Lachlan Formation.....	34
Figure 4-5 Specific yield distributions in Upper Cowra.....	34
Figure 4-6 Storage Coefficient in Lower Cowra	35
Figure 4-7 Storage Coefficient in Lachlan Formation.....	35
Figure 4-8 Vertical Leakage (1/d) between Upper and Lower Cowra.....	36
Figure 4-9 Leakage (1/d) between Lower Cowra and Lachlan Formation	36
Figure 4-10 Calibrated River Conductance in m ² /d/km.....	37
Figure 4-11 Layer 1 Scattergram of modelled versus measured heads and statistics results.	40
Figure 4-12 Layer 2 Scattergram of modelled versus measured heads and statistics results.	41
Figure 4-13 Layer 3 Scattergram of modelled versus measured heads and statistics results.	42
Figure 4-14 All Layers calibration assessment: scattergram of modelled versus measured heads, statistics and distribution of residuals results.....	43
Figure 4-15 Adjustable Model Parameter Sensitivities	45
Figure 4-16 Model Water Balance Summary for July 1986 to June 2008	46
Figure 4-17 Average Annual water balance for individual layers for July 1986 to June 2008	47
Figure 5-1 Average Annual water balance over dry scenario run June 2008 to July 2108	50
Figure 5-2 Average Annual water balance over medium scenario run June 2008 to July 2108.....	51
Figure 5-3 Average Annual water balance over wet scenario run June 2008 to July 2108.....	52
Figure 5-4 Dry Scenario yearly groundwater extractions over the 100 year simulation	53
Figure 5-5 Med Scenario yearly groundwater extractions over the 100 year simulation	53
Figure 5-6 Wet Scenario yearly groundwater extractions over the 100 year simulation.....	54
Figure 5-7 Dry Scenario yearly net river leakage over the 100 year simulation	54
Figure 5-8 Mid Scenario yearly net river leakage over the 100 year simulation	55
Figure 5-9 Wet Scenario yearly net river leakage over the 100 year simulation.....	55

Abstract

The model area is located in the central west of New South Wales. It comprises alluvial deposits along the Lachlan River from 20 km upstream of Cowra to Lake Cargelligo. The alluvium is commonly known as the Upper Lachlan groundwater source, (designated GWMA 011) for management purposes.

Most of the early groundwater extraction in the Upper Lachlan alluvium was limited to stock and domestic use and town water supply and most irrigation needs were met by surface water. With the reduction in river water supply for irrigation, the potential of groundwater in the Upper Lachlan as an alternative resource was recognised in the mid 1990s to late.

A groundwater flow model was developed for the Upper Lachlan alluvial aquifers to assist the community and resource managers to develop long term strategies to ensure environmentally responsible and economically sustainable use of this valuable natural resource.

The alluvial unconsolidated sediment sequence consists of two formations which are the Cowra and Lachlan Formation. Conceptually, for the purpose of this groundwater flow model the groundwater system is defined in terms of four layers;

- Layer 1- Upper Cowra
- Layer 2- Lower Cowra
- Layer 3- Lachlan
- Layer 4 Fractured Rock (inactive).

An inactive fourth layer has been included in the model to account for the fractured rock aquifer which is in direct contact with the overlying sediments. In time, this layer may be activated if there is evidence to suggest any significant interaction between the alluvial and fractured rock aquifers should this prove to be a significant of water.

The model calibration period is from July 1986 to June 2008. Recharge components to the aquifers are from rainfall, rivers, flood and irrigation. Discharge is predominantly through evapotranspiration, groundwater extraction and river leakage. Groundwater outflow occurs across the western boundary and there is no inflow from any of the boundaries. The direction of regional groundwater movement is generally from east to west.

Non linear parameter estimation (PEST) was used to aid calibration of the model based on observed water levels from NOW monitoring bores. Based on comparison between observed and simulated groundwater levels for the entire calibration period, the model achieved a good match with measured data in general with the exception of Zone 7. Low SRMS (scaled root mean square) values (less than 5%) were achieved for all three layers - confirming that the model is well calibrated overall. Poor calibration of bores in Zone 7 is attributed to the lack of shallow water table monitoring bores in the area.

The annual average total recharge is 186.48 GL from all recharge sources in the calibration period. The average rainfall recharge is about 59% of the total recharge. The total annual average discharge is 156.30 GL. The evapotranspiration is about 76% of this total while groundwater extraction makes up 11%. Evaporation is the dominant component of outflow over the calibration period.

“Dry”, “medium” and “wet” climate scenarios were formulated to examine the aquifer behaviour under “no pumping”, “current development” and “full entitlements” conditions. These scenarios showed that if there was no pumping in the region, water level would rise causing river leakage to decrease and evapotranspiration to increase. If there were high pumping, water levels would have declined causing evapotranspiration to decrease and river leakage to increase.

1. Introduction

The Upper Lachlan Valley is located in central western New South Wales. For groundwater management purposes this area is referred to as Groundwater Management Area (GWMA) 011. The area stretches from Lake Cargelligo in the west to 20 km east of Cowra. The groundwater system provides water for stock and domestic, irrigation, town water supply and industry in the region.

Within the Upper Lachlan Valley groundwater source there are two geological formations, which are the deeper Lachlan Formation and the shallower Cowra Formation. The Cowra Formation has separated into two distinct aquifers; layer 1- the shallower unconfined water table Upper Cowra aquifer and layer 2- deeper semi confined to confined Lower Cowra aquifer. Layer 3- the Lachlan Formation which has a maximum thickness of around 90 m. The Cowra Formation is generally 30-50 m thick in most areas. However, it can reach greater depths up to about 110 m in the south.

The GWMA 011 is embargoed for new groundwater entitlements. The current total entitlement is 184,575 ML/y. Groundwater extraction has risen in recent years from 18,700 ML in 2001/2002 to 84,600 ML in 2007/2008.

Conceptually, the groundwater system is divided into four major regional aquifers: an upper Cowra, a lower Cowra, a deeper Lachlan and fractured rock. There is no hydrogeological distinction between the Upper and Lower Cowra formation layers included in the model. For modelling purposes, an arbitrary thickness of Upper Cowra 20 m maximum in the centre of the valley was assumed. Fractured rock layer is an inactive layer.

Recharge mechanisms to the aquifer include rainfall recharge, river leakage, flood recharge and irrigation recharge. Discharges from the system are through evapotranspiration and groundwater pumping from all aquifers. The aquifer system receives no lateral flow through boundaries in the north, south and east. Groundwater flow out of the system is westward into the Lower Lachlan valley. Regional flow is from east to west.

A modular groundwater flow model (MODFLOW), using a non-uniform finite difference grid, was adopted for this study. Square cell dimensions vary from 500 m in the vicinity of the Lachlan River, and increase progressively to 2000 m away from the river to the north and south. The model grid is rotated 20 degrees anti clockwise. Grid size and rotation were selected to ensure an acceptable degree of detail along the river tract to provide better understanding of stream-aquifer interaction. The area covers approximately 50,960 km². The starting and ending model calibration period are July 1986 and June 2008 respectively. These dates were selected to include drought and flood conditions in the calibration simulation.

The groundwater flow model for the Upper Lachlan Valley was developed to:

- Aid understanding of the flow system
- Identify key recharge sources and quantify the contribution from each source
- Identify parts of the aquifer under stress
- Identify parts of the aquifer with development potential
- Aid assessment of the impact of groundwater development on river flow
- Aid understanding of the processes of river/aquifer water interchange
- Estimate recharge to the groundwater system
- Evaluate the impact of climate change on groundwater availability.

This report outlines the hydrogeology of the model area and development of the groundwater flow model.

2. Description of the model area

The extent of the Upper Lachlan Valley groundwater model area is shown in Figure 2-1. The model extent is defined by AMG coordinates 408000-666000 m E and 6160000-6370000 m N.

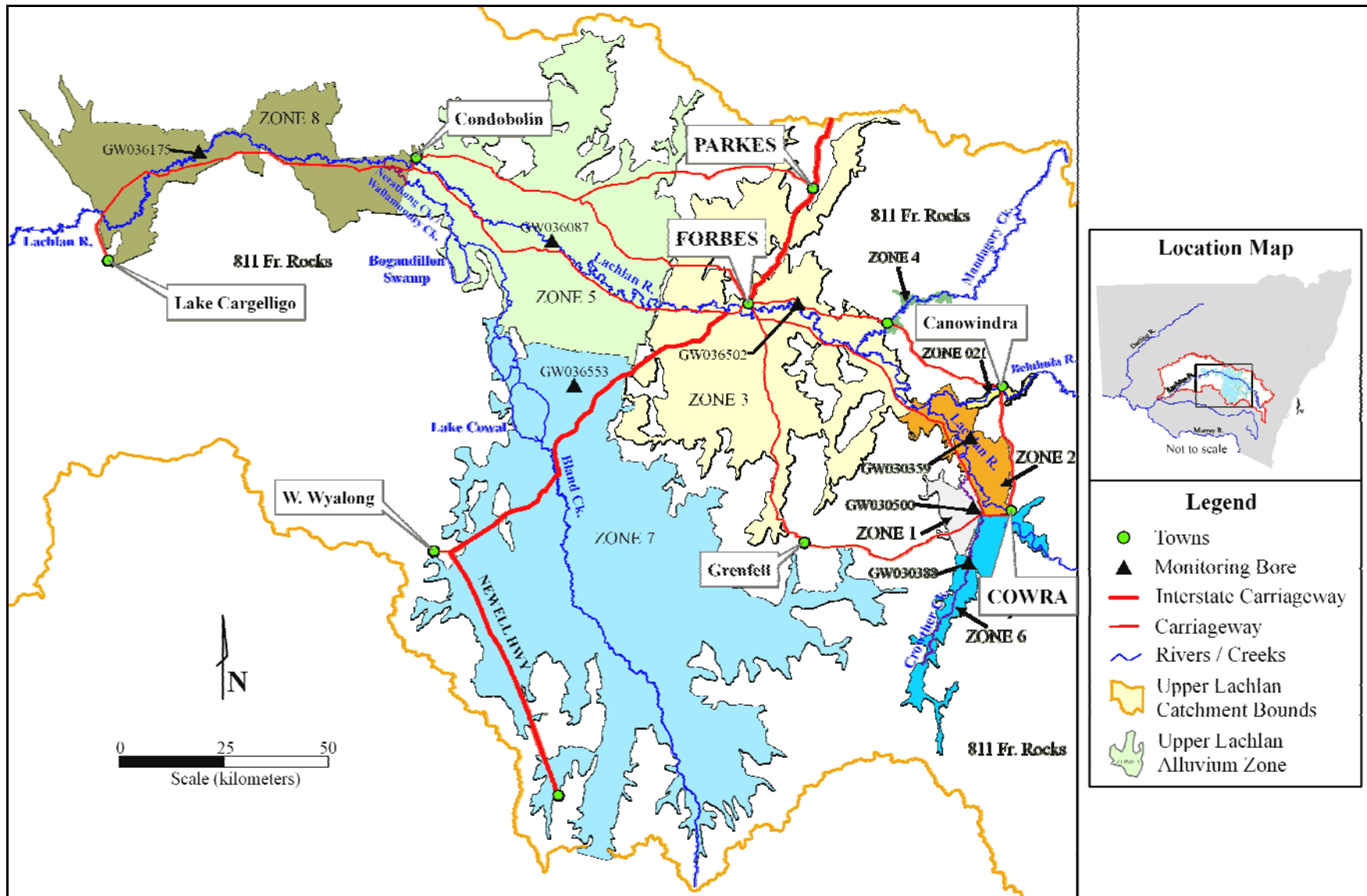
The major water courses in the study area includes the Lachlan River which flows from east to west, the lower end of the Belubula River and Mandagery Creek in the north-east, the lower end of Goobank Creek in the north and Crowther Creek in the south-east. Cowra, Forbes and Parkes are the main urban settlements located in the model area. Other towns in the area include Canowindra, Condobolin and West Wyalong.

The Newell Highway runs in the north-south direction in the central part of the model area.

The GWMA 011 has an area of 13087 km² and for management purposes the area is divided into eight zones:

- Zone 1 - Back Creek Cowra,
- Zone 2 - North of the Western Hwy Cowra to Gooloogong,
- Zone 3 - Gooloogong to Jemalong Gap,
- Zone 4 - Mandagery Creek,
- Zone 5 - Jemalong Gap to Condobolin,
- Zone 6 - South of the Western Hwy Cowra,
- Zone 7 - Bland Creek System
- Zone 8 - Condobolin to Lake Cargelligo

Figure 2-1 Location of the Upper Lachlan Valley

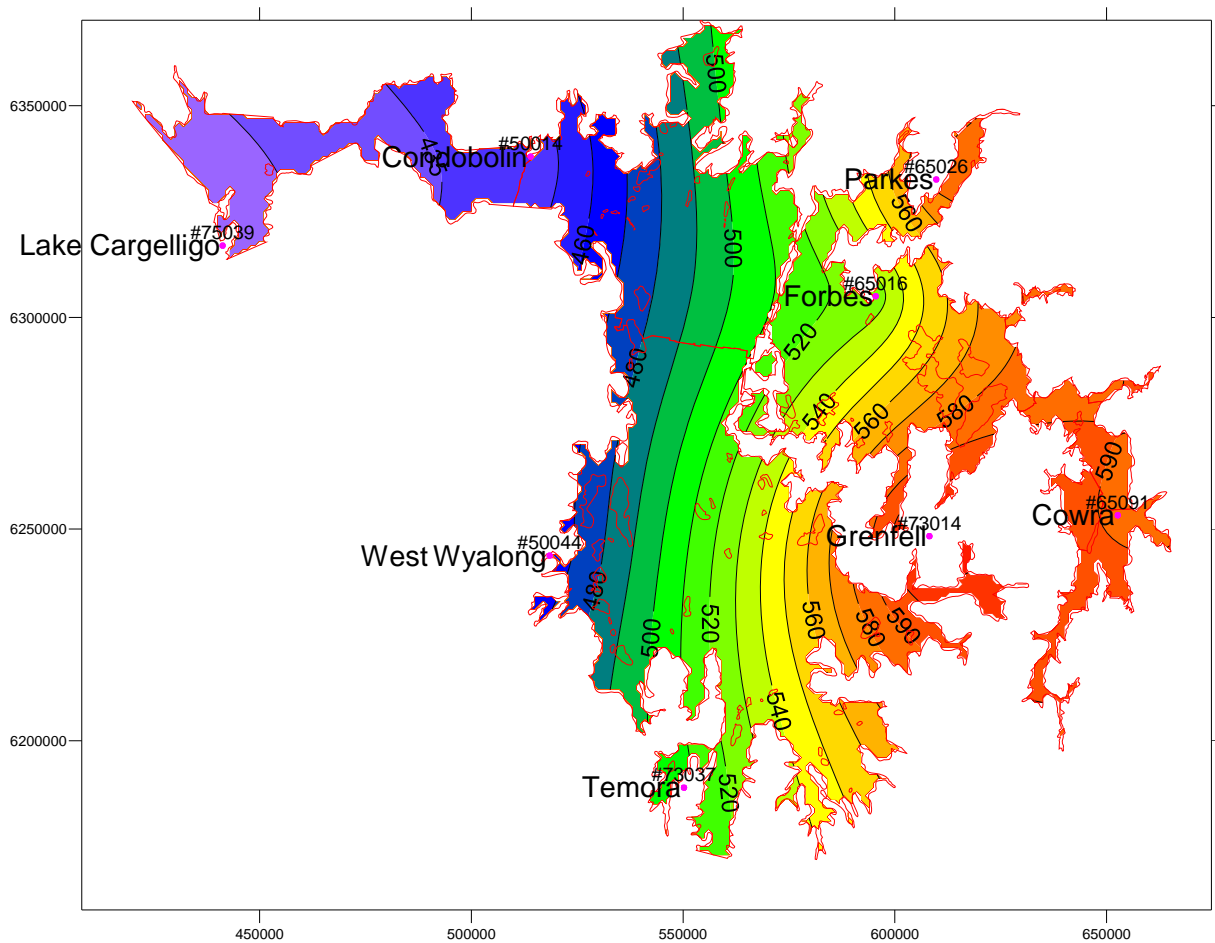


2.1 Rainfall and evaporation

2.1.1 Rainfall

Daily rainfall in the study area has been recorded at a number of weather stations at variable intervals. Rainfall records from eight stations monitored by the Australian Bureau of Meteorology were examined for the purpose of model construction. These stations (65091, 73014, 65016, 65026, 73037, 50044, 50014 and 75039) are shown in Figure 2-2 together with contours of average annual rainfall for the period 1986-2008.

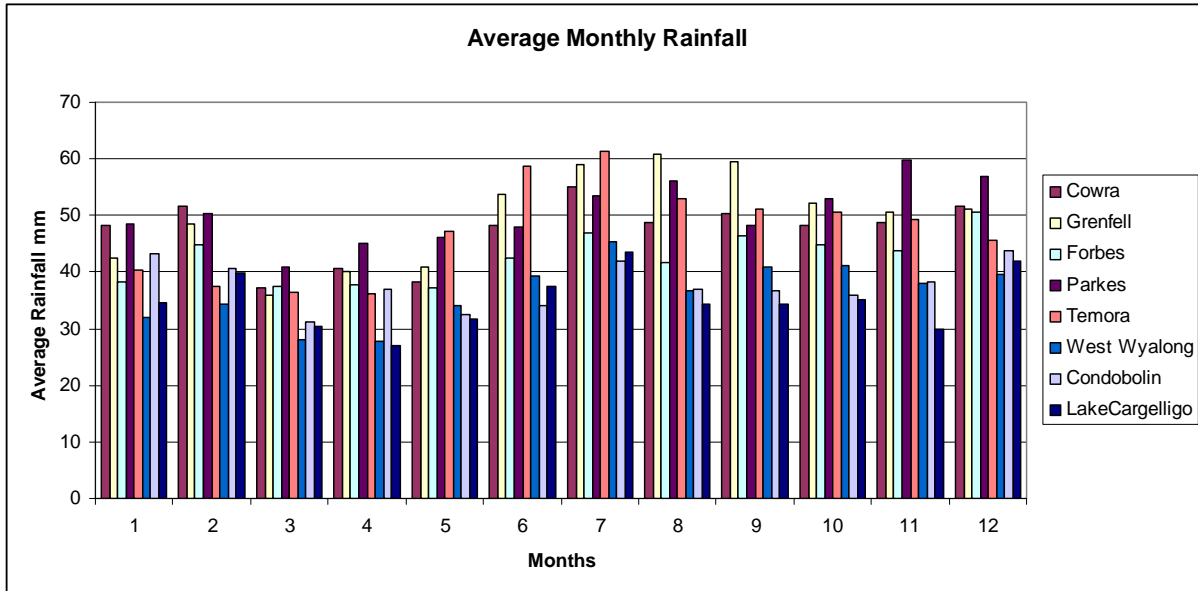
Figure 2-2 Rainfall stations and contours of average annual rainfall (1986-2008) in the model area



Rainfall in the Upper Lachlan Valley generally decreases with decreasing elevation towards the west. Contours of mean annual rainfall in Figure 2-2 show the high rainfall contour (620 mm/year) lies along the eastern margins of the basin. Average annual rainfall, for the same period, ranges from 421 mm at Lake Cargelligo to 619 mm at Grenfell, a difference of 198 mm a year over a distance of 258 km.

The average monthly rainfall for the study area is given in Figure 2.3. Over 35 percent of the annual rainfall at Forbes occurs between June and September. July with average rainfalls of approximately 47 mm is the wettest months. March and May are the driest months with the average rainfall around 37 mm respectively.

Figure 2-3 Average monthly Rainfall (mm) registered by eight Meteorological Stations in the model area



The cumulative residual-mass curve in Figure 2-4 provides a good visual representation of the rainfall history. The residual mass curve is calculated by subtracting the mean monthly rainfall for a given month from the recorded rainfall for the same month, and adding the difference to a rolling sum. A falling trend indicates a period of lower than average rainfall, whereas the reverse is true for rising trends. From 1908 to 1946, the rainfall was below average; and this is considered a dry period. From early 1947 to early 1965, the annual rainfall increased markedly to a record high. Between 1965 and 1968 shows a drop in average rainfall and a rise during the next ten years which indicates higher than average rainfall.

Changes in the residual mass curve can be compared with changes in bore water levels to examine links between long-term rainfall trends and fluctuations of groundwater level. Figure 2-5 demonstrates that there is a strong relationship between the rainfall residual mass curve and fluctuations of water table in the model area.

Summer mean maximum temperatures are greater than 30°C in most areas. In winter, minimum temperatures of less than 3°C are common.

Figure 2-4 Residual Mass Curve of Rainfall for the period in the model area 1889-2007

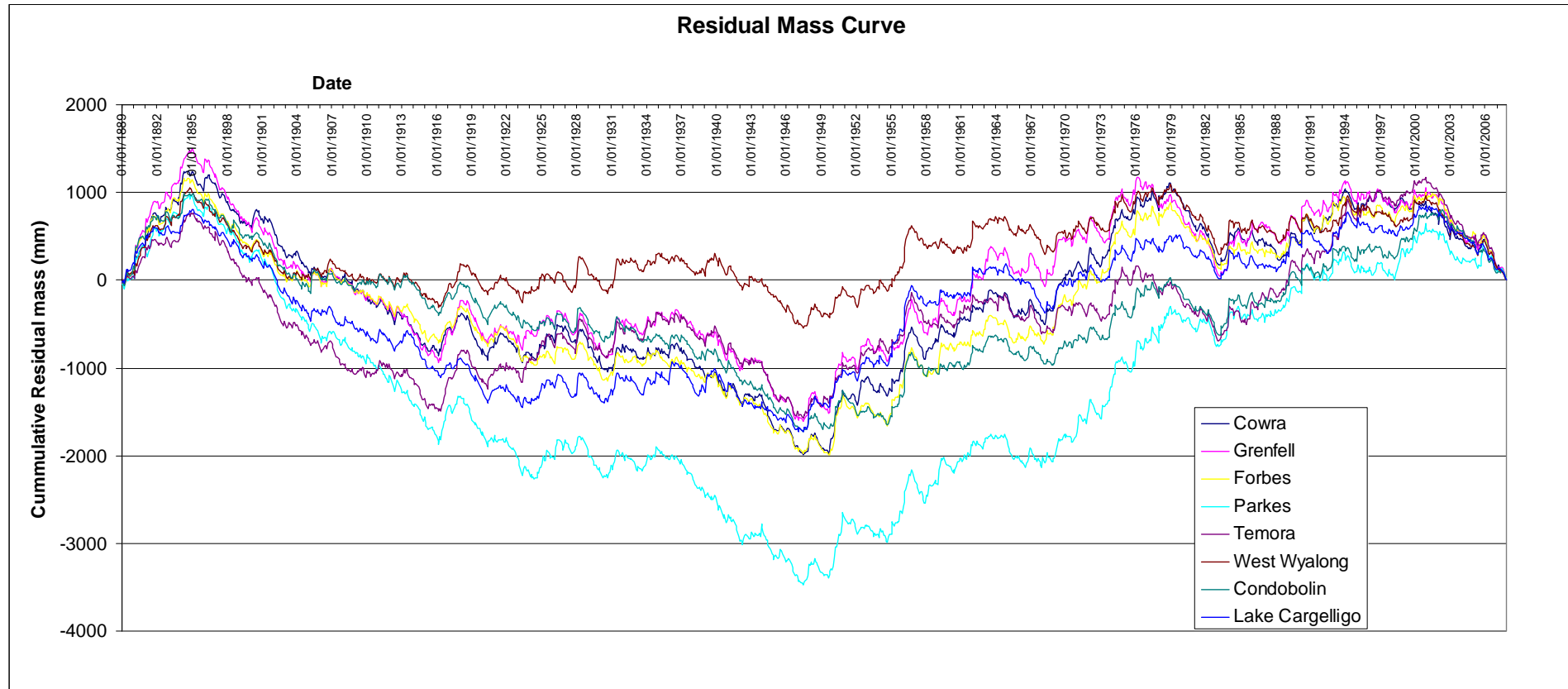
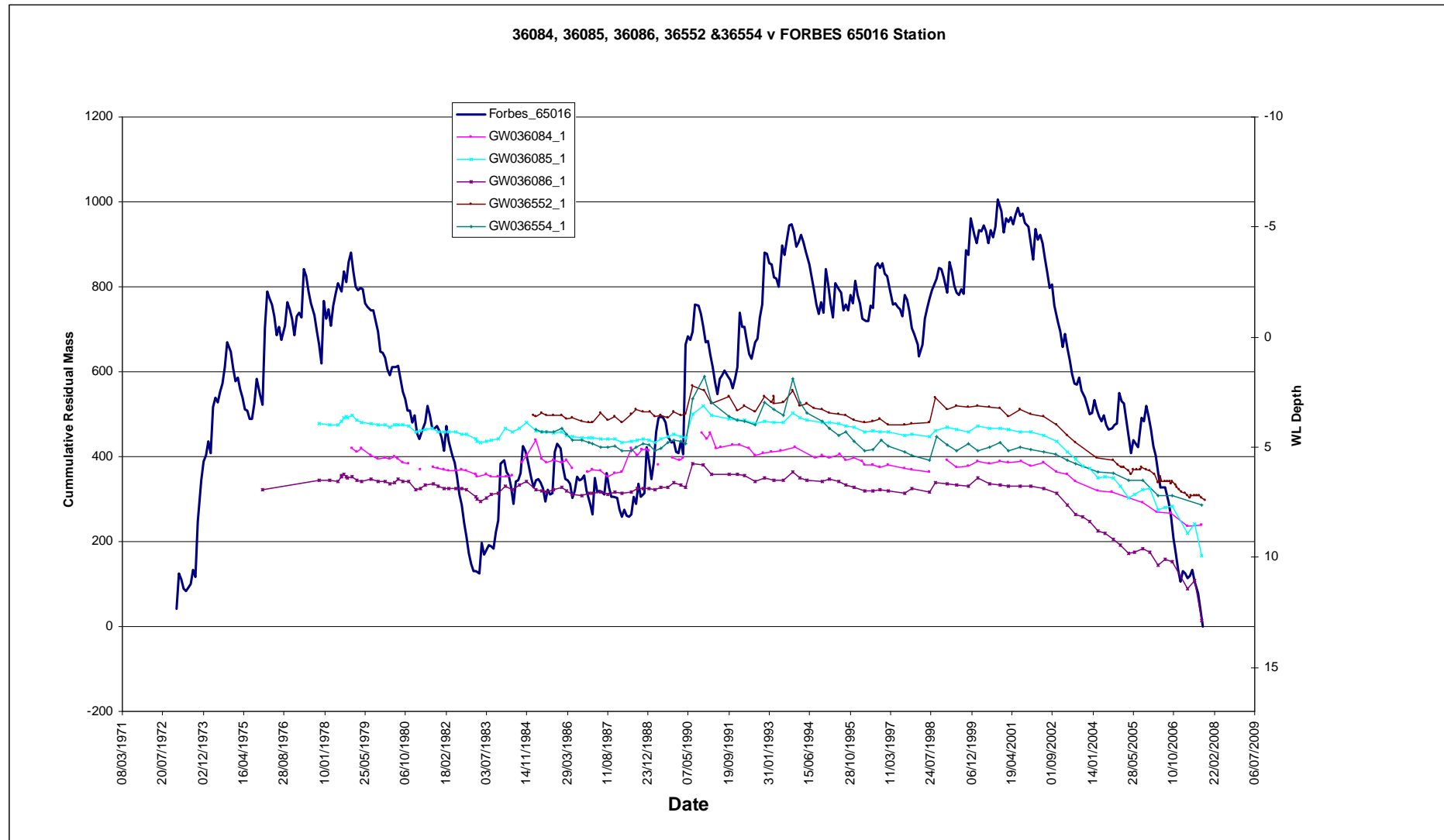


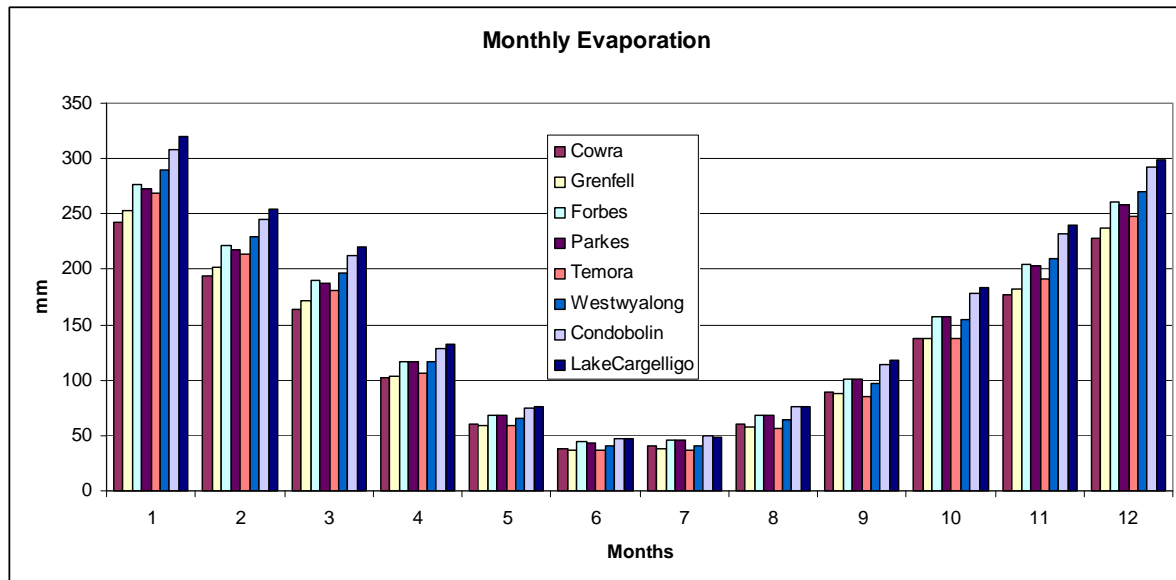
Figure 2-5 Residual Mass Curve of Rainfall (65016) against water levels in monitoring bores of 36064_1, 36085_1, 36086_1, 36552_1 and 26554_1



2.1.2 Evaporation

The weather stations providing rainfall data for the model also provided evaporation data. The average monthly evaporation data for these stations are shown in Figure 2-6. The average annual evaporation is between from 1534 to 2014mm (1986-2008). Highest monthly evaporation occurs in December and January in response to high the summer temperatures. Lowest monthly evaporation occurs in June and July.

Figure 2-6 Monthly average evaporation data between 1986 and 2008



2.2 Geology

The regional geology of the area has been studied by Gates and Williams (1988), Bish and Gates (1991) and Muller and Lennox (1999). The following description is reproduced from the latter reference.

“It can be seen that much of the central part of the area is covered by unconsolidated alluvial and colluvial sediments. With the exception of some coarse-grained Jurassic sediment in the north and the Carboniferous granites to the east, most rock types were formed prior to the Carboniferous period (354 million years ago). Ordovician metasediments are extensive throughout the area as are Silurian-Devonian granites and granodiorites. Volcanic rocks are extensive in the east and in many cases are comagmatic with adjacent plutonic rocks. These igneous rocks have been major source of material for the sedimentary rocks of the region. Depositional environment for sedimentary rocks would have been dominantly marine or marginal for rocks of early Devonian age or older. Transitional and freshwater environments existed after this time. Structurally, the area is quite complex with several orogenic episodes deforming and displacing the strata between the Ordovician and Carboniferous periods. This activity was associated with the formation of the Lachlan Fold Belt. After this time, conditions in the study area stabilised and erosional processes dominated until the advent of the Cainozoic, when both erosional and depositional processes formed the present day landscapes”.

2.3 Hydrogeology

The alluvial unconsolidated sediment sequence is divided into two major aquifer formations, the Cowra Formation and the deeper Lachlan Formation. The Cowra Formation unconformably overlies the Lachlan Formation and basement rocks. It is generally 30-50 m thick in most areas. However it can reach greater thickness - up to about 110 m - in Zone 7. It consists mainly of clay with interbedded moderately sorted sand and gravel. The Cowra Formation is divided into two aquifers in the model area, the Upper Cowra unconfined water table aquifer and the Lower Cowra semi confined to unconfined aquifer. The Lachlan Formation occurs in the deep incised palaeo channel of the Lachlan River and the maximum thickness is around 90 m. This Formation consists of subrounded to rounded, grey to off white sand and gravel with larger amounts of interbedded brown to yellow to grey clay. Representative cross sections for lines depicted in Figure 2-7 are presented in Figure 2-8. The fractured rock (layer 4) shown with a minimal thickness that does not represent reality.

The water quality in the Cowra formation deteriorates with distance from the Lachlan River and its tributaries as discussed by O'Rourke (2007)

Figure 2-7 Location of model cross-sections

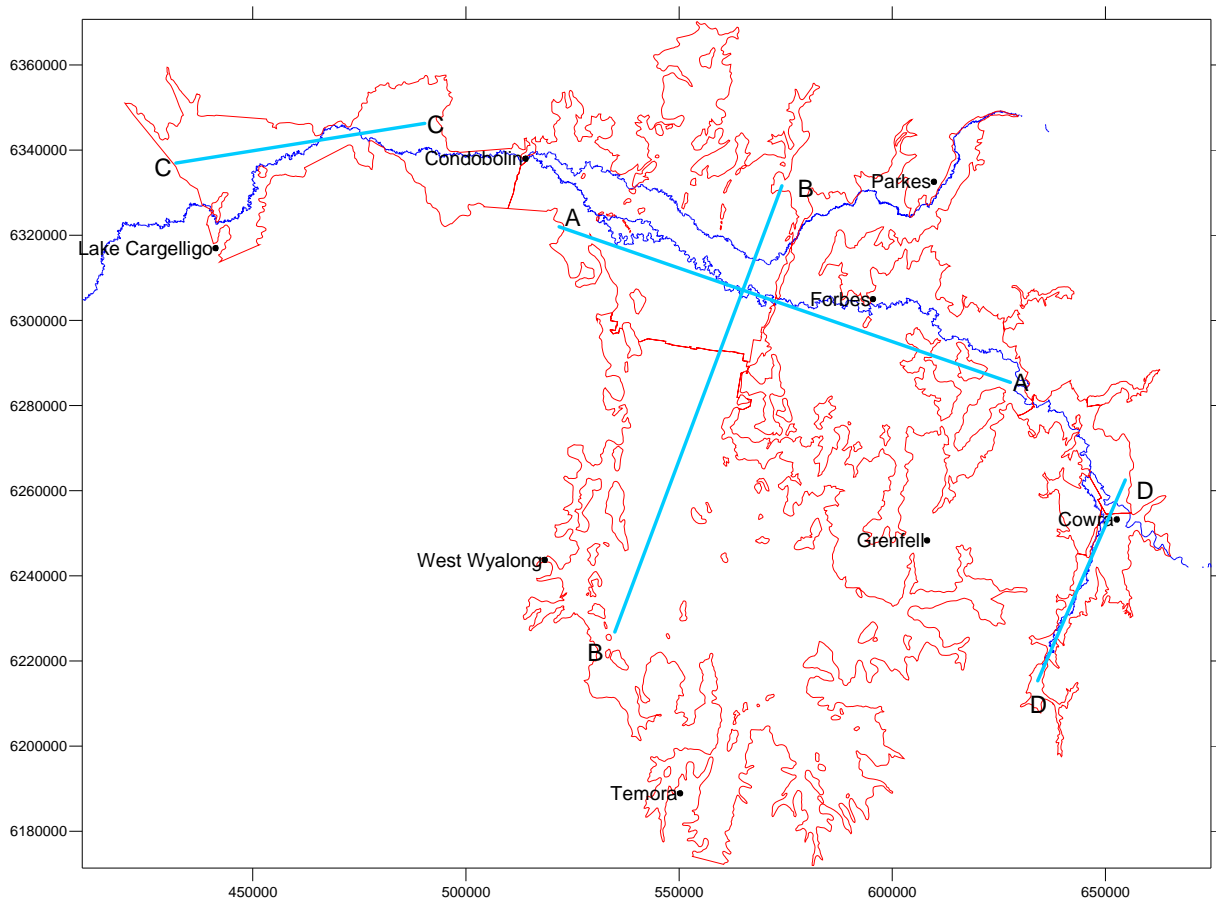
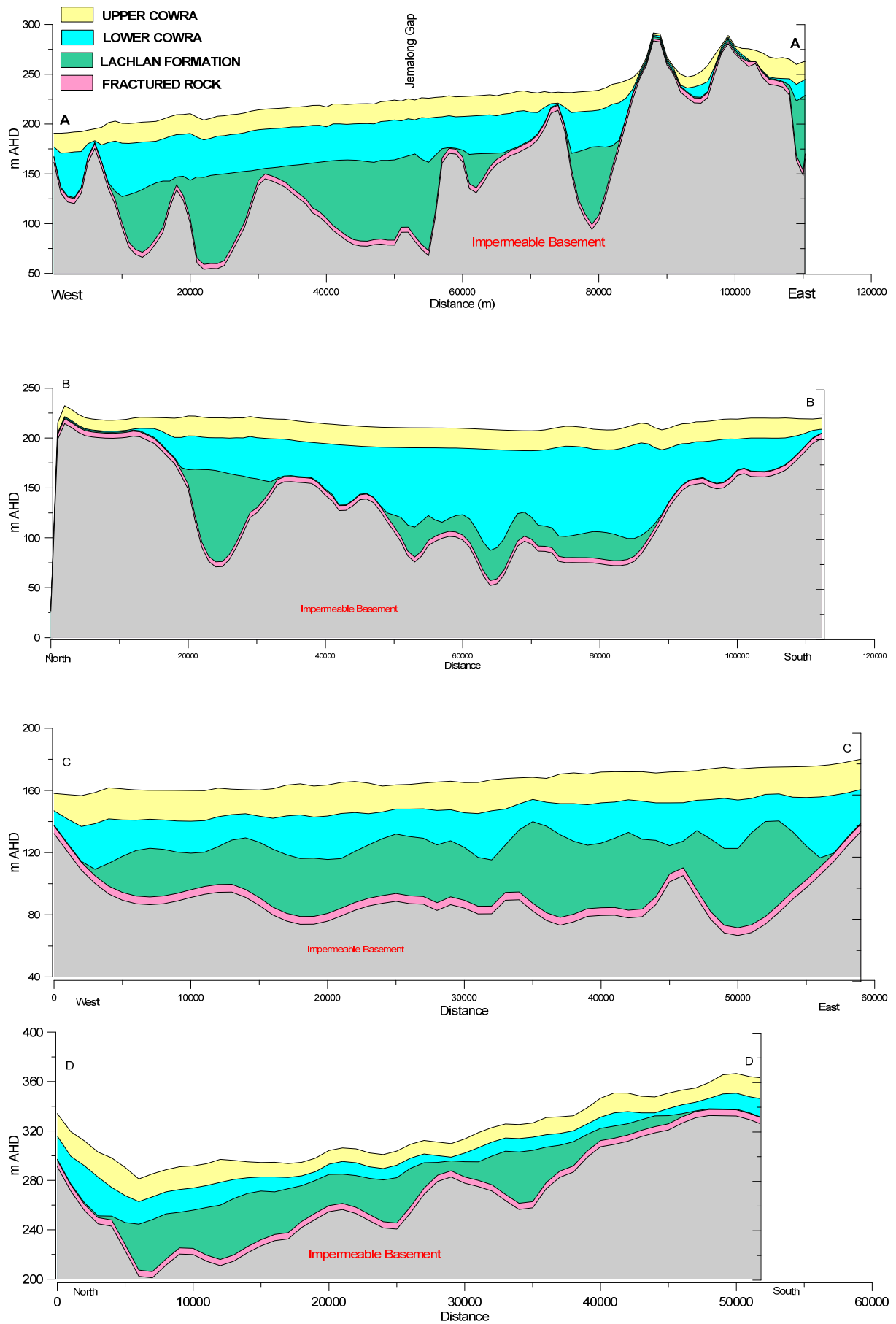


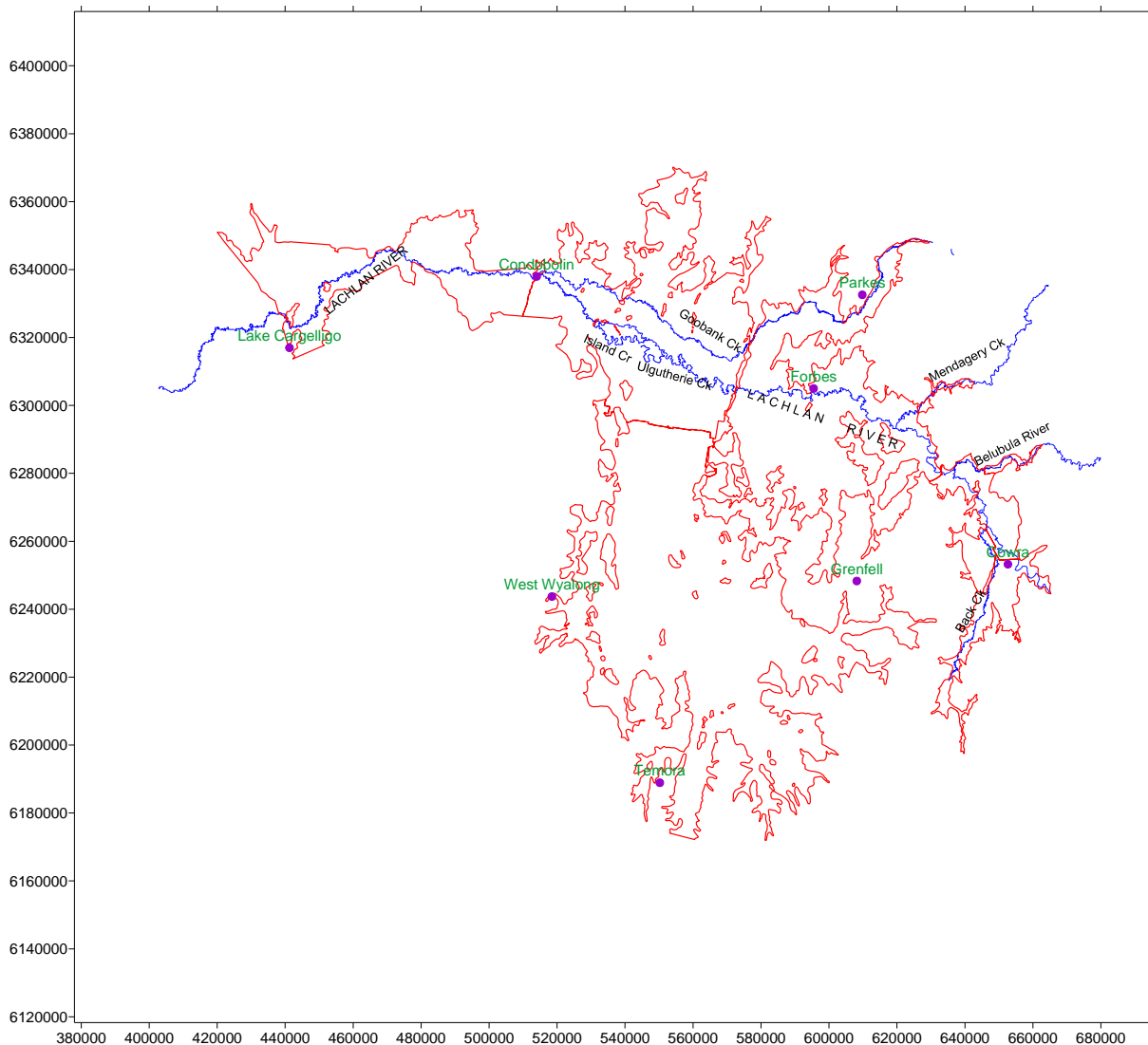
Figure 2-8 Cross section of the model area



2.4 Surface water

The Lachlan River is one of the major recharge sources in the Upper Lachlan GWMA. The Lachlan River directly overlies the alluvial aquifers. Interaction between the Lachlan River and the aquifer system is known to have an important influence on groundwater levels within the model area. The Lachlan and Belubula Rivers are regulated from water stored in Wyangala and Carcoar Dams respectively. Minor unregulated tributaries include Back Creek, Mandagery Creek, Island Creek, Ulgutherie Creek and Goobank Creek in the study area. The Lachlan River and its branches in GWMA 011 are shown in Figure 2.9.

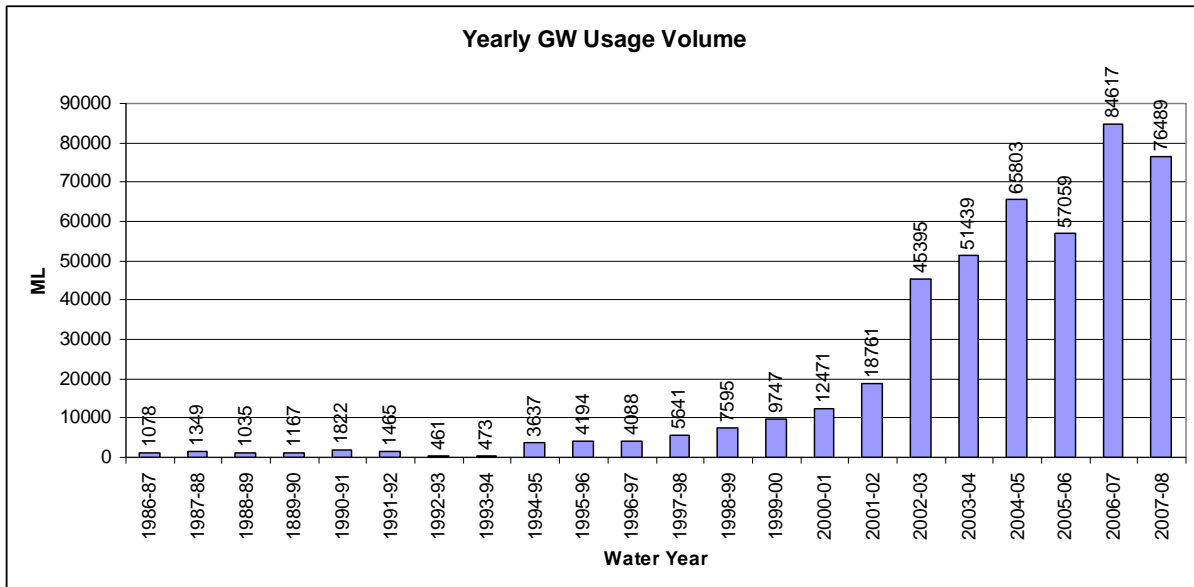
Figure 2-9 The rivers and creeks in the model area



2.5 Groundwater usage

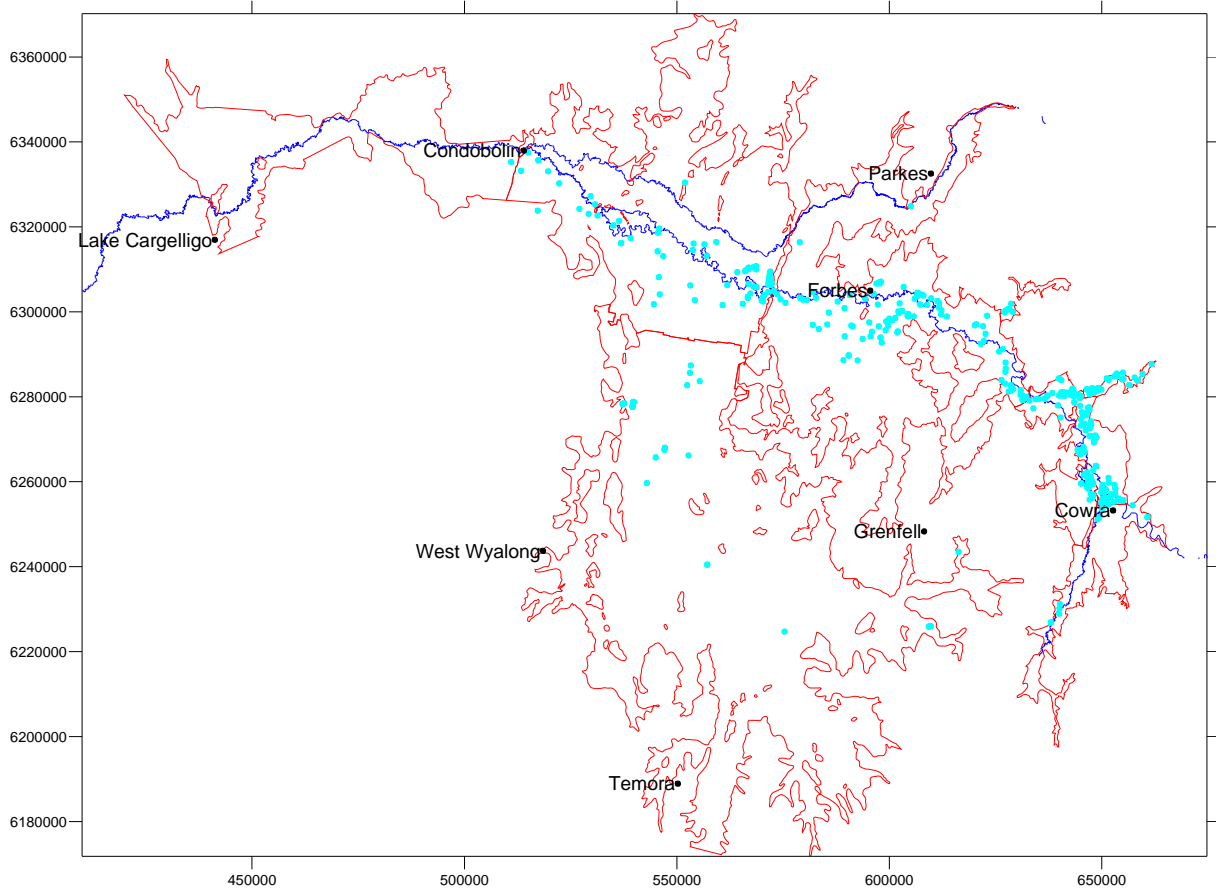
Groundwater from the alluvium of the Upper Lachlan Valley is used extensively for irrigation, town and rural community water supplies and stock and domestic requirements. Most high yield bores are used for irrigation and town water supply. The volume of groundwater extraction from the Upper Lachlan GWMA for the water years 1986–2008 is shown in Figure 2-10.

Figure 2-10 Groundwater usage pattern for each water year in the Upper Lachlan GWMA (1986-2008)



There is little available data for usage prior to 1998. However this has little impact on the model development since data are available for the major part of the calibration period (July 1986 to June 2008). Reliable metered groundwater usage data are available in NOW databases from 1998/1999 to the present. There has been a considerable increase in groundwater usage volumes and the area irrigated by groundwater since 1994 since the implementation of the Murray Basin surface water cap. As a consequence of this measure, groundwater use partially replaced the use of surface water. The locations of the currently 388 active groundwater pumping wells are presented in Figure 2-11.

Figure 2-11 Groundwater usage bores in the model area



3. Model development

A numerical groundwater model is a computer-based mathematical representation of a natural hydrogeological system that is based on a conceptual model of that system. The mathematical model is a set of equations which, subject to certain assumptions and boundary conditions, describes the essential physical features and processes of the groundwater system. The set of equations is solved using numerical methods (e.g. finite differences).

The numerical model is developed with MODFLOW 2000 finite difference software (McDonald & Harbaugh, 1988), using the Groundwater Vistas™ (Version 5.41) graphical user interface in a Windows environment.

Nine MODFLOW packages are used in this model:

- Basic (BAS) package,
- Block Centred Flow (BCF) package,
- Discretization (DIS) package
- Constant Head Boundary (CHD) package,
- Recharge (RCH) package,
- Well (WEL) package,
- Evapotranspiration (EVT) package
- River (RIV) package,
- Pre-conditioned Conjugate Gradient (GMG) package.

This chapter describes the data analysis and processing required to develop the model under the MODFLOW framework.

3.1 Conceptual model

A conceptual model is a simplified presentation of the groundwater flow system including major hydrostratigraphic units and boundary conditions. Such a conceptual model for the Upper Lachlan groundwater model is illustrated in Figure 3-1.

Conceptually, the groundwater system is defined in terms of four layers, designated Upper Cowra, Lower Cowra, Lachlan and fractured rock.

The Upper Cowra (layer 1) in the upper alluvium is an unconfined aquifer and its thickness has a fixed maximum value of 20 m if the total thickness of the Cowra (Upper and Lower) Formation exceeds 40 m. The Lower Cowra (layer 2) in the lower alluvium of the Cowra Formation is an unconfined/confined aquifer. The Lachlan Formation aquifer (layer 3) in the deep alluvium is also conceptualised as unconfined /confined. Layer 4 is an inactive fractured rock layer included in the model to facilitate future modifications should data become available to indicate hydraulic connection with the overlying alluvial aquifers.

The system is assumed to be enclosed by impermeable basement.

The western boundary is a flow boundary where either groundwater potential or flow-rates can be prescribed as a function of time and position. Significant fluxes of groundwater across this boundary (shown in Figure 3-2) are expected due to connectivity with adjoining aquifers. The boundaries to the east, north and south are treated as no-flow boundaries

The major recharge sources of the aquifers are identified as rainfall, irrigation, floods and the river system comprising the Lachlan River, Belubula River, Mandagery Creek, Goobank Creek, Back Creek, Island Creek and Ulgutherie Creek. Discharge from the aquifer is mainly due to evapotranspiration, groundwater extraction and outflow through the western boundary.

Figure 3-1 Conceptual Model

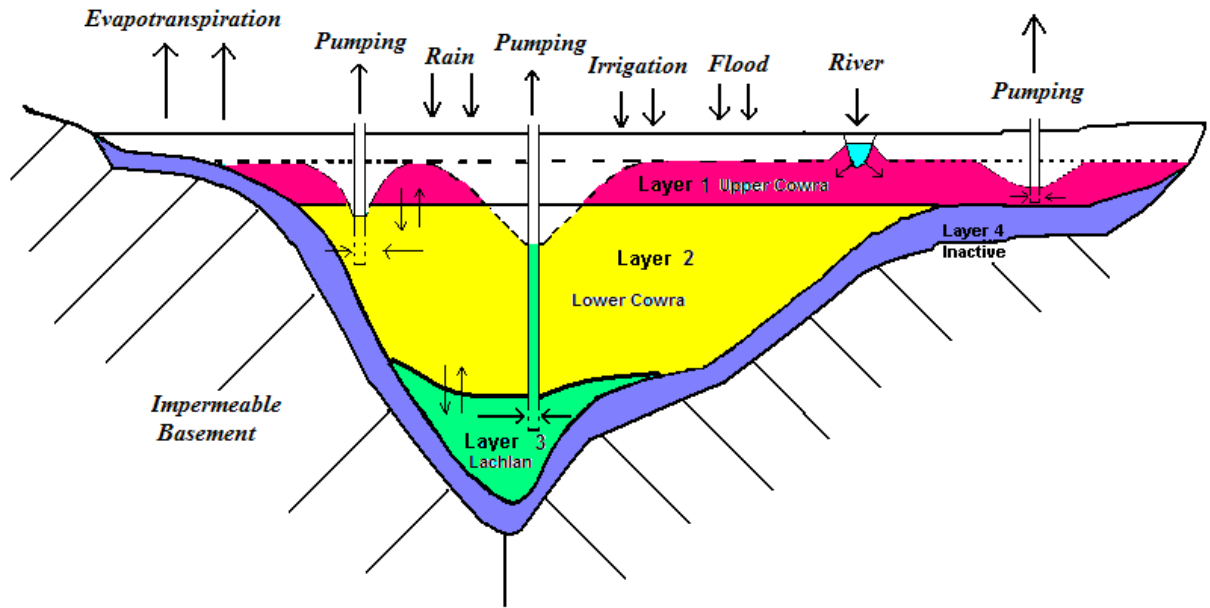
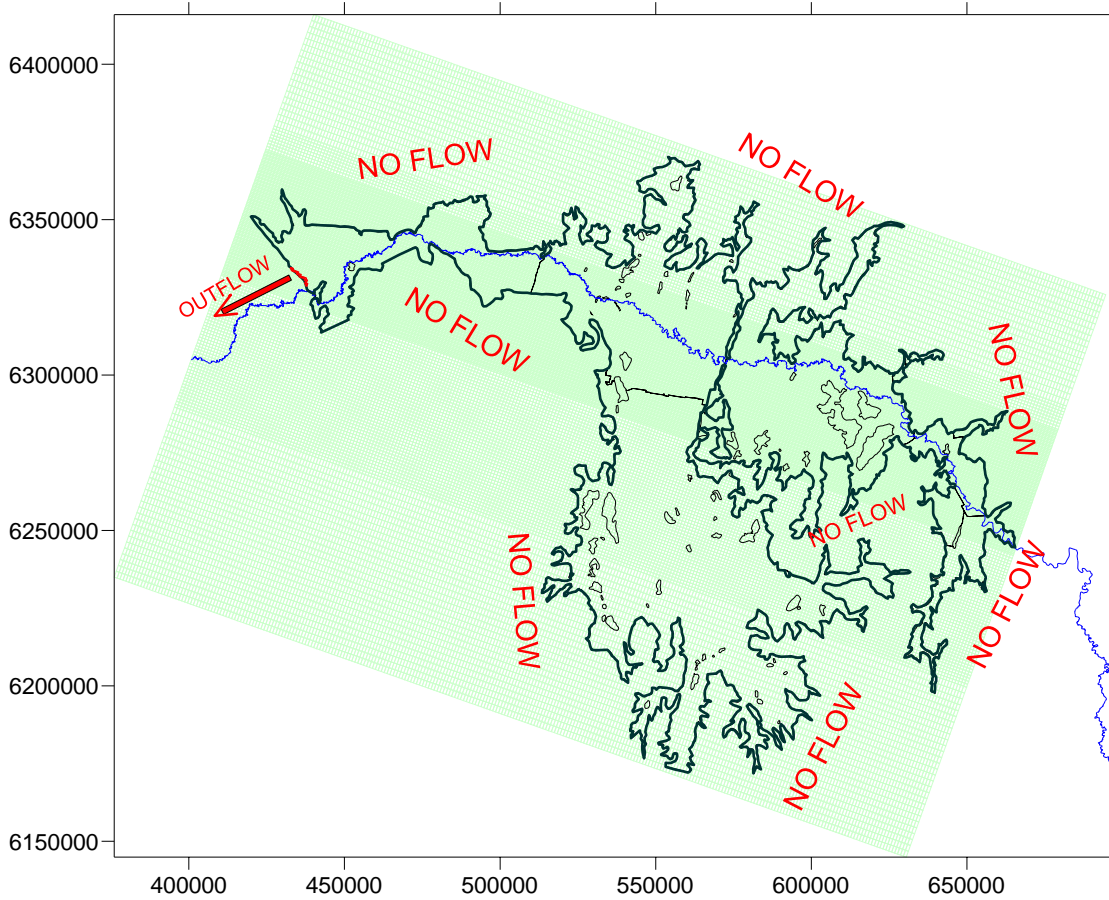


Figure 3-2 Conceptual Model – Plan View



3.2 Model discretisation

Use of MODFLOW software requires discretisation of the model spatially as well as temporally. Spatial discretisation is achieved by specifying an orthogonal set of rows and columns to form a mesh over the model area. While a regular mesh with uniform row and column widths yields the most accurate form of the finite difference solution, often it becomes necessary to refine the mesh in key areas of interest. In the current grid, row widths are appropriately sized to ensure an acceptable degree of detail along the river tract to provide a better understanding of stream-aquifer interaction. In order to produce a numerically efficient model, the grid is rotated 20 degrees anticlockwise (Figure 3-3) relative to the Australian Map Grid (AMG) to minimise its overall size. The grid cells falling outside the model boundaries and outcrop areas are designated as inactive. Data pertaining to the model grid are summarised in Table 3-1.

The model calibration period is from July 1986 to June 2008. According to the rainfall residual mass curves presented in Chapter 2 (Figure 2-4), this start date appears to be within a period of relatively stable climatic conditions. In addition, over this period, a significant set of observed water level data are available within the model area, for meaningful comparison with corresponding model predictions. Transient simulation of a MODFLOW numerical model needs the calibration period to be discretised into several stress periods. Stress periods are periods within which the various model stresses are assumed to remain constant and for which data are available or can reasonably be inferred. The model computes the groundwater elevation at the centre of each active grid cell in the model space, at each stress period during simulation. MODFLOW's approach to solving the mathematics of groundwater flow also requires that stress periods be further discretised into a number of time steps using a suitable time step multiplier. Time discretisation parameters are summarised in Table 3-2.

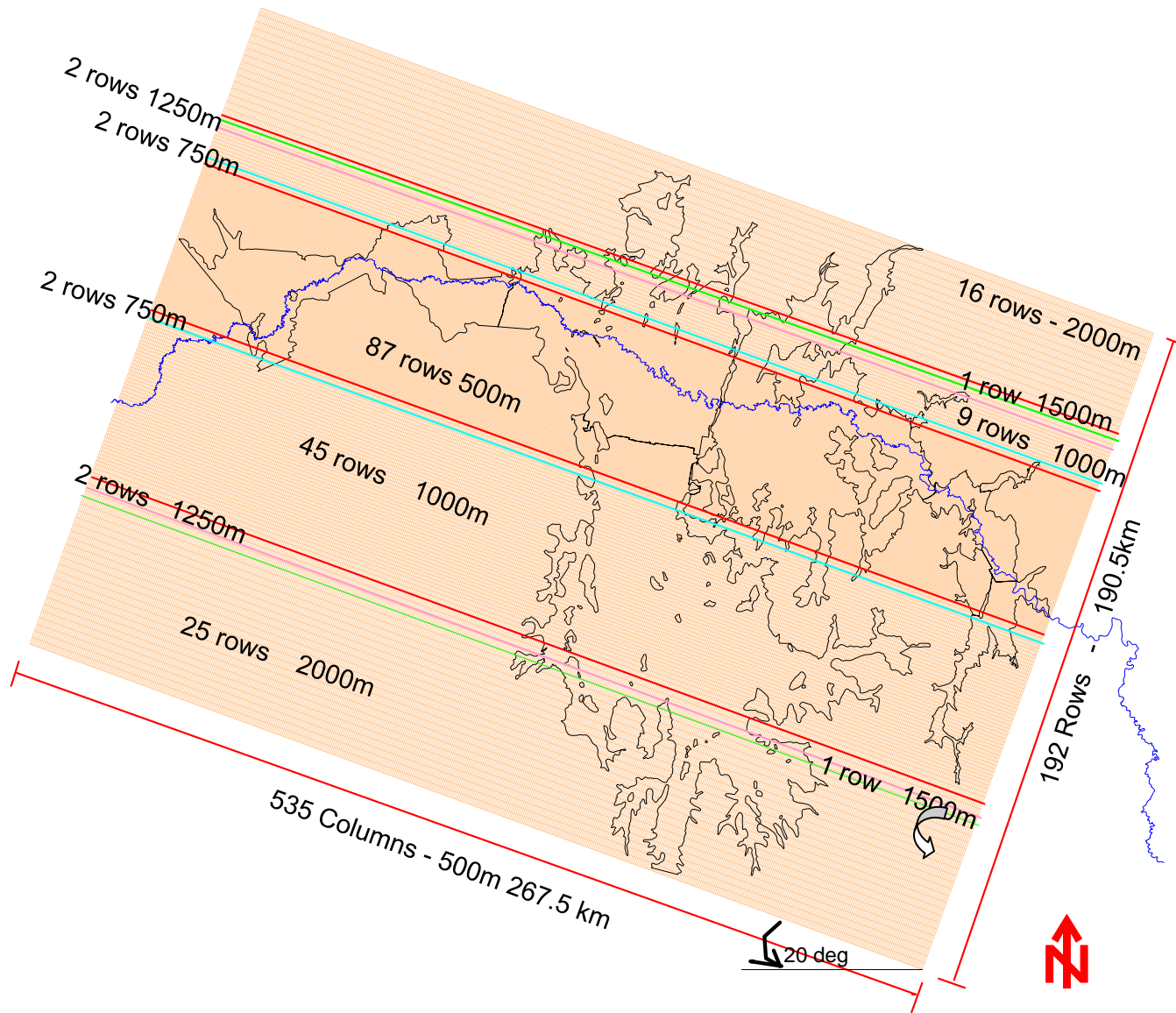
Table 3-1 Model Grid Specifications

South-west corner easting, northing:	378 000, 6 237 000m AMG
Angle of rotation relative to AMG:	20 degrees (anticlockwise)
No. of layers	4
No. of columns:	535
No. of rows:	192
Column width	500 m
Row width (varied)	500 - 2000 m
Total Cells (active + inactive):	410880

Table 3-2 Model Time-Discretisation Parameters

Stress period length:	1 month (30.44 days)
No. of stress periods:	264
No. of Time steps	10 (in each stress period)
Time step multiplier	1.2
Start of calibration period:	July 1986
End of calibration period:	June, 2008
Calibration period length:	22 years

Figure 3-3 Grid details



The following five surface elevation data sets are required to be specified in m AHD, for each active cell in the current model to define aquifer geometry.

- Natural surface (which is also the top of the Upper Cowra Formation)
- Bottom of Upper Cowra Formation (which is also the top of the Lower Cowra Formation)
- Bottom of Lower Cowra Formation (which is also the top of the Lachlan Formation)
- Bottom of Lachlan Formation (which is the hydraulic basement as well as the top of the Fractured Rock) while layer 4 is inactive
- Hydraulic basement bed surface (which is also the bottom of the fractured rock)

Topographic DEM data were used to define the natural surface elevation of the model. Data for the elevations of the four remaining surfaces were obtained from several sources which included Murray Basin Hydrogeological Map Series CARGELLIGO scale 1:250 000, Barnett (2008), SKM Upper Lachlan Groundwater Model Calibration Report and Coffey Geosciences Pty Ltd Cowal Gold Mine Groundwater supply modelling study (2006). Surfer™ software was used to create all five layer elevations using available data before importing into the model. Contour maps showing the three model layer thicknesses are presented in Appendix 1.

3.3 Initial heads

The MODFLOW numerical model requires the specification of head for every active cell in each layer at the start of the calibration period. Transient models require initial conditions closely matching natural conditions at the start of the simulation. The initial conditions are the heads from which the model estimates the changes in the system due to the stresses applied. Therefore, any errors associated with assumptions made to obtain such data are likely to impact overall model performance.

Water-level data for each piezometer at the first sampling date on or after 1st July 1986 were extracted from the NOW's Groundwater Data System (GDS) for observation bores in the study area. Water-level data were manually inspected to remove 'bad' or 'suspect' values, then the initial heads of all layers specified in the model were obtained using SURFER™ software. This process caused some cells at the margins of layers 1 and 2 to start as dry (that is, the interpolated heads were below the layer base), because there are fewer observation bores near the lateral boundaries of the model area and layers 1 and 2 generally rise in elevation towards these boundaries. The starting heads in these cells were therefore specified as a nominal height above the bottom of layer 1. The resulting SURFER 'grid' files were imported directly into Groundwater Vistas for analysis. The starting heads contours are graphically displayed in Appendix 2.

3.4 Aquifer parameters

Transient numerical models require knowledge of hydraulic conductivity and storage capacity of the aquifer medium in each cell to compute the flow between adjacent cells and the rate of movement of water to and from storage. Usually, the parameters such as hydraulic conductivity and storativity of material forming the aquifer vary across the model area laterally as well as vertically. Aquifer parameters are generally estimated from pumping tests.

Following pumping test analysis, Anderson (1993) suggested ranges of aquifer transmissivity for the depth range 24.4 to 60 m. Transmissivity varied from 49 to 1200 m²/d around the Jemalong and Wyldes Plains Irrigation Districts. There is no trend evident either spatially, or with depth. Several NOW irrigation bores have been pump tested. Bore 25165, of the Mulguthrie Section, was pump tested at a depth of 60.9-70 m, giving rise to a transmissivity of 71 m²/d. Similarly, bores 36551 and

36523 of the Corinella section were pump tested. For bore 36551, the aquifer tested was at a depth of 60.47-63.76 m and the transmissivity value determined was 780 m²/d. The zone tested in bore 36523 was a much deeper Lachlan Formation aquifer (119.6-122.6 m) and transmissivity was found to be 1160 m²/d.

Megalla and Kalf, (1973) recommended specific yield value of 0.10 for the alluvials in the region and Coffey (2006) used a value of 0.04.

Based on the calibrated aquifer parameters, Coffey (2006) estimated hydraulic conductivity to be in range 3 - 28 m/d for the Lachlan Formation and 1 m/d for the Cowra Formation. They estimated vertical leakance between the Cowra and Lachlan Formation to be $5.3 \times 10^{-7} \text{ d}^{-1}$.

Barnett and Muller (2008) used calibrated hydraulic conductivity values from 1 to 10 m/d for the Upper and Lower Cowra Formation and between 10 and 100 m/d for the Lachlan Formation.

These values were used to identify upper and lower hydraulic property bounds and initial estimates for the model. Some values were changed to obtain a better calibration during the calibration process.

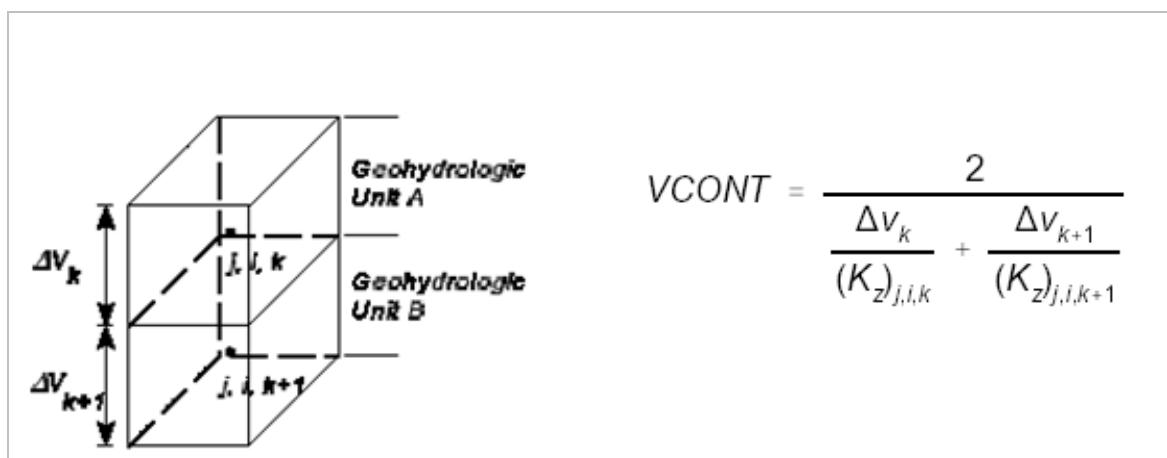
Specification of hydraulic conductivity (in X- and Y- directions) and storage factors (specific yield and storage coefficient) for each zone is needed in Groundwater Vistas. For the Upper Cowra Formation, which is unconfined, specific yield is used in MODFLOW computations. For the Lower Cowra and Lachlan aquifer, which are designated as 'confined/unconfined', both specific yield and storage coefficient are needed. As long as the aquifer remains confined during simulation, the assigned specific yield values have no impact on the model. If it becomes unconfined at any stage during simulation, then MODFLOW uses specific yield in place of storage coefficient in computations.

For a model consisting of more than one layer a vertical conductance term, known as vertical leakance (VCONT) is also required for all but the lower most layer. This parameter represents the leakage occurring between two model layers and is defined in terms of layer thicknesses and vertical hydraulic conductivities as shown in Figure 3-4.

In Groundwater Vistas, the user has the option either to specify vertical leakance for each parameter zone or to allow MODFLOW to compute vertical leakance based on the above relationship. However, the latter will require specification of the hydraulic conductivity in the vertical direction in each zone.

Aquifer parameters together with layer elevations are written into the block-centred-flow (BCF) package in MODFLOW.

Figure 3-4 Definition of Vertical Leakance Parameter (VCONT)
(from Chiang & Kinzelbach, 1996)



3.5 Boundary conditions

Boundary conditions determine where water enters or leaves the model domain and in what quantity. Commonly three different boundary conditions are identified in groundwater modelling. They are specified head, specified flow and mixed type (head dependent) boundaries. The discussion in this section is limited to the relationships between the spatial boundaries of model flow domain and the external environment.

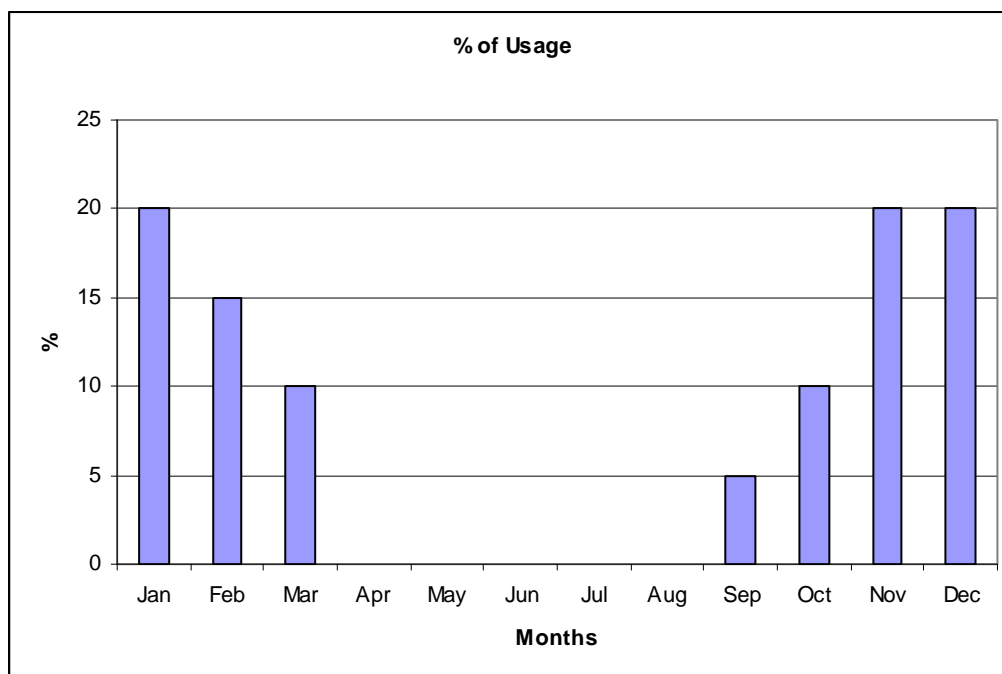
Model boundaries in the east, north and south are specified as 'no-flow' which means that no groundwater flow occurs across these boundaries. The western boundary is designated as a 'constant head boundary (CHD) in which the head varied with time.

3.6 Well package

The well package is designed to represent extraction of water from cells and to account for such losses in the finite difference equations. Recharging and discharging wells have positive and negative rates respectively. For each cell in each layer, only one value for net discharge can be specified for a given stress period.

This groundwater model simulates monthly stress periods and requires monthly frequency for data. Usage data prior to 1998 were relatively small and unreliable. However, after 1998 reliable annual groundwater usage data is available. In order to simulate pumping in the model it was necessary to derive monthly usage patterns from the yearly usage data by applying a specified percentage distribution. Assumed pumping schedule is shown in Figure 3-5. However, the actual pattern of usage may vary with the purpose of the bore. For a listing of the bores used in the well package, refer to Appendix 3.

Figure 3-5 Assumed monthly pumping and irrigation schedule



The model runs from July 1986 to June 2008; however before 1998 the usage data set is incomplete for the model period. A twelve year gap in usage data at the beginning of the model has implications for the calibration of the model. If the applied stress from groundwater extraction is not accurate the model may not represent real conditions and may not calibrate properly as discussed in Bilge (2001) and Salotti (1997).

3.7 Recharge

The recharge package adds terms representing distributed recharge to the finite difference equation. In this study, the aquifer is recharged by rainfall, flood, irrigation and stream leakage. Recharge relative contributions are further explained in section 4.6. All recharge sources may vary spatially as well as temporally. Recharge due to river leakage is considered separately under stream/aquifer interaction as discussed in Section 3.8. The remaining sources rainfall, flood and irrigation, are simulated in the model using MODFLOW's recharge package. Recharge is applied to the highest active layer.

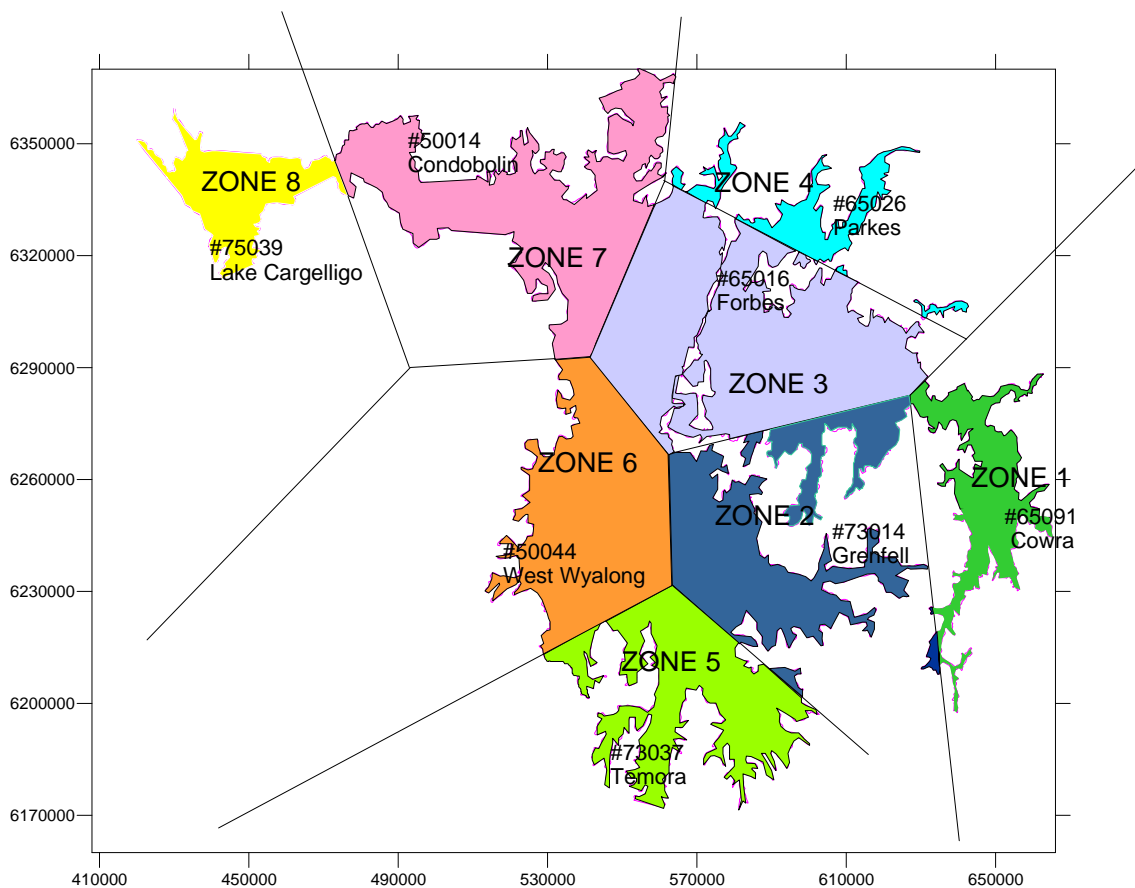
3.7.1 Rainfall Recharge

Recharge from rainfall can occur in a number of ways. For example, it can occur through direct infiltration beyond the root zone. Rainfall induced recharge can occur through side-slope run-off and ephemeral streams which may include lagoons and flood runners. As mentioned in Section 2.1, changes in the residual mass curves developed for the region compare well with changes in bore water levels in undeveloped areas indicating a strong link between long-term rainfall trends and fluctuations of groundwater level.

A rainfall recharge rate of 2 % and bounds between 0.1 % and 5 % of average annual rainfall were based on Dawes et al (2000) which provides estimates for medium scale catchments in the Liverpool Ranges of NSW, were used in initial model calibration attempts. These values were subsequently changed to obtain a better model calibration.

The assumed area of influence of each rainfall station based on the Thiessen method is shown in Figure 3-6.

Figure 3-6 Rainfall Recharge & Evaporation Distribution

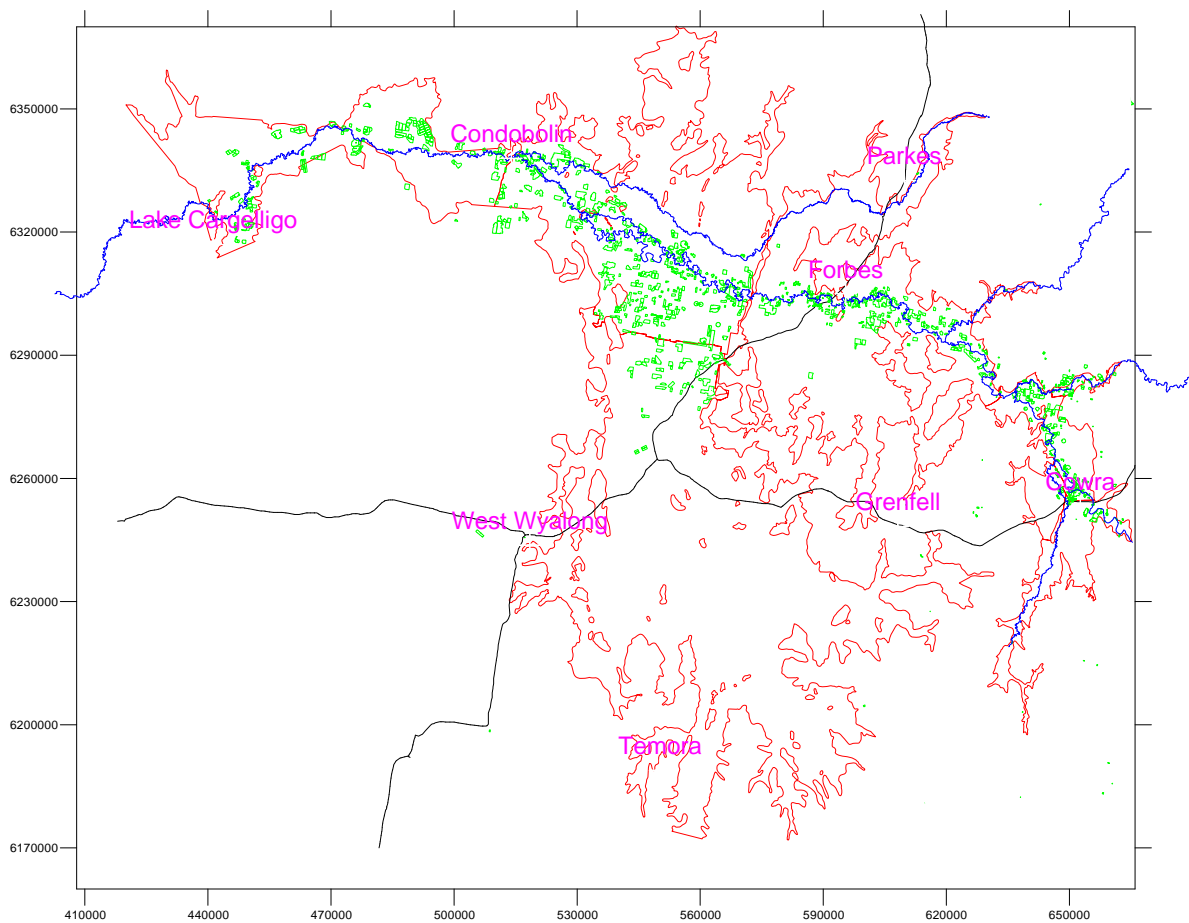


3.7.2 Irrigation Recharge

Leakage from crop irrigation systems is a source of artificial recharge to the aquifer system. The irrigation recharge areas within the model are based on the department's GIS Land Use Classification Mapping in 2000 as shown in Figure 3-7. These areas are assumed to be constant throughout the calibration period (July 1986 - June 2008) but irrigation recharge rates are varied proportionately based on the historical record of surface water diversion.

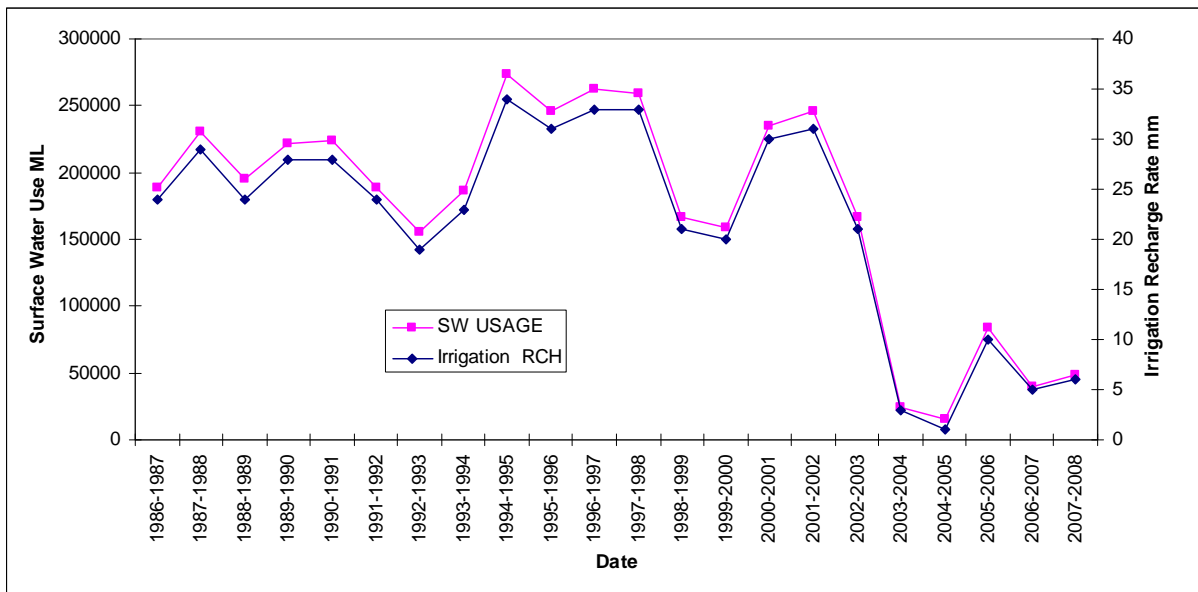
The standard irrigation application rate for non-rice crop farmlands is 6 ML/ha/yr. Of this, about 5 ML/ha/yr is assumed to be lost through evaporation. Therefore, only 1ML/ha/yr is available for irrigation recharge. This is equivalent to 100 mm of water per farmland hectare per year which is the maximum irrigation recharge available after irrigation efficiency, crop interception and initial soil moisture are taken into account Prathapar (pers. comm.).

Figure 3-7 Irrigation recharge areas



It is reasonable to assume that the component of irrigation recharge returns to the groundwater regime to be between 20 and 40 mm/ha/yr. In the current model surface water use during the calibration period (1986-2008) and spatial irrigated area water year 2000-2001 are available however, the pattern of spatial growth of irrigated area over the years is not known accurately. Irrigation recharge of 30 mm/ha/yr in the water year 2000-2001 was assumed and the level of recharge for other years was estimated proportionately based on historical records of surface water diversion in each year. These diversions are shown in Figure 3-8. The monthly irrigation schedule shown in Figure 3-2 was applied to the annual diversions to obtain monthly components of irrigation recharge. While this approach makes sure that the aquifer system received the full complement of irrigation recharge every year, it fails to replicate accurately any local impacts on the water table due to irrigation practice.

Figure 3-8 Assumed yearly irrigation recharge rates

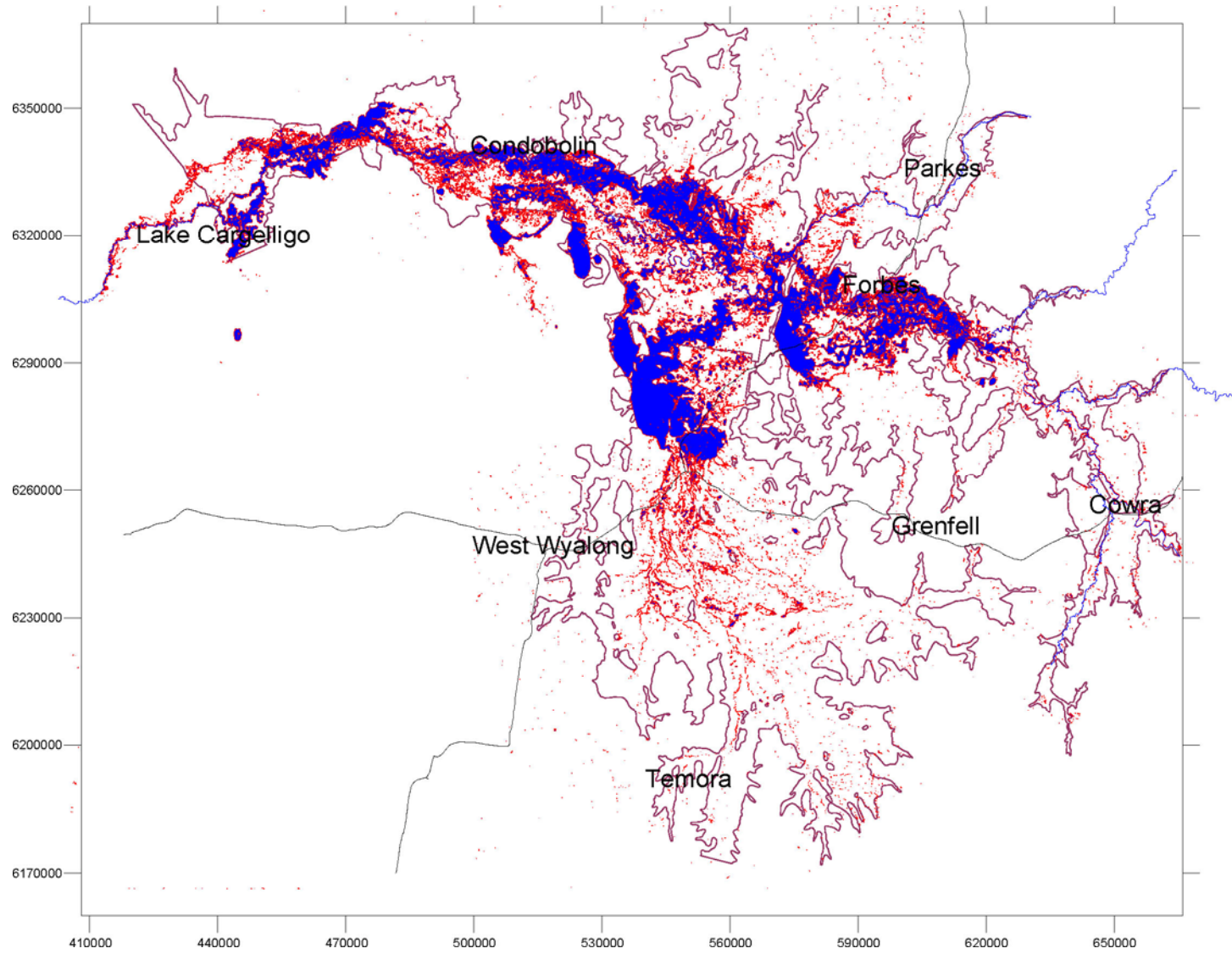


3.7.3 Flood Recharge

In the period from July 1986 to June 2008 two flood events occurred within the model area, a major event occurred in April-August 1990 and a minor event in June-July 1998. For the model, only the major event was taken as a recharge contributor. For this event the area coverage and the model hydrographs response are clearly visible. The inundated area during the 1990 flood is shown in Figure 3-9, based on available GIS flood maps.

The inundated area is divided into eight Thiessen polygons identical to the rainfall zones shown in Figure 3-6 for calibration purposes. Initial flood recharge fluxes for each zone varied from 0.0002 to 0.005 m/d. These values were adjusted during calibration. The period of flood inundation was seven months from May 1990 to November 1990.

Figure 3-9 Flood recharge areas



3.8 River aquifer interaction

Some interaction between streams and the shallow aquifer exists in most alluvial formations. The model indicates the Lachlan River suffers considerable losses to groundwater along its course. It is likely that increased groundwater pumping in the vicinity of the river in recent years has contributed to some of these losses.

MODFLOW (McDonald and Harbaugh, 1988) simulates leakage between a river and the aquifer as a vertical flow through the riverbed. The direction of leakage through a river cell depends on the relative positions of the groundwater level (H_{ijk}) and the river stage ($HRIV$). The rate of leakage ($QRIV$) is controlled by the head and the conductance ($CRIV$) of the riverbed within a particular river cell (see Equation 3.1).

$$QRIV = CRIV (HRIV - H_{ijk}), \text{ for } H_{ijk} > RBOT \quad (\text{Equation 3.1})$$

$$CRIV = KLW / M$$

where,

material	K	=	the conductivity of the riverbed
	L	=	the river reach length
	W	=	the river width
	M	=	the thickness of riverbed material

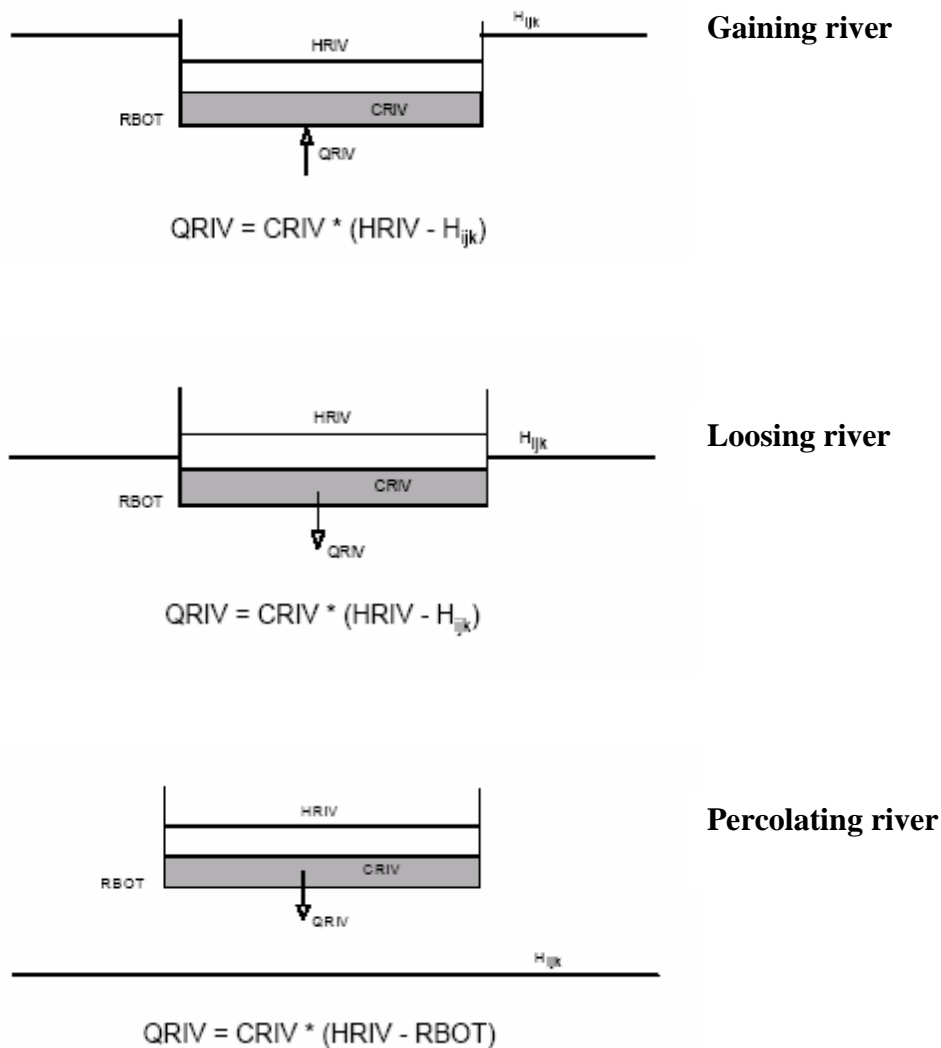
If $(HRIV - H_{ijk}) < 0$, then the seepage is in the direction of the river (a gaining river cell, see Figure 3-10). If $(HRIV - H_{ijk}) > 0$, then the seepage is in the direction of the aquifer (a losing river cell, see Figure 3-10). In both these situations, it is assumed that the head in the aquifer is above the river bottom elevation ($RBOT$). However, there may be instances where the groundwater level (H_{ijk}) falls below the river bottom. In such a situation, MODFLOW assumes a constant seepage from the river (a percolating river cell). The rate of flow from the river is solved by Equation 3.2 independent of further head decline of the aquifer (a percolating river cell as shown in Figure 3-10).

$$QRIV = CRIV (HRIV - RBOT), \text{ for } H_{ijk} \leq RBOT \quad (\text{Equation 3.2})$$

Of the four parameters contributing to $CRIV$, only the river reach length (L) is known accurately. River width (W), river bed thickness (M) and hydraulic conductivity (K) in each river cell are difficult to estimate with any confidence. Hence, the lumped parameter, KW/M , is assumed initially and adjusted during the calibration process.

The parameters required in MODFLOW's river package to simulate stream/aquifer interaction for each designated river cell are the layer number, row and column of the cell, river stage, river bottom elevation and river conductance. Groundwater VistasTM allows the specification of a reach number as well.

Figure 3-10 MODFLOW conceptualisation of river/aquifer interaction



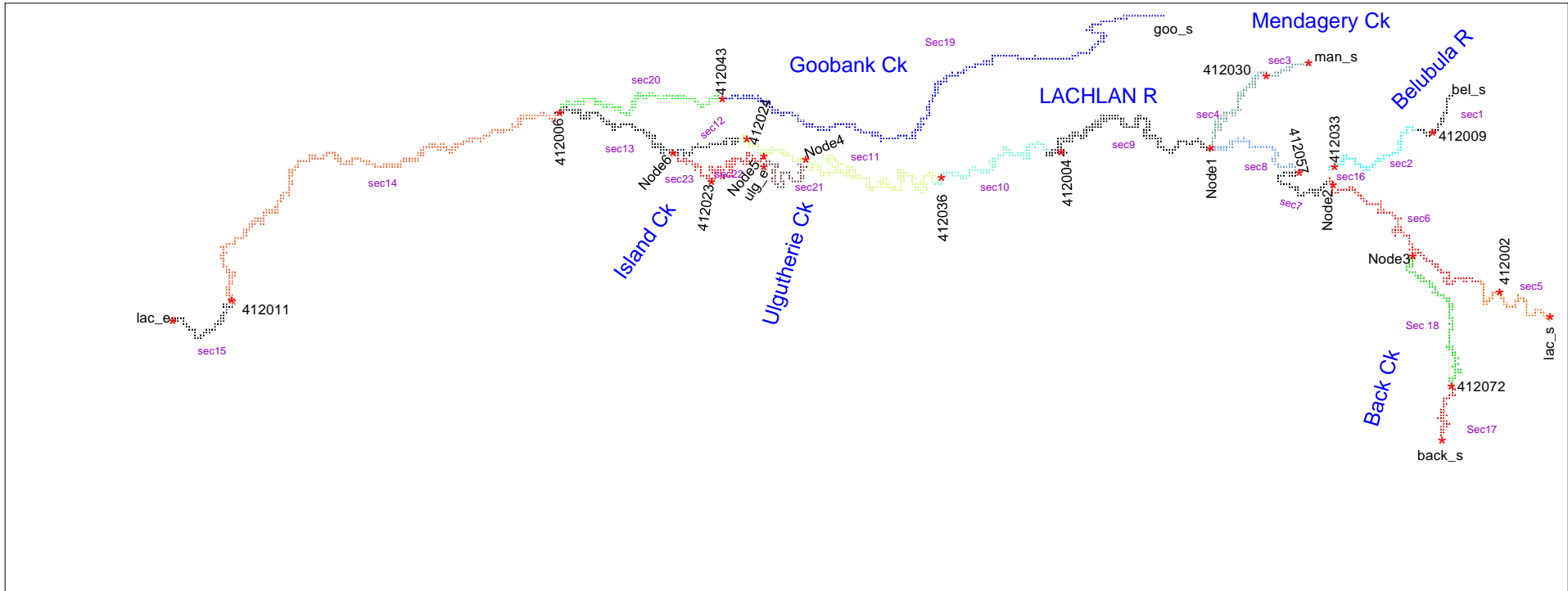
There are thirteen gauging stations along the stretch of the river considered in this study. Of these, only seven stations have continuous records of river gauging data covering the entire model calibration period. River hydrographs at the seven stations, gauging station and weirs are given in Appendix 4.

The preparation of input data for MODFLOW involves a number of tasks, which are listed below:

- Digitising river reach for the Lachlan River and processing river data to obtain river length within a cell.
- Extractions of river stage data for each gauging station covering the model calibration period.
- Estimation of missing data through interpolation.
- Processing riverbed data from available gauging station elevations.
- Establishment of hypothetical gauging stations and estimation of river stage data.
- Preparation of the surface topography map of the model area on a cell-by-cell basis.
- Processing data using a modified version of 'VMRIVER' software developed by Demetriou (1995) to create the river boundary file for Visual MODFLOW.

A schematic diagram of the 23 sections and thirteen gauging stations used in the model is presented in Figure 3-11. The river package has a total of 2037 river cells belonging to twenty three sections. River hydrographs and river gauging station and weirs are given in Appendix 4.

Figure 3-11 Schematic diagram of the river sections and gauging stations



3.9 Evaporation

MODFLOW's evapotranspiration (EVT) package simulates the effects of plant transpiration and direct evaporation in removing water from the saturated groundwater regime (McDonald & Harbaugh, 1988). As implemented in MODFLOW, for each model surface cell a maximum rate of evapotranspiration (ET) is specified for each surface cell together with an ET surface elevation and an 'extinction depth'. When the water table depth is at or above the ET surface, evapotranspiration occurs at the maximum specified rate. When the water table lies below the extinction depth, zero evapotranspiration occurs. Between these two depths, evapotranspiration varies linearly.

Eight evapotranspiration zones were introduced in the model area, identical to the distribution of recharge zones presented in Figure 3-6. A starting value of 10% of the potential evaporation (m/d) recorded at weather stations were specified as the initial evapotranspiration rate at the ground surface in all eight zones. The extinction depth was varied from 3 to 9 meters below the surface across the model area. Evapotranspiration is applied to the highest active layer.

3.10 Solver

The 'Geometric Multigrid (GMG)' is used as the mathematical solver in this model. The parameter settings for the package are shown in Table 3-3.

Table 3-3 Parameter settings in GMG solver package

Maximum Inner Iterations	500
Maximum Outer Iterations	1
Head Change Criterion for Convergence	0.001
Inner Convergence Criterion	0.1
Relaxation Parameter	0
Adaptive Damping Flag	0
Output Control Flag	4
Damping parameter	1.0

4. Model calibration

Calibration of a numerical groundwater flow model can be accomplished by determining a set of parameters, boundary conditions and stresses that produce simulated heads and fluxes in order to match field-measured values within a pre-established range of error. Finding this set of values from a set of observed heads amounts to solving the inverse problem (Anderson, Gates & Mount, 1993).

During the calibration process, important model parameters are adjusted, within realistic limits, to produce the best match between simulated and observed data. The process begins with an initial estimation of parameters (hydraulic conductivity horizontal and vertical, specific yield, recharge, boundary conditions, etc.) for each active cell in the model grid. Adjustment of parameters can be done manually or automatically. Automatic calibration method was attempted in the current model.

PEST (Doherty, 2005) is nonlinear parameter estimation software which is used in automatically calibrating complex groundwater models. PEST was used in "regularisation mode" coupled with "pilot points" as a method of spatial parameterisation to calibrate the current model. A total of 1845 estimable parameters were used. PEST software can automatically adjust model parameters to minimise the discrepancies between the observed data and model predicted values (residuals). The objective function (ϕ), defined as the 'sum of squares of weighted residuals' is used as a calibration statistic. In a mathematical sense, a lower objective function indicates better model calibration.

The starting and ending times of the model calibration period are 1/7/1986 and 30/06/2008 respectively.

Water level data from observation bores in the model area were utilised to obtain target results for calibration. Thirty-four observation bores in layer 1, ninety four bores in layer 2 and fifty in layer 3 were used for the model. Their spatial distribution is shown in Appendix 5.

4.1 Automatic calibration

Nonlinear parameter estimation software is commonly used in calibrating complex groundwater models. PEST is one such nonlinear parameter estimator which is powerful and model independent. PEST was used in "regularisation mode" coupled with "pilot points" as a method of spatial parameterisation to calibrate the current model. SVD-Assist is a powerful new model calibration tool available in PEST which embodies a hybrid regularisation methodology that combines the strengths of subspace methods, for example singular value decomposition (truncated SVD), and Tikhonov regularisation methodologies.

In the pilot point parameterisation scheme, parameter values are assigned to a set of points distributed throughout the model domain. These parameter values are then spatially interpolated to the individual cells of the model grid using the spatial interpolation method 'kriging'. Regularisation across the entire model domain is allowed to take place with 'preferred parameter' values included as 'regularisation observations' to enforce a smoothing condition. The fundamental purpose of regularisation is to prevent extreme parameter values at pilot points and to produce a smooth parameter distribution.

The number of pilot points used in each layer varied and the parameters estimated are summarised below:

- layer 1 hydraulic conductivity ($kx1_1$ to $kx1_164$)
- layer 1 specific yield ($sy1_1$ to $sy1_164$)
- leakance between the layers ($le1_1$ to $le1_164$)

- layer 2 hydraulic conductivity ($kx2_1$ to $kx2_221$)
- layer 2 storage coefficient ($ss2_1$ to $ss2_221$)
- layer 2 specific yield ($sy2_1$ to $sy2_221$)
- leakance between the layers ($le2_1$ to $le2_156$)
- layer 3 hydraulic conductivity ($kx3_1$ to $kx3_156$)
- layer 3 storage coefficient ($ss3_1$ to $ss3_156$)
- layer 3 specific yield ($sy3_1$ to $sy3_156$)

Zone based rainfall, flood recharge ($prain1$ to $prain8$ and $fflux$ to $fflux$) and evapotranspiration ($pevt1$ to $pevt9$) parameters were also included as adjustable parameters. The number of river reaches was increased from one to forty one ($riv1$ to $riv41$) to allow better estimates of river/aquifer interaction.

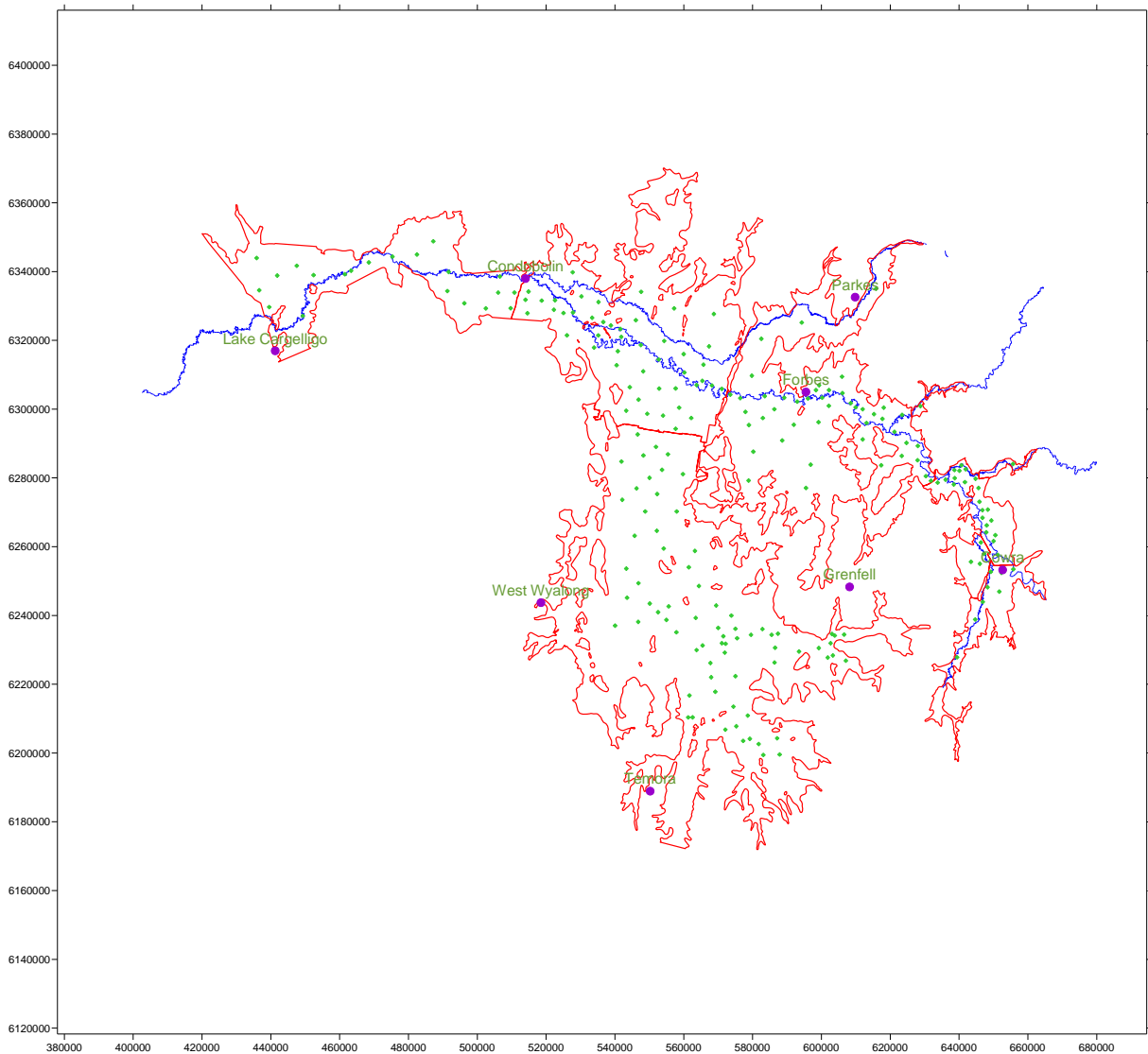
The locations of pilot points used for layer 2 of the model (Lower Cowra Formation) are shown in Figure 4-1. For the other layers, with lesser active area, a subset of these was used. Model parameters representing different hydraulic properties at each of the pilot points are named uniquely. This nomenclature is summarised in Table 4-1.

Table 4-1 Model Parameters

LAYER	Hydraulic Property	No. of Pilot Points	Parameters Names
1	Hydraulic Conductivity	164	$kx1_1$ to $kx1_164$
1	Specific yield	164	$sy1_1$ to $sy1_164$
1	Leakance	164	$le1_1$ to $le1_164$
2	Hydraulic Conductivity	221	$kx2_1$ to $kx2_221$
2	Specific yield	221	$sy2_1$ to $sy2_221$
2	Leakance	156	$le2_1$ to $le2_156$
2	Storage coefficient	221	$ss2_1$ to $ss2_221$
3	Hydraulic Conductivity	156	$kx3_1$ to $kx3_156$
3	Specific yield	156	$sy3_1$ to $sy3_156$
3	Storage coefficient	156	$ss3_1$ to $ss3_156$
	Rainfall	8	$prain 1$ to $prain 8$
	Flood	8	$fflux1$ to $flux8$
	Evapotranspiration	9	$pevt1$ to $pevt 9$
	River	41	$riv1$ to $riv 41$
	Total	1845	

All parameters in each group assumed an initial value equal to the average parameter value obtained from a previous model by Coffey (2006) and Barnett & Muller, (2008) with some adjustments based on available pumping test analysis. Furthermore, all parameters in each group were subjected to the same constraints in the form of minimum and maximum values.

Altogether, there were 1845 parameters, 16836 observations with non-zero weight and 17 observation groups listed in the PEST control file. The SVD-assist parameter estimation process requires a pre-SVD-assist PEST run which is carried out specifically for the purpose of calculation of derivatives. SVD-assisted parameter estimation was then carried out using 600 super parameters which are essentially linear combinations of base parameters.

Figure 4-1 Location of pilot points in the Lower Cowra Formation

4.2 Final estimates of aquifer parameters

The calibration of model parameters was a major task. The calibrated parameters include horizontal hydraulic conductivity (K_h) for all layers, VCONT (vertical leakage) between layer 1 and layer 2 and layer 2 and layer 3; storage coefficient (S) of the lower layers, which are unconfined/confined; and specific yield (S_y) of the layer 1, which is unconfined. The calibrated hydraulic conductivity values of Upper Cowra vary from 30 to 0.01 m/d; for the Lower Cowra layer the values range from 40 to 0.01 m/d. The Lachlan Formation has conductivity values ranging from 1 to 100 m/d. The calibrated values of minimum and maximum specific yield of layer 1 are between 0.02 and 0.3 respectively. The calibrated specific storage (S_s) ranges from 10^{-4} to 10^{-6} for deeper layers.

Figure 4-2 shows the calibrated horizontal hydraulic conductivity (K_h) values for the Upper Cowra Formation. A variation in K_h values is evident in this diagram. Areas of high K_h exist along the ancient Lachlan palaeo channel part of the model area. These areas have values between 5 and 30 m/d. Most of the Upper Cowra aquifer has K_h values between 5 and 10 m/d.

Figure 4-3 shows the calibrated K_h values for the Lower Cowra Formation. A large part of this layer shows moderate to high values in the range of 5 to 35 m/d. Values are higher in the Lower Cowra Formation than in the Upper Cowra Formation.

For the Lachlan Formation horizontal hydraulic conductivity values vary between 1 and 100 m/d over the model area as shown in Figure 4-4.

In auto-calibration changes to specific yield (S_y) values were typically aimed at improving the calibration for the upper layer of Cowra. With lower S_y values, the model would typically become more sensitive to recharge rates, and would tend to create higher simulated heads in layer 1. Figure 4-5 shows the distribution of (S_y) values for layer 1. These values range from 0.06 to 0.14, indicating a medium degree of variability in the sediments of the layer1 formation.

Parameters representing the storage coefficient (S) of the Lower Cowra and Lachlan Formations were important. Changes to S values were usually aimed at increasing or decreasing the simulated pressure ranges to match those caused by seasonal pumping. This typically required orders-of-magnitude changes in S for each run. The layer 2 formation storage coefficient distribution in Figure 4-6 shows values around 10^{-6} , with little spatial variability. The storage coefficient in the Lachlan Formation is about $8.8e-5$ with very little spatial variability as shown in Figure 4-7.

Figures 4-8 and 4-9 show the calibrated vertical leakance VCONT values for the Upper Cowra Formation (layer 1) and the Lower Cowra Formation (layer 2), respectively. VCONT values are significantly higher in layer 1, ranging from 0.01 to 0.001 m/d.

Calibrated river conductance is represented in Figure 4-10. It varies from 1 to 2000 $m^2/d/km$. The conductance is, nevertheless difficult to assess by model calibration, as it can be varied by several orders of magnitude without much apparent effect as discussed by Merrick, (1989).

The remaining calibrated parameters are listed in Table 4-2.

Figure 4-2 Hydraulic Conductivity (m/d) distributions in Upper Cowra (Layer 1)

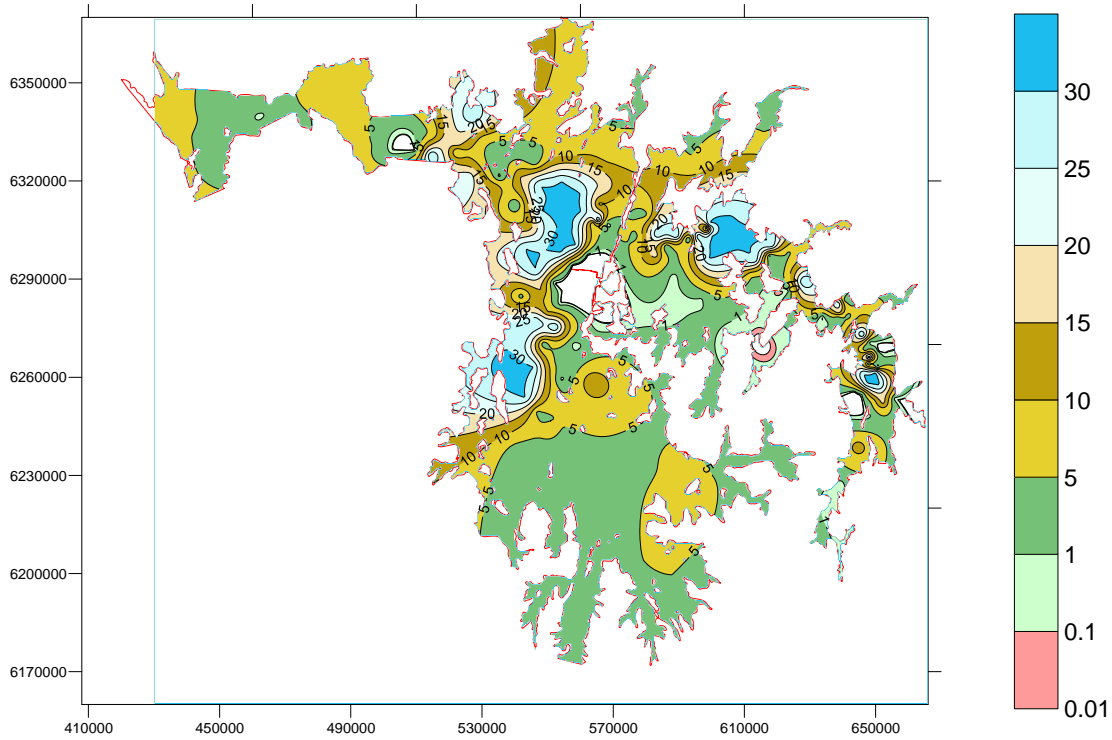


Figure 4-3 Hydraulic Conductivity (m/d) distributions in Lower Cowra (Layer 2)

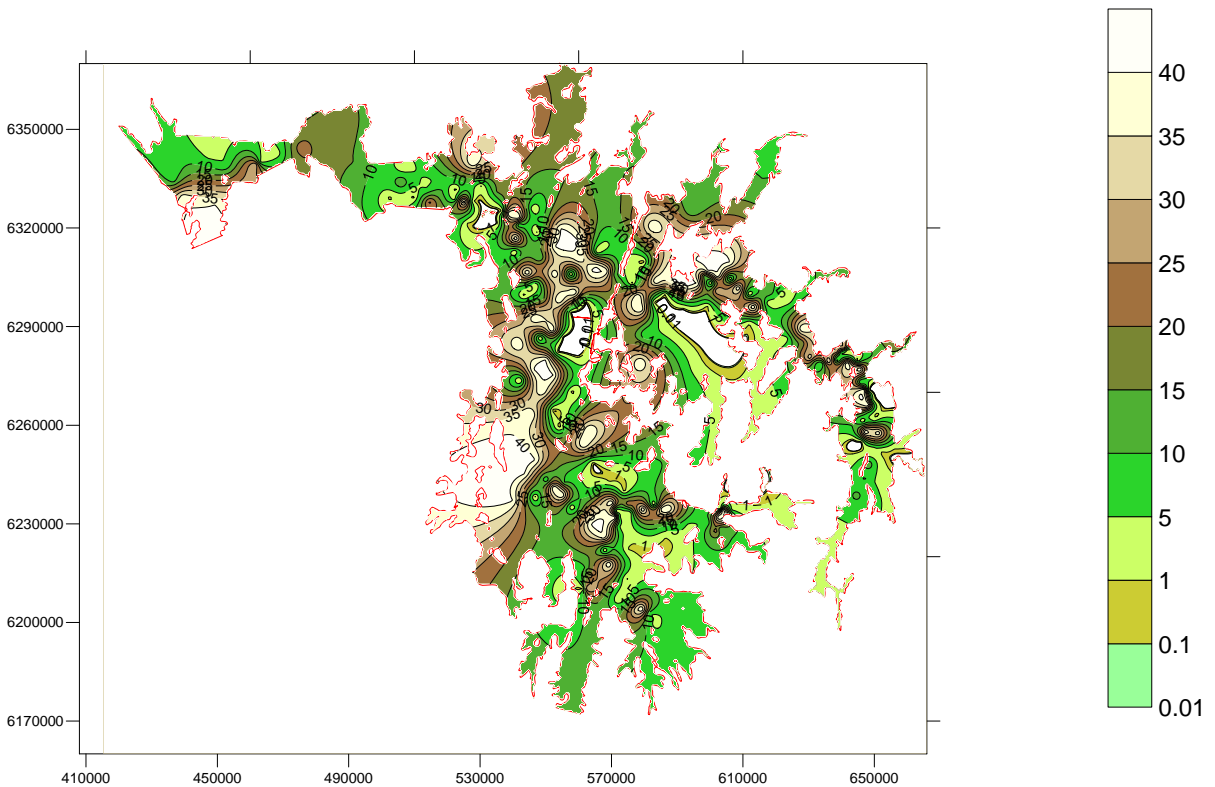


Figure 4-4 Hydraulic Conductivity (m/d) distributions in Lachlan Formation

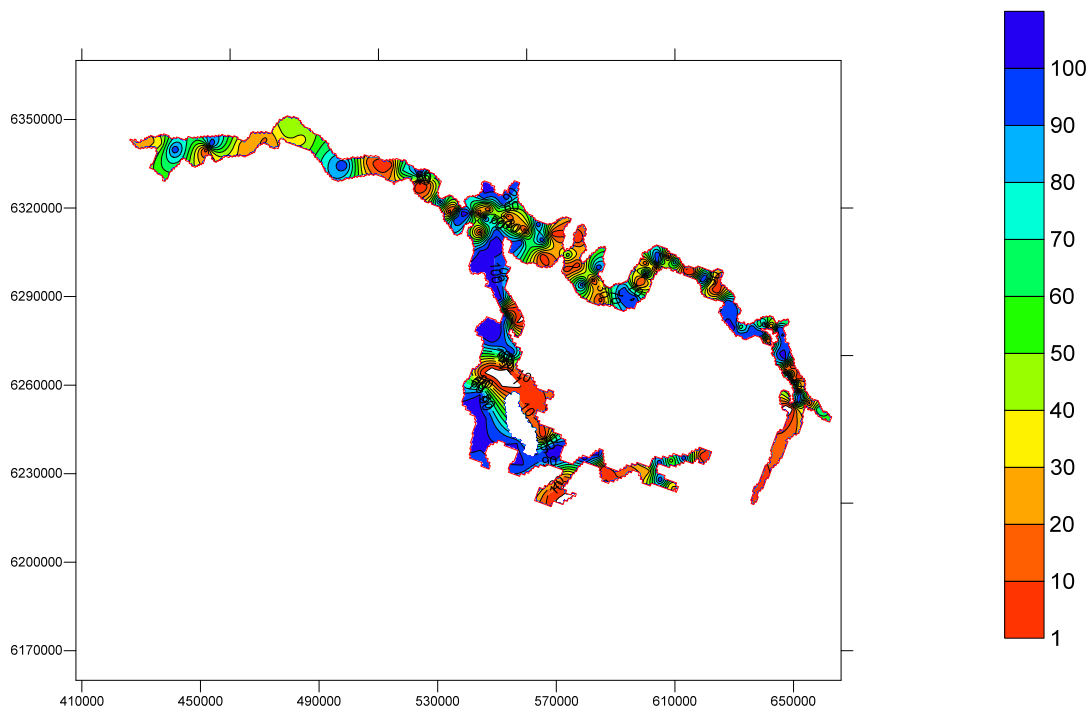


Figure 4-5 Specific yield distributions in Upper Cowra

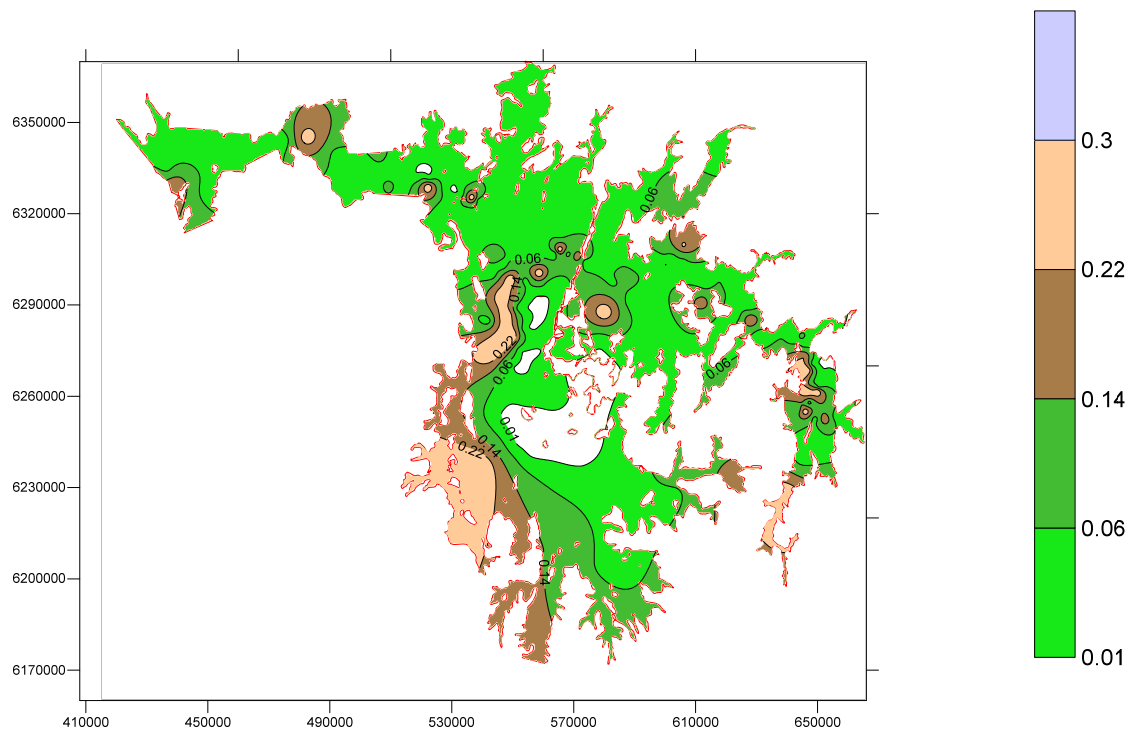


Figure 4-6 Storage Coefficient in Lower Cowra

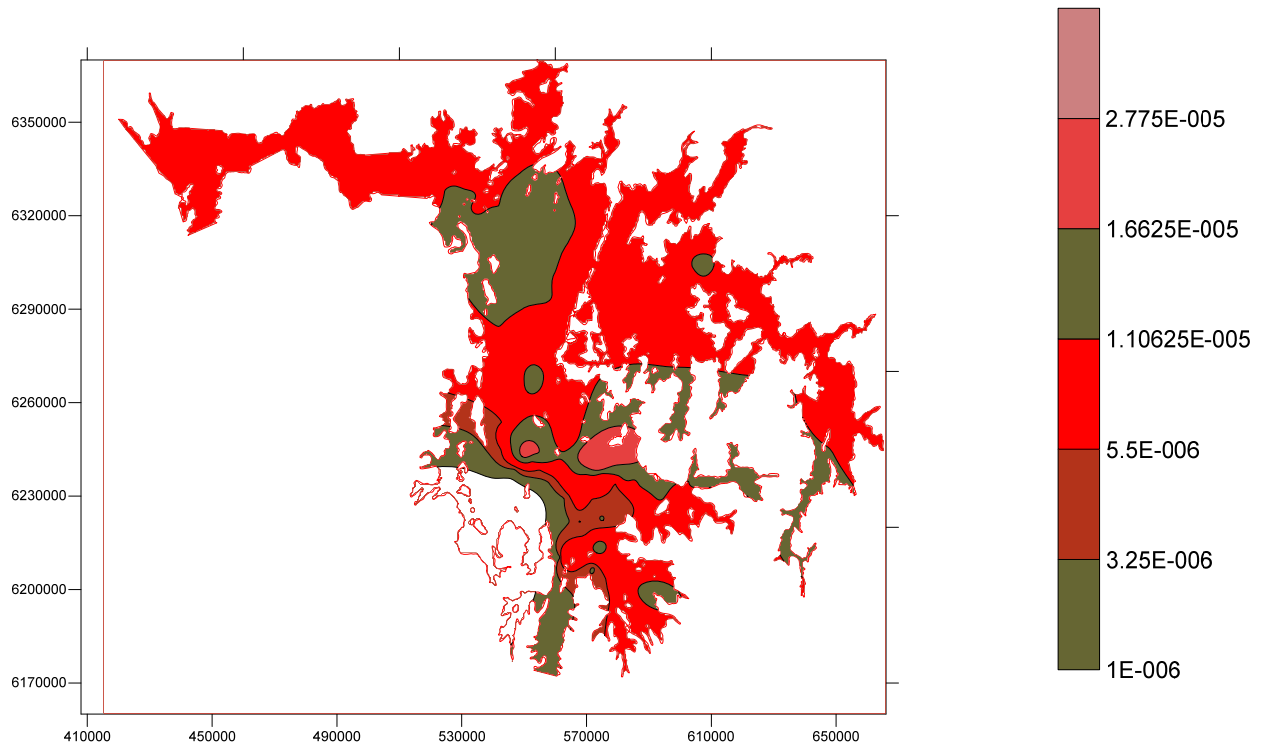


Figure 4-7 Storage Coefficient in Lachlan Formation

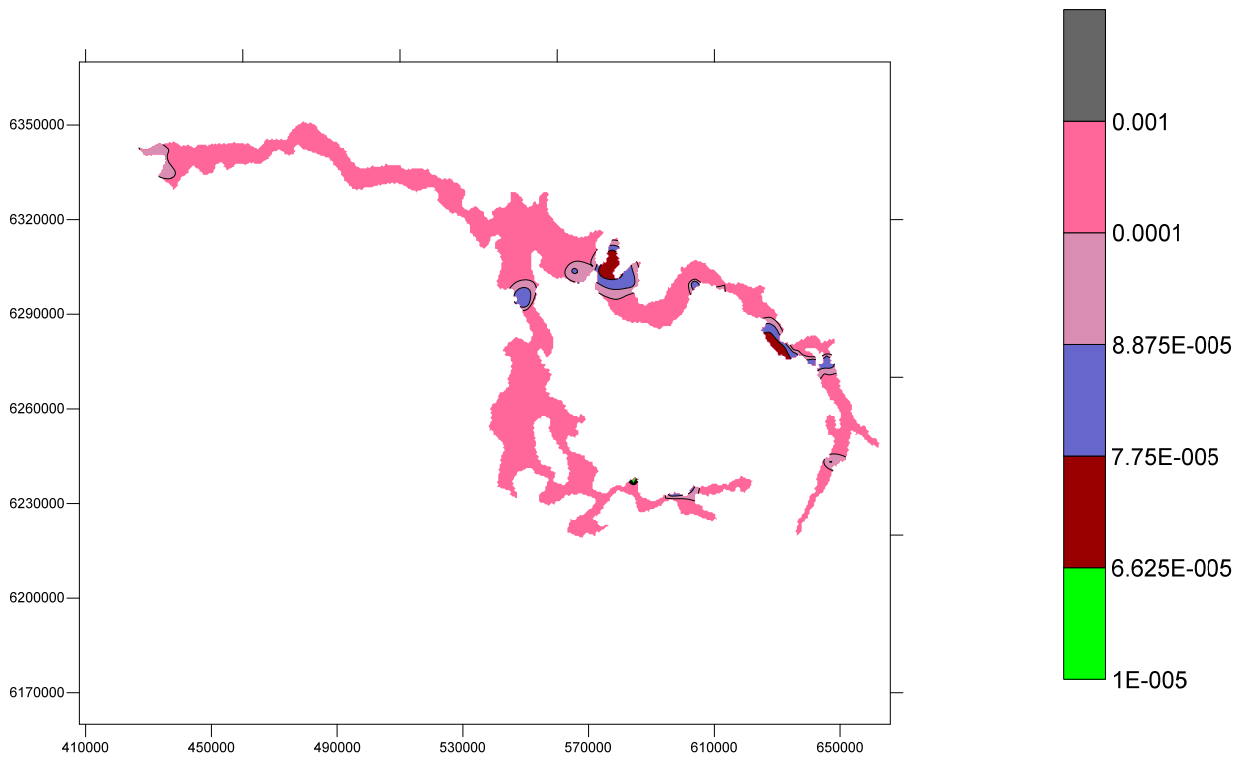


Figure 4-8 Vertical Leakance (1/d) between Upper and Lower Cowra

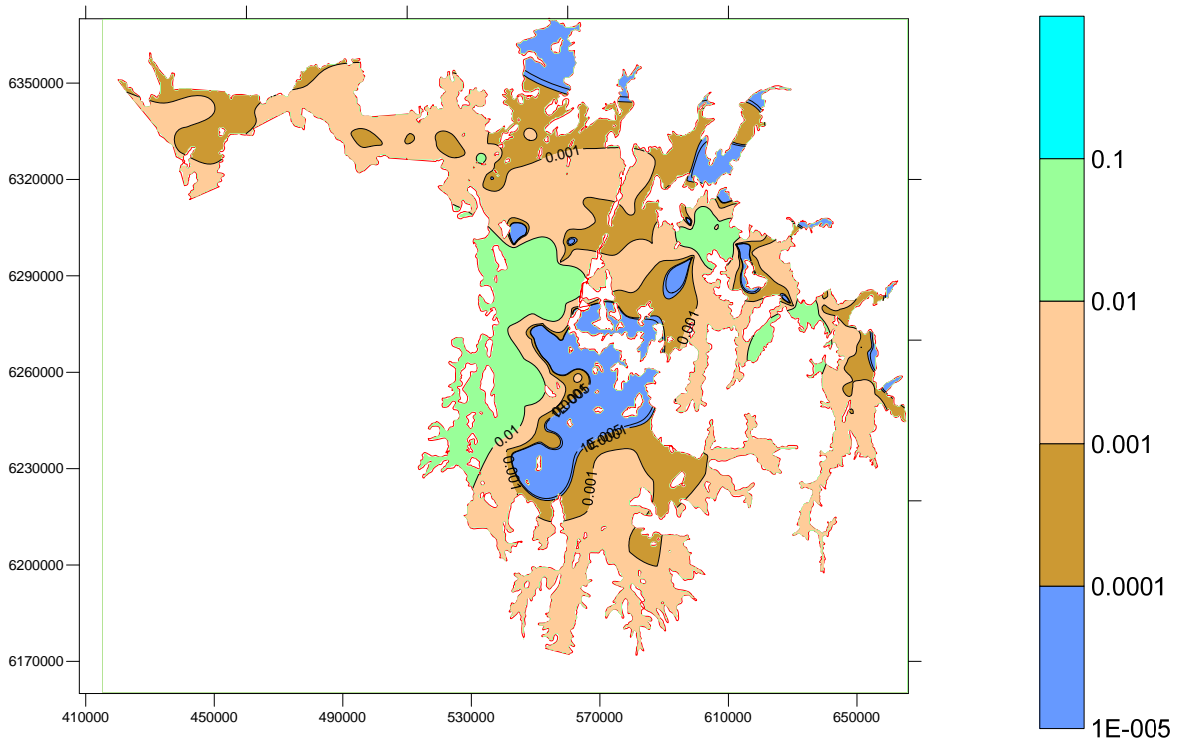


Figure 4-9 Leakance (1/d) between Lower Cowra and Lachlan Formation

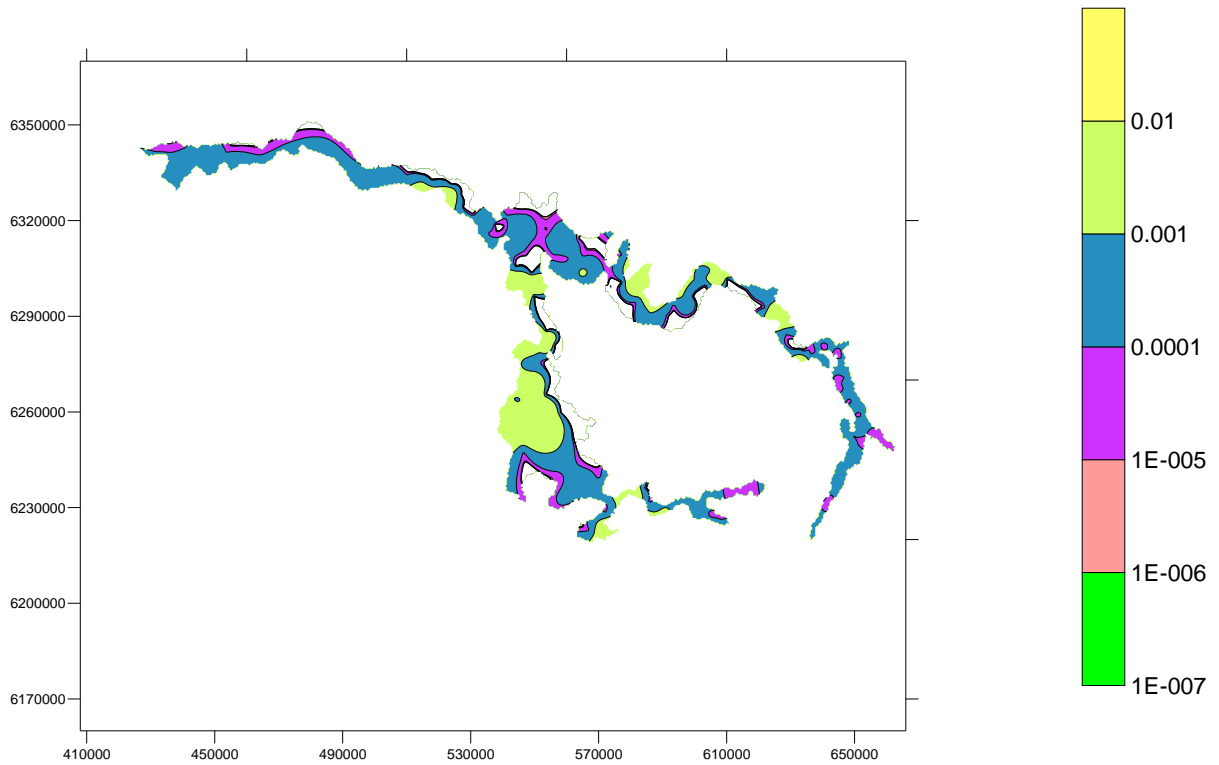


Figure 4-10 Calibrated River Conductance in $m^2/d/km$.

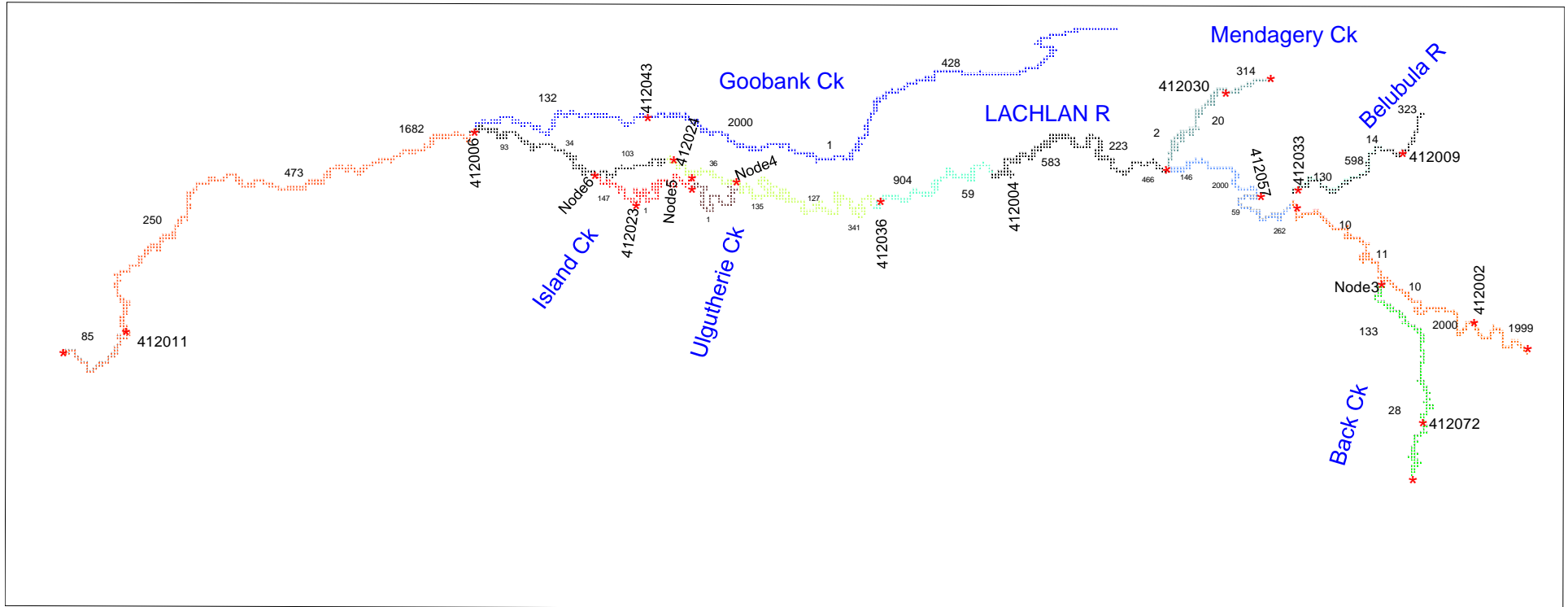


Table 4-2 Calibrated Model Parameters.

RIVER

	River Bed Hydraulic Conductivity
Parameter	m ² /d/km
riv1	323.5
riv2	14.3
riv3	598.0
riv4	130.2
riv5	313.6
riv6	20.4
riv7	2.5
riv8	1999.2
riv9	1999.9
riv10	10.0
riv11	10.6
riv12	10.1
riv13	262.4
riv14	58.6
riv15	2000.0
riv16	145.6
riv17	465.5
riv18	222.9
riv19	583.4
riv20	58.7
riv21	904.3
riv22	341.4
riv23	127.0
riv24	135.4
riv25	36.1
riv26	103.1
riv27	33.7
riv28	93.5
riv29	1681.6
riv30	472.6
riv31	250.1
riv32	84.8
riv33	27.8
riv34	132.8
riv35	428.0
riv36	1.0
riv37	2000.0
riv38	131.9
riv39	1.0
riv40	1.0
riv41	147.2

RAINFALL

Parameter	Rate (%)
prain1	1.9
prain2	0.1
prain3	2.9
prain4	3.0
prain5	0.1
prain6	0.1
prain7	3.0
prain8	3.0

FLOOD

Parameter	mm
fflux1	0.2-5
fflux2	0.2-5
fflux3	0.2-5
fflux4	0.05-1.25
fflux5	0.2-5
fflux6	0.05-1.25
fflux7	0.05-1.25
fflux8	0.2-5

EVAPORATION

Parameter	Rate (%)	Extinction Depth (m)
pevt1	5	6
pevt2	1	4
pevt3	25	9
pevt4	5	4
pevt5	7.5	4
pevt6	25	9
pevt7	25	8
pevt8	4.8	3
pevt9	4.9	5

4.3 Head response

Plots of observed and simulated hydrographs for each calibration bores are presented in Appendix 6. These comparison plots are presented in eight groups primarily based on their location. The locations of these bores are shown in Appendix 5. There are total 174 hydrograph in Appendix 6.

Except in zone 7, most monitoring bores show that water levels in layers 1 and 2 sharply increased in response to the flood event of 1990. Following the flood event water levels remained generally steady until the year 2000. After that the water levels show a sharp decline which is attributed to increased groundwater usage coupled with drought conditions.

Most of the monitoring bores in layer 3 also follow the same trend as that observed in layers 1 & 2. However, at some of the calibration bores, simulated water levels do not fluctuate as much as the corresponding observed water levels. In particular, predicted drawdowns are often less than that measured. This may be attributed to the lack of monthly pumping data. Accurate monthly pumping records are necessary to quantify the amount of aquifer stress. Pumping records are not reliable before 1998 and after this only annual totals were reported. But the groundwater model simulates monthly stress period and ideally requires monthly pumping values.

Simulated and observed water levels in zone 7 do not match well suggesting the model is poorly calibrated in this area. A poor match in this area was also noted in Coffey (2006). In zones 1 and 2 the simulated and observed heads show a similar trend but simulated values are higher than observed values in all layers. Reasons for these mismatches are unclear but it is likely that knowledge of the local geology was not sufficient to have allowed construction of a realistic model in this area.

In the remaining zones the model mostly matches the observed pattern well.

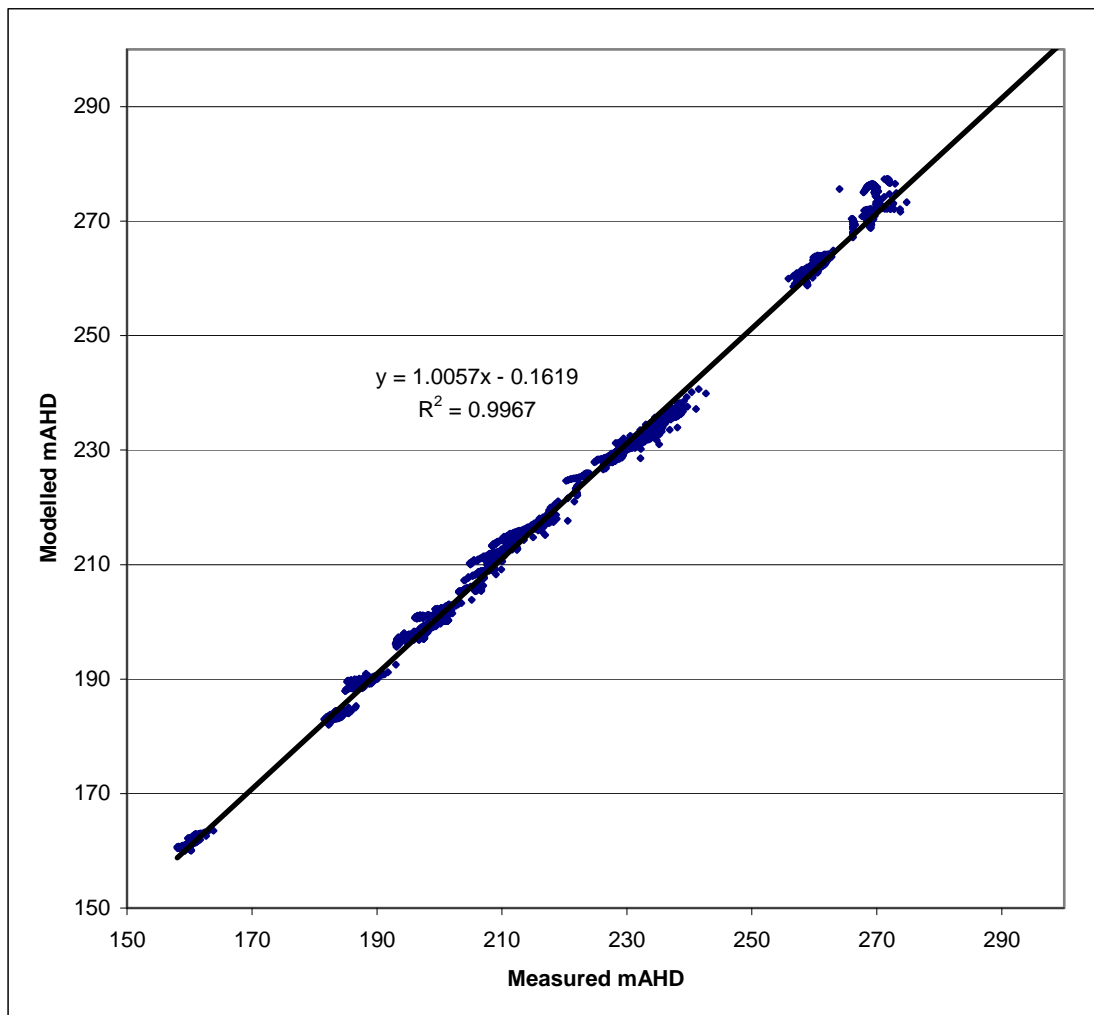
4.4 Calibration assesment

The modelling guidelines by Middlemis, et al., (2001) recommend evaluation of the degree of calibration of a groundwater model using both qualitative (visual comparison) and quantitative (statistical) means. Quantitative measures assessing calibration usually involve mathematical and graphical comparisons between measured and simulated aquifer heads and the calculation of statistics regarding residuals.

Figures 4-11 to 4-13 provide, for each layer, scattergrams of the simulated water levels. In diagrams of this sort, a 45° line through the origin represents a perfect calibration with a coefficient of determination of one ($R^2 = 1$). The extent of scatter about this line is regarded as a measure of the goodness of model calibration. Some minor discrepancies between the observed and simulated aquifer heads are to be expected in a model of this magnitude. Low SRMS (scaled root mean square) value (less than 5%) is normally regarded as another indicator of a well calibrated model. According to these criteria, this model is well calibrated.

For layer 1, simulated values are closely clustered about the 45° line with a root mean square (RMS) of 2.01 meters and a mean sum of residuals of 1.41 meters for 3175 observation data.

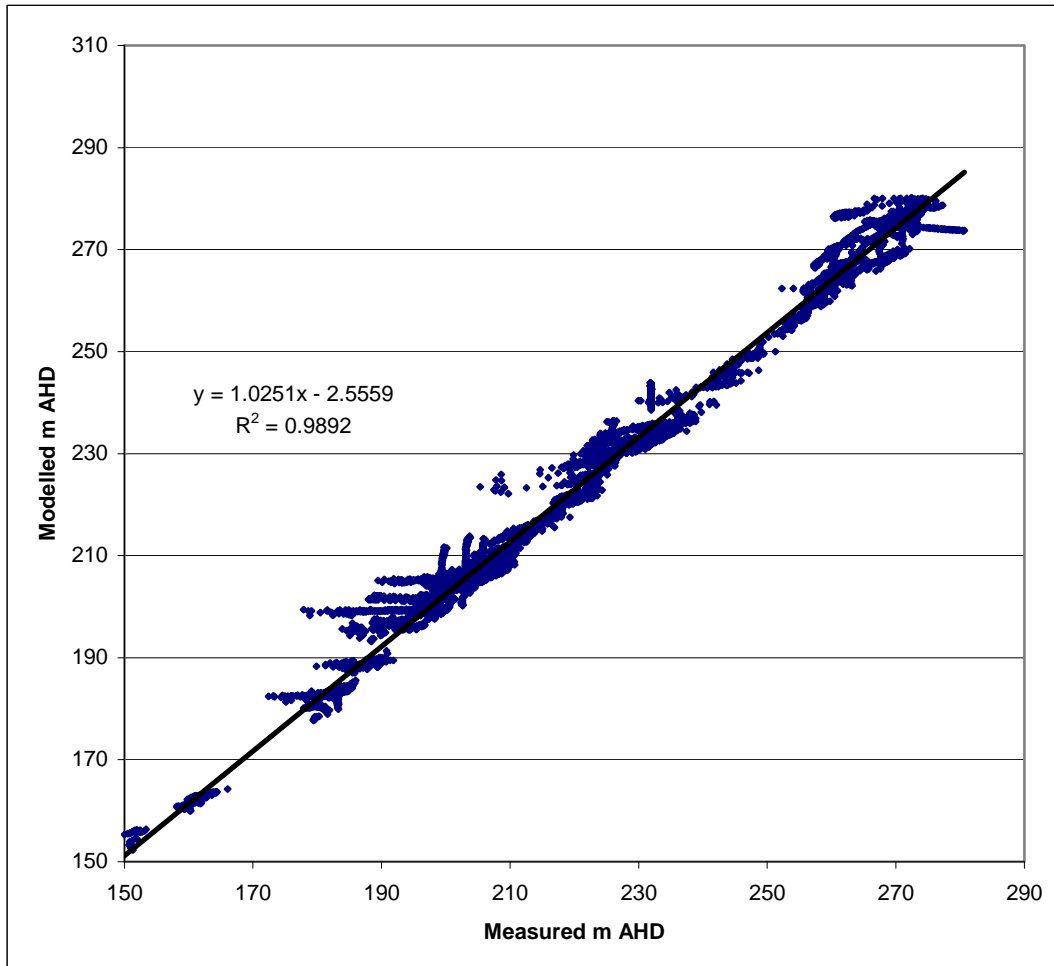
Figure 4-11 Layer 1 Scattergram of modelled versus measured heads and statistics results.



Sum of Squares (m**2)	SSQ =	12784.33	m**2
Mean Sum of Squares (m)	MSSQ =	4.03	m
Root Mean Square (m)	RMS =	2.01	m
Scaled Root Mean Square (%)	SRMS =	1.37	%
Root Mean Fraction Square (%)	RMFS =	0.87	%
Scaled Root Mean Fraction Square (%)	SRMFS =	1.30	%
Sum of Residuals (m)	SR =	4479.08	m
Mean Sum of Residuals (m)	MSR =	1.41	m
Scaled Mean Sum of Residuals (%)	SMSR =	0.96	%
Coefficient of Determination (tend to unity)	CD =	0.98	

The scattergram plot of Layer 2 Figure 4-12 shows scatter with a RMS value of 4.84 metres for 7515 observation data points.

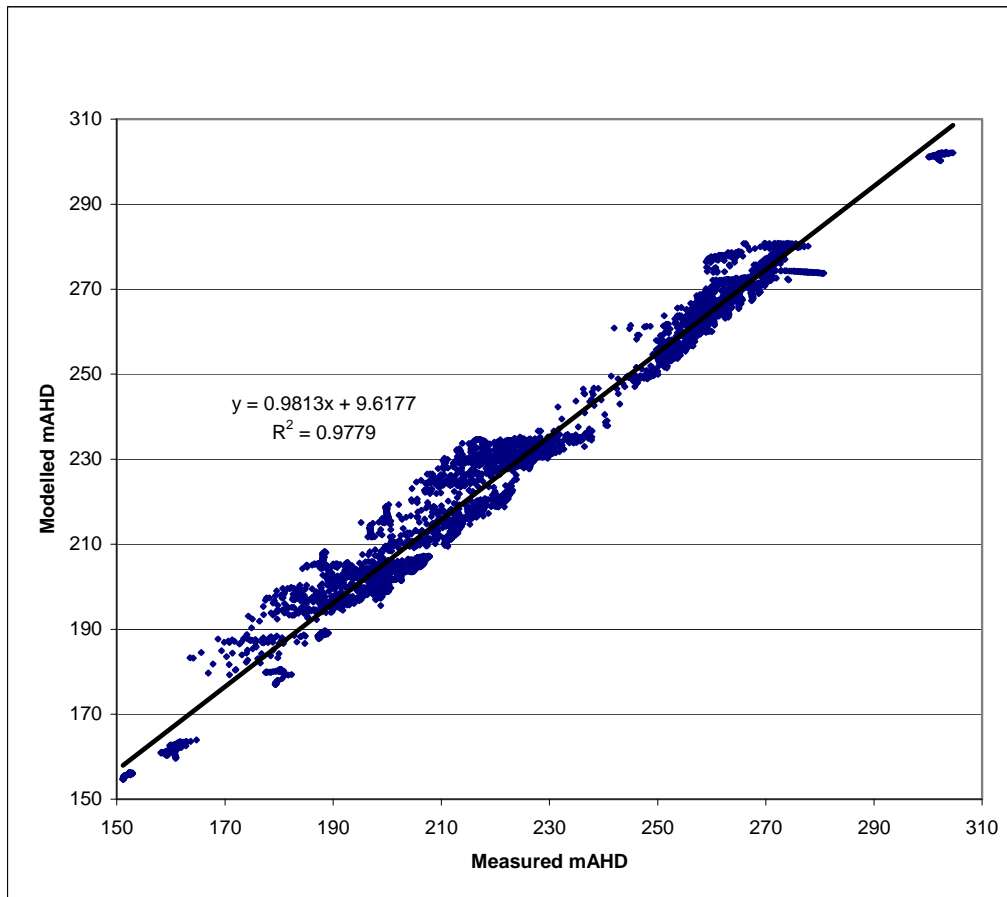
Figure 4-12 Layer 2 Scattergram of modelled versus measured heads and statistics results.



Sum of Squares (m**2)	SSQ =	176109.83	m**2
Mean Sum of Squares (m)	MSSQ =	23.43	m
Root Mean Square (m)	RMS =	4.84	m
Scaled Root Mean Square (%)	SRMS =	3.68	%
Root Mean Fraction Square (%)	RMFS =	2.29	%
Scaled Root Mean Fraction Square (%)	SRMFS =	3.84	%
Sum of Residuals (m)	SR =	24519.70	m
Mean Sum of Residuals (m)	MSR =	3.26	m
Scaled Mean Sum of Residuals (%)	SMSR =	2.48	%
Coefficient of Determination (tend to unity)	CD =	1.08	

The scattergram for layer 3 shown in Fig. 4-13 recorded a RMS of 7.16 meters for 5948 observation data points.

Figure 4-13 Layer 3 Scattergram of modelled versus measured heads and statistics results.

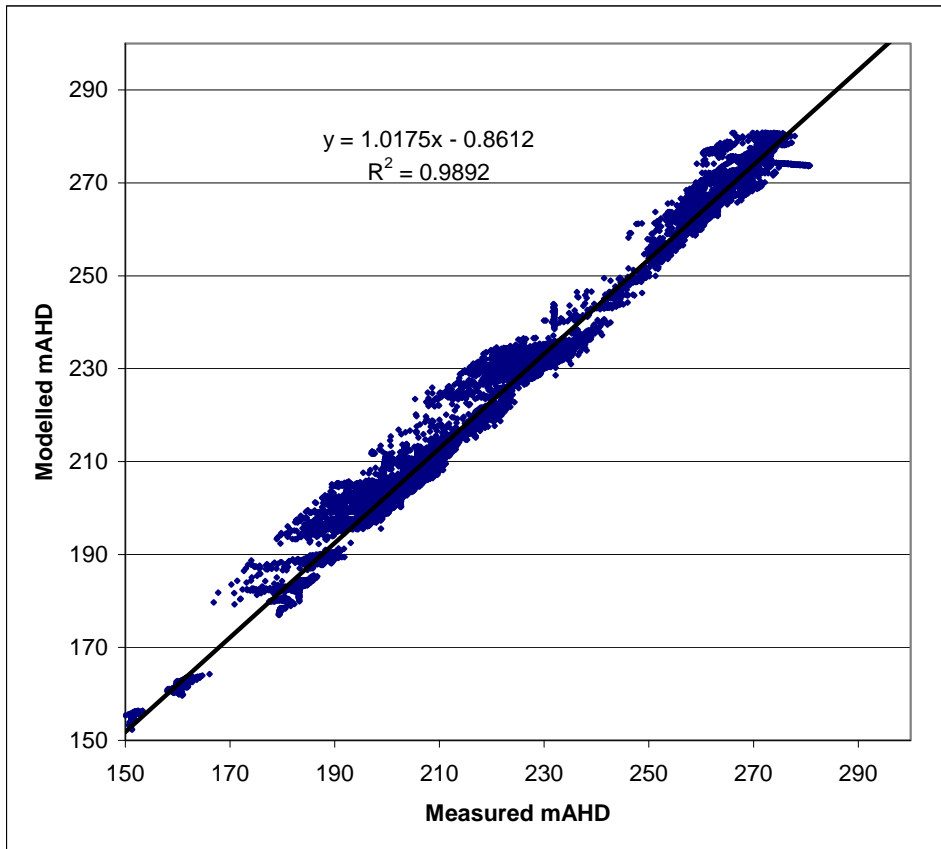


Sum of Squares (m**2)	SSQ =	304776.02	m**2
Mean Sum of Squares (m)	MSSQ =	51.24	m
Root Mean Square (m)	RMS =	7.16	m
Scaled Root Mean Square (%)	SRMS =	4.46	%
Root Mean Fraction Square (%)	RMFS =	1.84	%
Scaled Root Mean Fraction Square (%)	SRMFS =	2.58	%
Sum of Residuals (m)	SR =	14876.54	m
Mean Sum of Residuals (m)	MSR =	2.50	m
Scaled Mean Sum of Residuals (%)	SMSR =	1.56	%
Coefficient of Determination (tend to unity)	CD =	1.18	

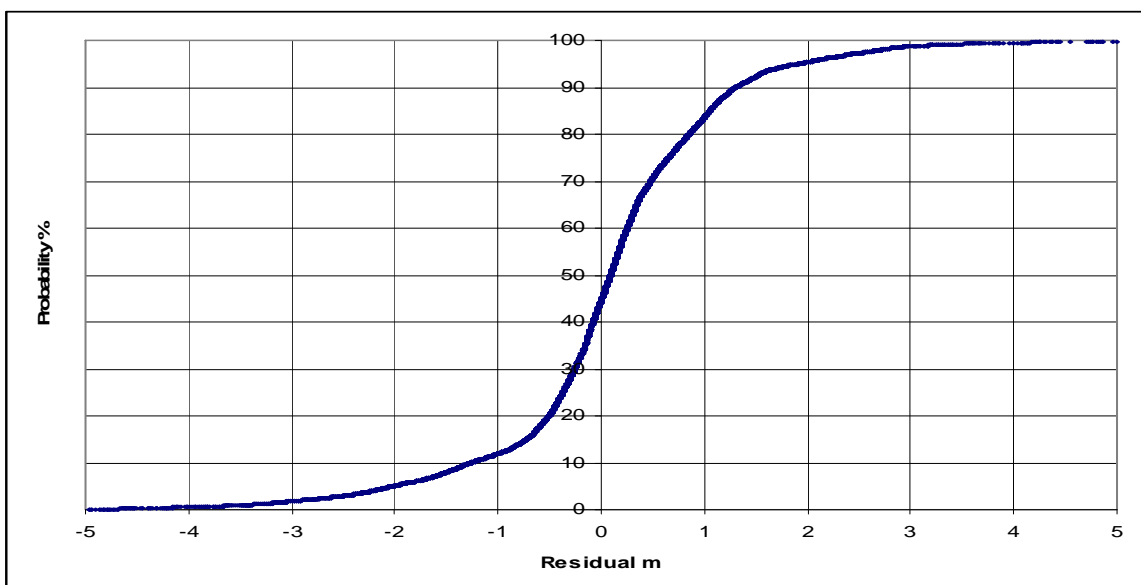
Figure 4-14 is a plot of the simulated heads versus the observed heads for all observations in all layers over the calibration period. RMS of 5.45 m, scaled RMS of 3.4% and sum of mean residual values of 2.10 m for a total of 16836 observation data points indicates reasonably good calibration performance. Middlemis et al. (2001) suggested a criterion of about 5% for the scaled RMS to be regarded as a well calibrated model. A correlation coefficient of 0.9892 (nearly 1) also indicates a strong relationship between the simulated and the observed heads.

Second plot presents the distribution of residuals (the difference between observed and simulated head) in all layers. A positive residual indicates an underestimate by the model where as a negative residual is an overestimate. The plot indicates overall that the model slightly over estimates the water levels over the model domain. In summary 70% of simulated heads in all layers are within 1 metre of the corresponding observed water levels.

Figure 4-14 All Layers calibration assessment: scattergram of modelled versus measured heads, statistics and distribution of residuals results.



Sum of Squares (m**2)	SSQ =	493671	m**2
Mean Sum of Squares (m)	MSSQ =	29.67	m
Root Mean Square (m)	RMS =	5.45	m
Scale Root Mean Square (%)	SRMS =	3.40	%
Root Mean Fraction Square (%)	RMFS =	2.08	%
Scaled Root Mean Fraction Square (%)	SRMFS =	2.88	%
Sum of Residuals (m)	SR =	34976.63	m
Mean Sum of Residuals (m)	MSR =	2.10	m
Scaled Mean Sum of Residuals (%)	SMSR =	1.31	%



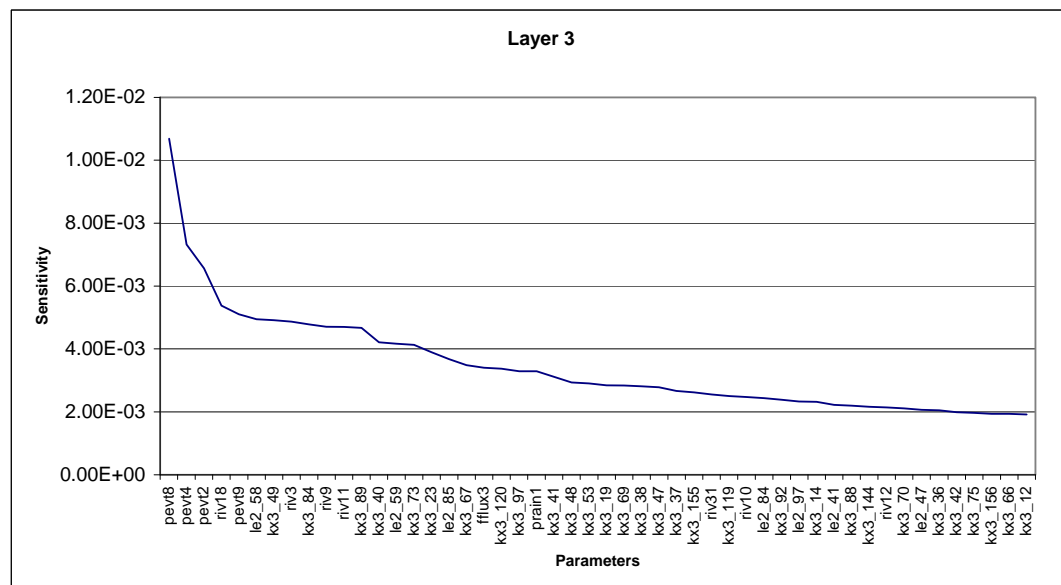
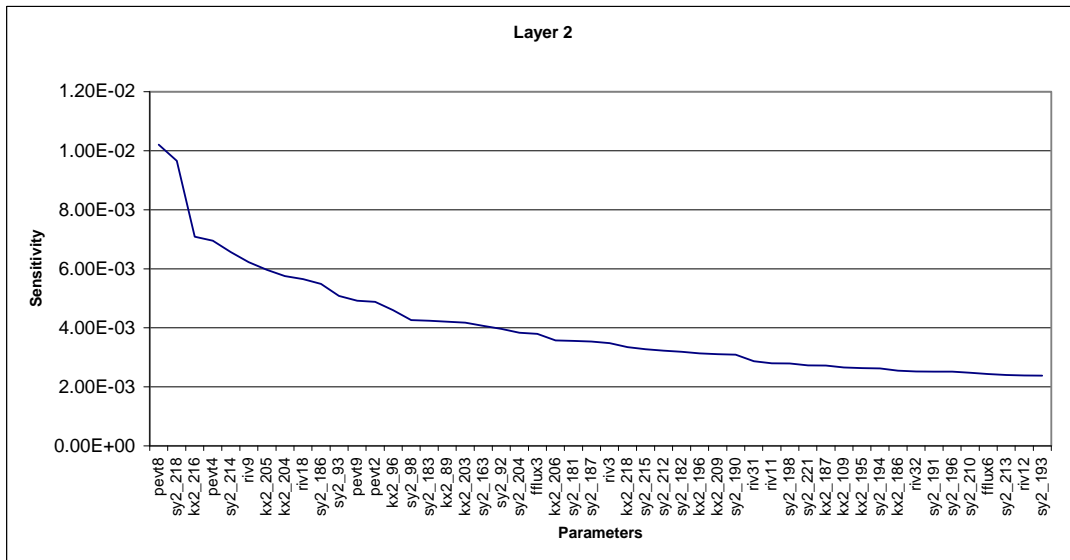
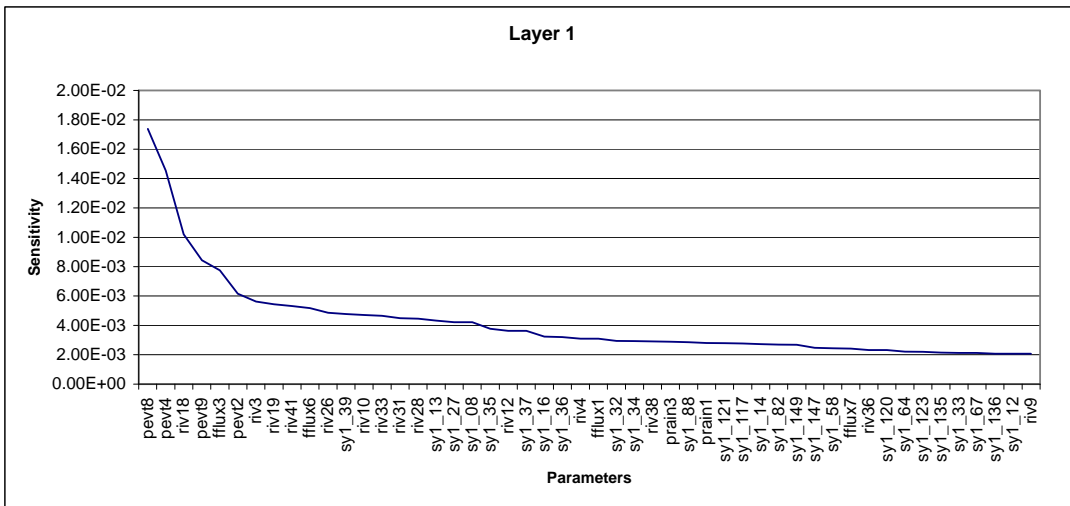
4.5 Sensitivity analysis

.A product of the use of PEST is a table of parameter sensitivity values that provides a guide to the relative extent to which each model adjustable parameter affects the simulated groundwater levels. The most sensitive parameters make a significant contribution to the behaviour of the model while those that are least sensitive contribute very little and have a wide range of acceptable values. The parameter sensitivities that PEST provides are not absolute measures. They vary, depending on the parameter combinations used. Nevertheless, they provide a very useful guide to the relative importance of the adjustable model parameters.

Figure 4-15 shows a plot of parameter sensitivities provided by PEST for the parameter set chosen to represent the calibrated model. Because of the large number of adjustable model parameters, only the 50 most sensitive parameters are represented for each layer in the diagram.

Evapotranspiration parameters are the most sensitive and river, hydraulic conductivity specific yield and flood seem to have a moderate influence on model outcomes. Storage coefficient is the least sensitive of model parameters

Figure 4-15 Adjustable Model Parameter Sensitivities



4.6 Water balance

The water balances presented in this chapter are based on the most recent calibration run which spans the 22 years from July 1986 to June 2008 and they pertain to the whole of the model area is shown in Figure 2.7. Figure 4-16 presents a summary of water balance components for the calibrated model showing annual volumes averaged over the 22 year calibration period.

Figure 4-16 Model Water Balance Summary for July 1986 to June 2008

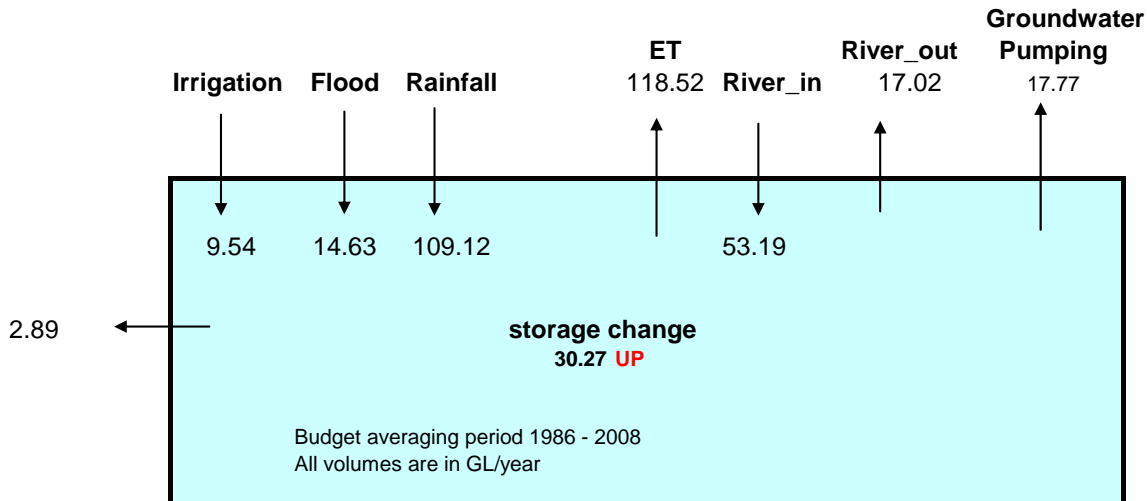


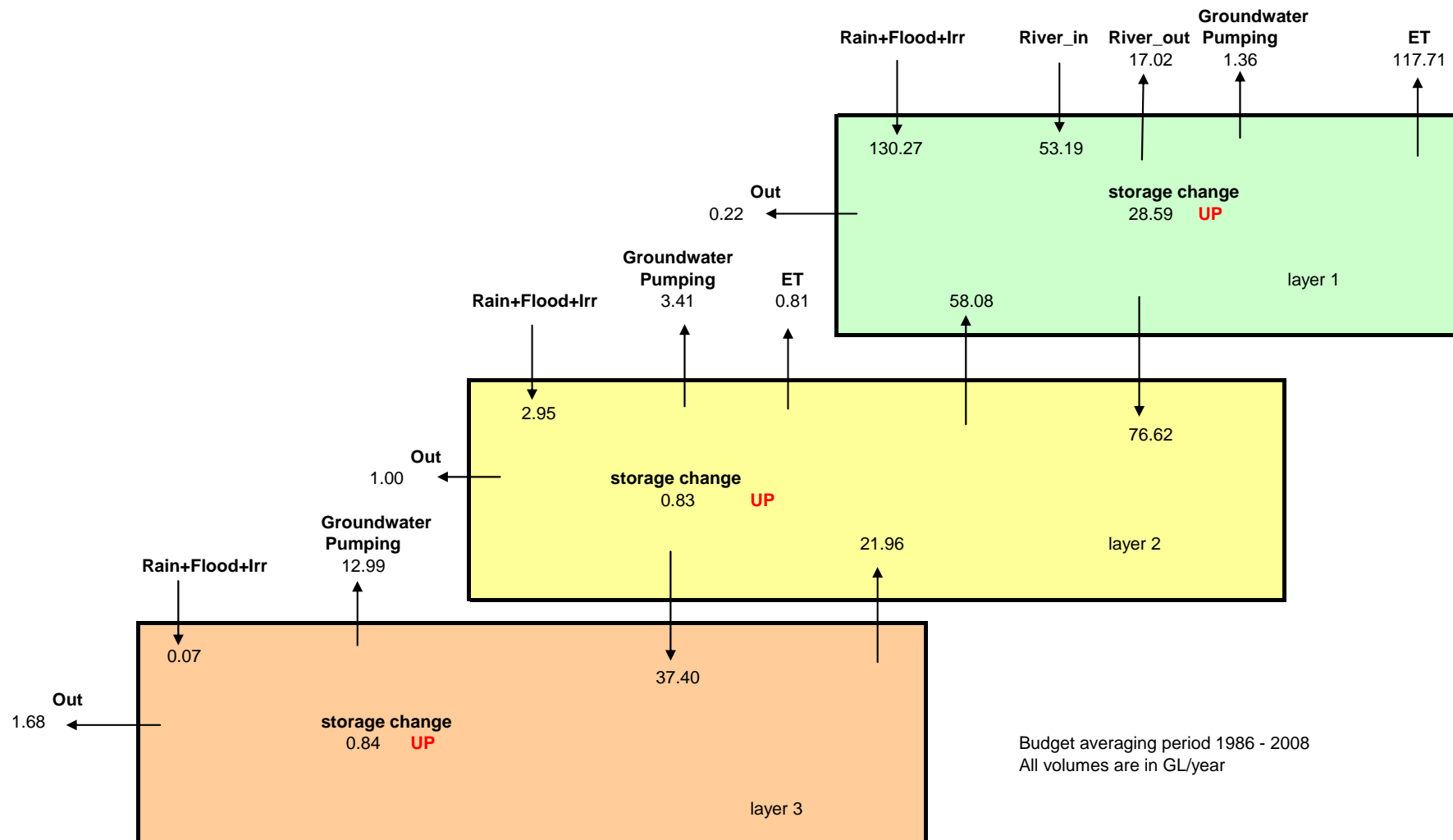
Figure 4-16 summarises the amount of water being transferred into and out of storage by stresses such as rainfall, irrigation, river, flood, evapotranspiration, boundary flows and extraction.

The annual average total recharge from all sources in the calibration period is 186.47 GL. This figure represents a summation of contributions from rainfall recharge, river, flood, irrigation, evapotranspiration and lateral flow. The average rainfall recharge is about 58.5 % of the total recharge. River, flood and irrigation recharge contributions relative to total recharge are 28.5%, 7.8% and 5.2%, respectively.

The total annual average outflow in the GWMA 011 is 156.20 (118.52+17.02+17.77+2.89) GL. The evapotranspiration is about 75.8% of this total while the groundwater abstraction makes up 11.4%. River and lateral flow contributions relative to total outflow are 10.9% and 1.9%, respectively. Evaporation is the dominant discharge source over the calibration period.

Figure 4-17 provides a breakdown of a water budget on a layer basis. The groundwater usage figures averaged over the 22 years are deceptive since heavy pumping started after 2000.

Figure 4-17 Average Annual water balance for individual layers for July 1986 to June 2008



It is important to realise that the recharge calculated is distributed over the entire model area which may not occur in practice in certain area thus the aquifer system cannot cope with high rates of groundwater extraction (even if they are consistent with recognised sustainable yield). This has direct implications for the area of high yielding bores around Forbes and Cowra.

5. Scenario runs

An objective of the groundwater flow model was to generate various scenarios for aquifer management purposes. 'Dry', 'wet' and 'medium' scenarios were formulated to examine the aquifer behaviour under "no pumping", "current development" and "entitlements" conditions. It is hoped that the results of these scenarios will aid in the formulation of an appropriate aquifer management strategy for the Upper Lachlan Aquifer system.

The selection of 'dry', 'wet' and 'medium' conditions is based on the historical rainfall pattern going back about 100 years. These data sets identified as C_{dry} , C_{wet} and C_{med} were supplied by CSIRO. Each set of climate data was used to prepare relevant MODFLOW recharge and evapotranspiration packages.

For the MODFLOW river package, Integrated Quantity and Quality Model (IQQM) model generated monthly flow data for the chosen period were converted to corresponding monthly river stage at gauging stations along the Lachlan River, Belubula River, Goobank Creek and Back Creek for each climatic variation (C_{dry} , C_{wet} and C_{med}).

For the 'wet' scenario five flood events were applied over the 100 year period, based on exceedance of the river stage height of 5.7 metres at the gauging stations 412004 and 412002 in Figure 3-11. With the same criterion, three flood events were applied for the 'dry' and 'med' climatic variations. Floods were applied over the area inundated by the 1990 flood.

Irrigation recharge was maintained at the 2000/2001 level in the absence of any other irrigated area spatial distribution data.

Heads at outflow CHD boundaries were fixed at long-term average values.

The three different climatic variation scenarios were run for three different groundwater extraction limits: 'no pumping', 'current development' and 'maximum allocation'. The combination of three climate scenarios and three pumping scenarios yielded nine scenarios in total.

The 'no pumping scenario' represents the natural condition where zero pumping occurs. The 'current development scenario' corresponds to the 2006-2007 water year in which the highest groundwater usage (84.6 GL) was recorded. These data sets were applied from the end of the calibration period to June 2108. In order to assess the current development situation. The 'entitlements' scenario corresponds to the maximum allocation limit of 174.6 GL/year. These data were recycled 100 times to allow simulation to year 2108.

All nine scenarios ('dry_no pumping', 'dry_current development', 'dry_maximum allocation', 'wet_no pumping', 'wet_current development', 'wet_maximum allocation', 'med_no pumping', 'med_current development' and 'med_maximum allocation') were applied from the end of the calibration period (July 2008), finishing at June, 2108.

5.1 Scenario water balance

Scenario results are provided in Figures 5-1 to 5-3. These diagrams show water balance components (GL/yr) averaged over the 100 year period.

The major differences in the dry, wet and medium scenarios relate to groundwater pumping.

Comparison of the 'dry_current development' with 'dry_maximum allocation' scenario result show river leakage is greater by 5 GL/yr and evapotranspiration deplete from 138 to 120 GL/yr. The 'dry_no pumping' scenario shows that evapotranspiration was increased to 171 GL/yr and net river leakage decreased from 100 GL/yr to 62 GL/yr (Figure 5.1). For the wet scenario recharge (rainfall+flood+irrigation) is 146 and net river leakage is 106 GL/yr in wet_max_allocation scenario,

however in the wet current development river net leakage declined to 101 and evapotranspiration rose up to 178 GL/yr. Wet no pumping scenario net river leakage is 67 GL/yr in Figure 5.2.

These illustrate that if there was no pumping in the region, water levels would have risen causing river leakage to decrease and evapotranspiration to increase. If there was high pumping, water level would have depleted causing evapotranspiration to decrease and river leakage to increase.

Evapotranspiration is the dominant discharge process over each scenario run.

In the early stages of each scenario run, it was noted that some of the bores failed to maintain the pumping rates specified in the model and as a result of those pumping locations became dry (as shown in Figures 5-4 to 5-6). Water levels in these areas can exhibit gradually declining trends. In the dry, wet and med scenarios with the maximum allocation, the groundwater system reaches a new equilibrium after year 55 and the system maintains groundwater pumping rates at approximately 96-99 GL/yr.

Net river leakages over the one hundred year period from 1895 to 1995 in each scenario are shown in Figure 5-7 to 5-9. As expected river leakage increases with pumping in all three scenarios.

Figure 5-1 Average Annual water balance over dry scenario run June 2008 to July 2108

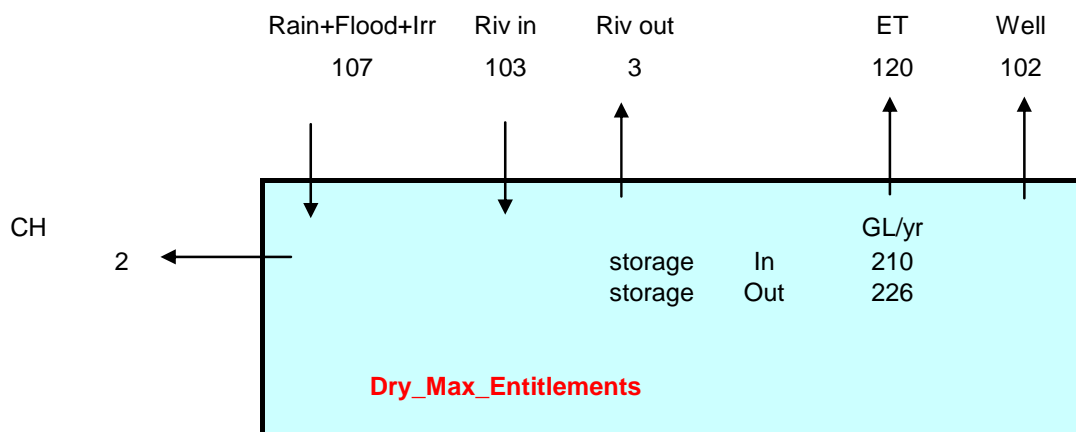
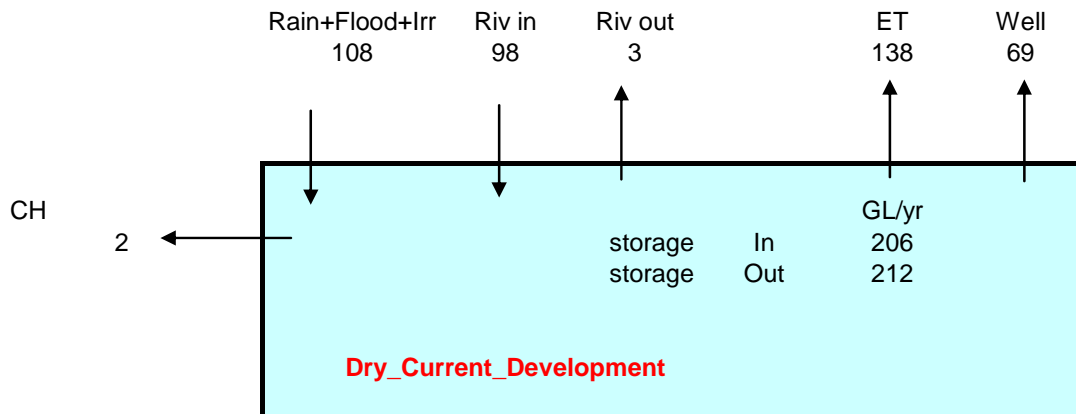
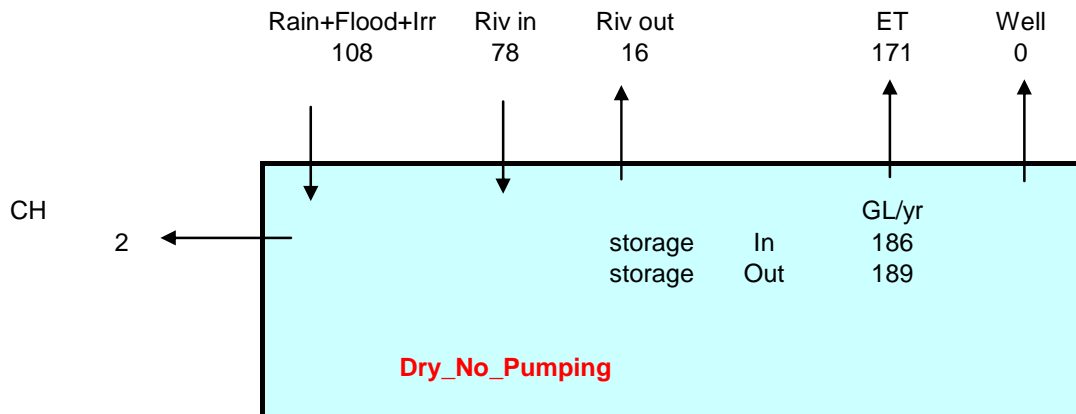


Figure 5-2 Average Annual water balance over medium scenario run June 2008 to July 2108

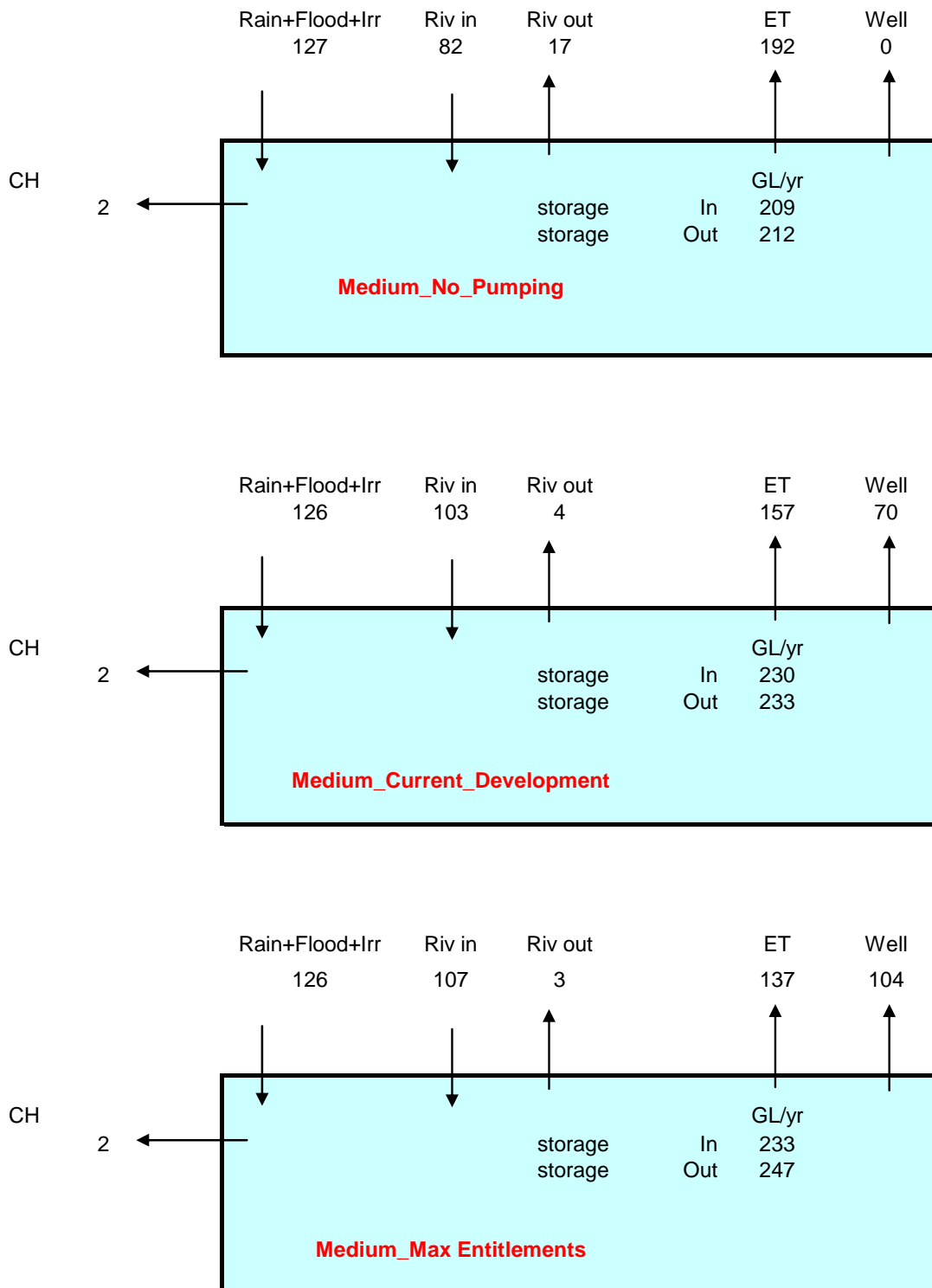


Figure 5-3 Average Annual water balance over wet scenario run June 2008 to July 2108

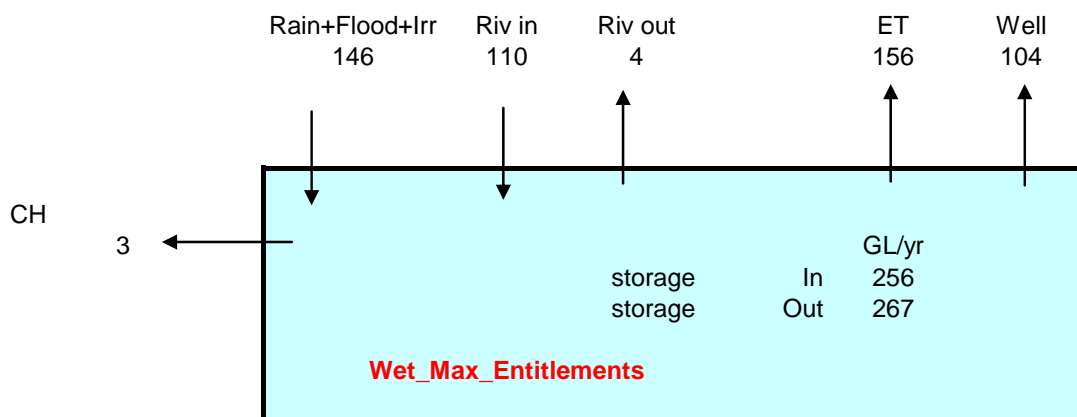
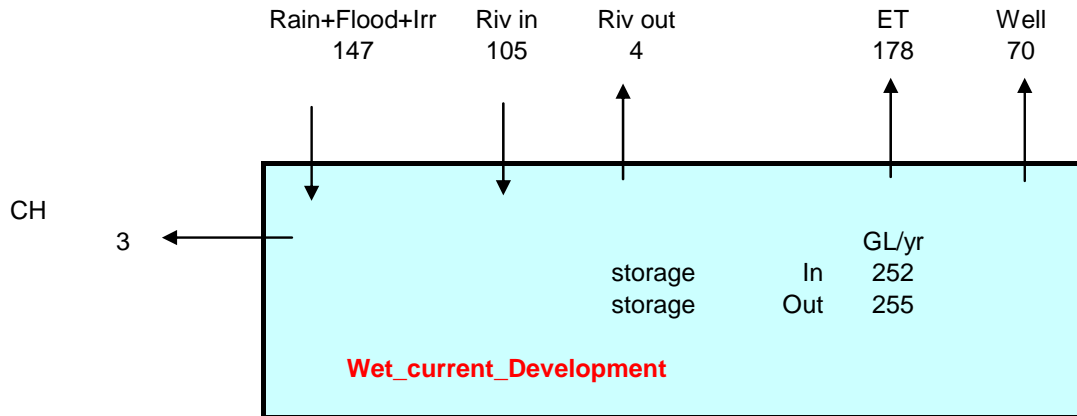
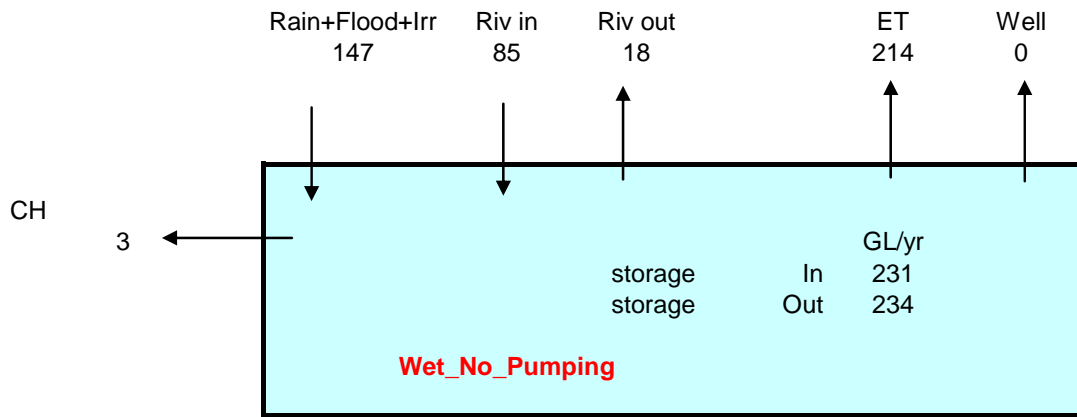


Figure 5-4 Dry Scenario yearly groundwater extractions over the 100 year simulation

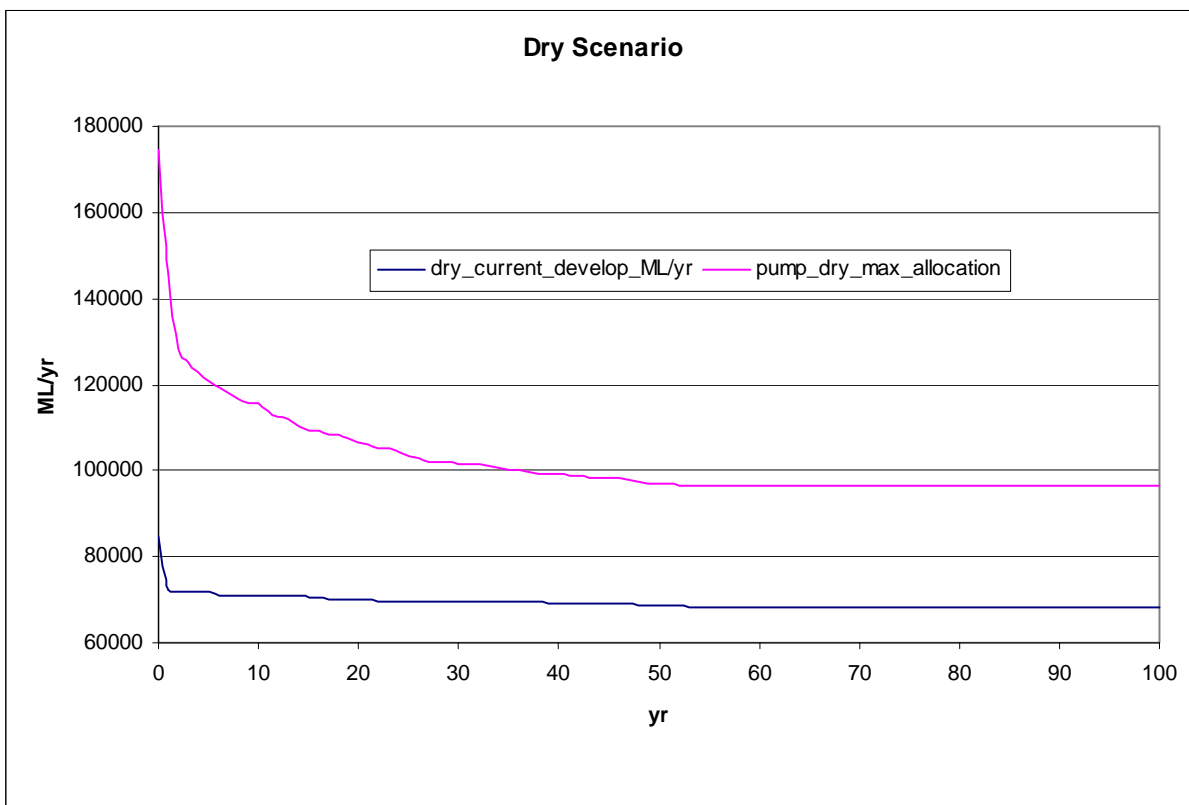


Figure 5-5 Med Scenario yearly groundwater extractions over the 100 year simulation

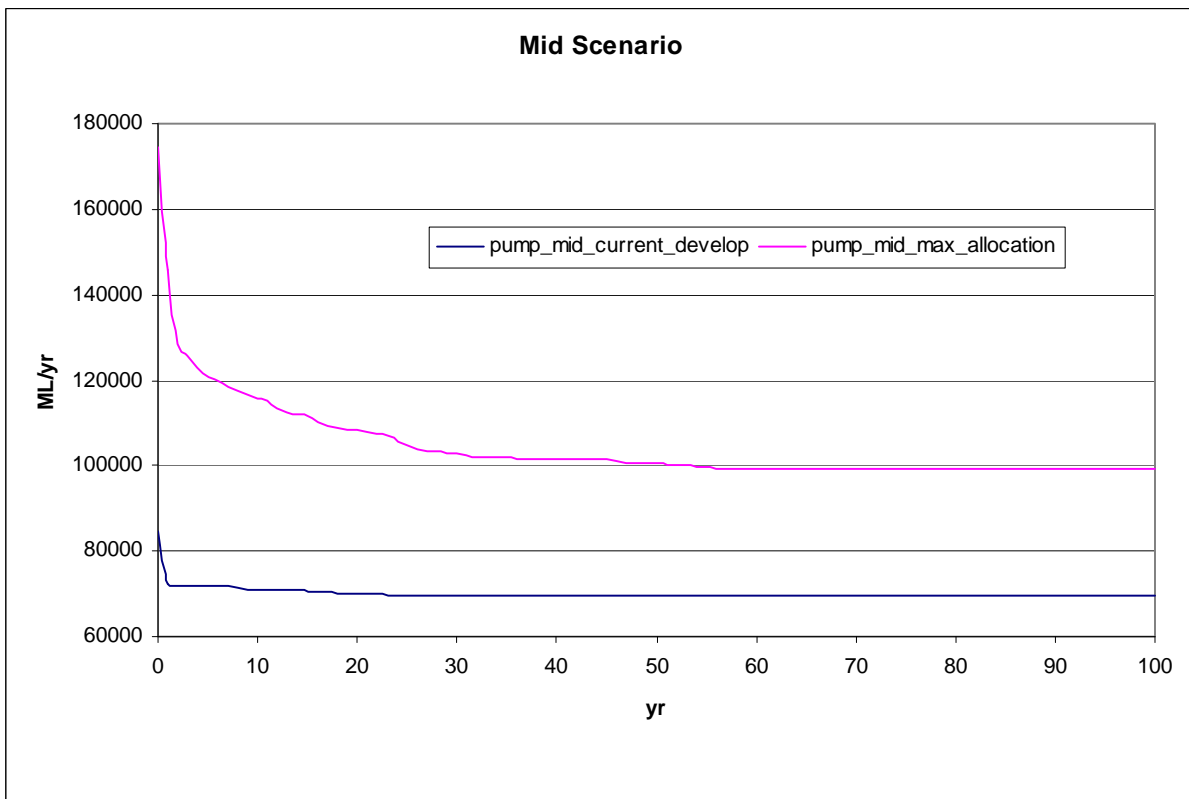


Figure 5-6 Wet Scenario yearly groundwater extractions over the 100 year simulation

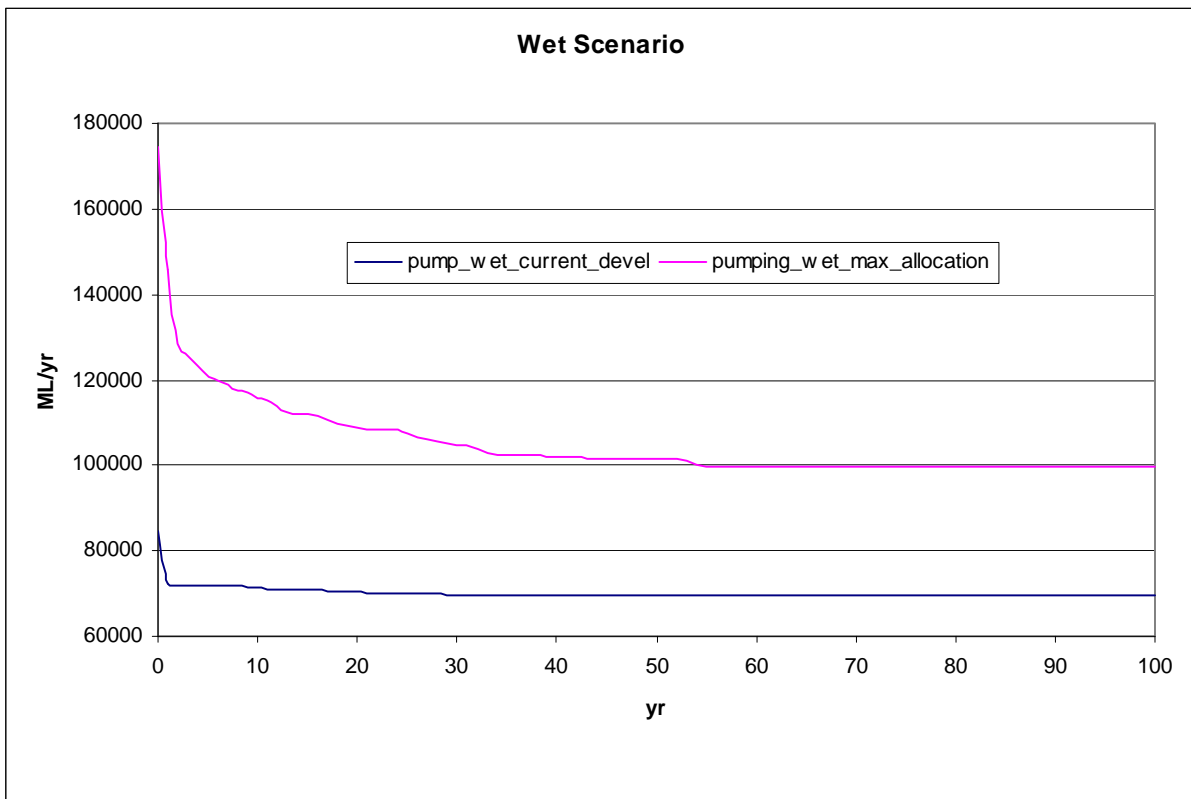


Figure 5-7 Dry Scenario yearly net river leakage over the 100 year simulation

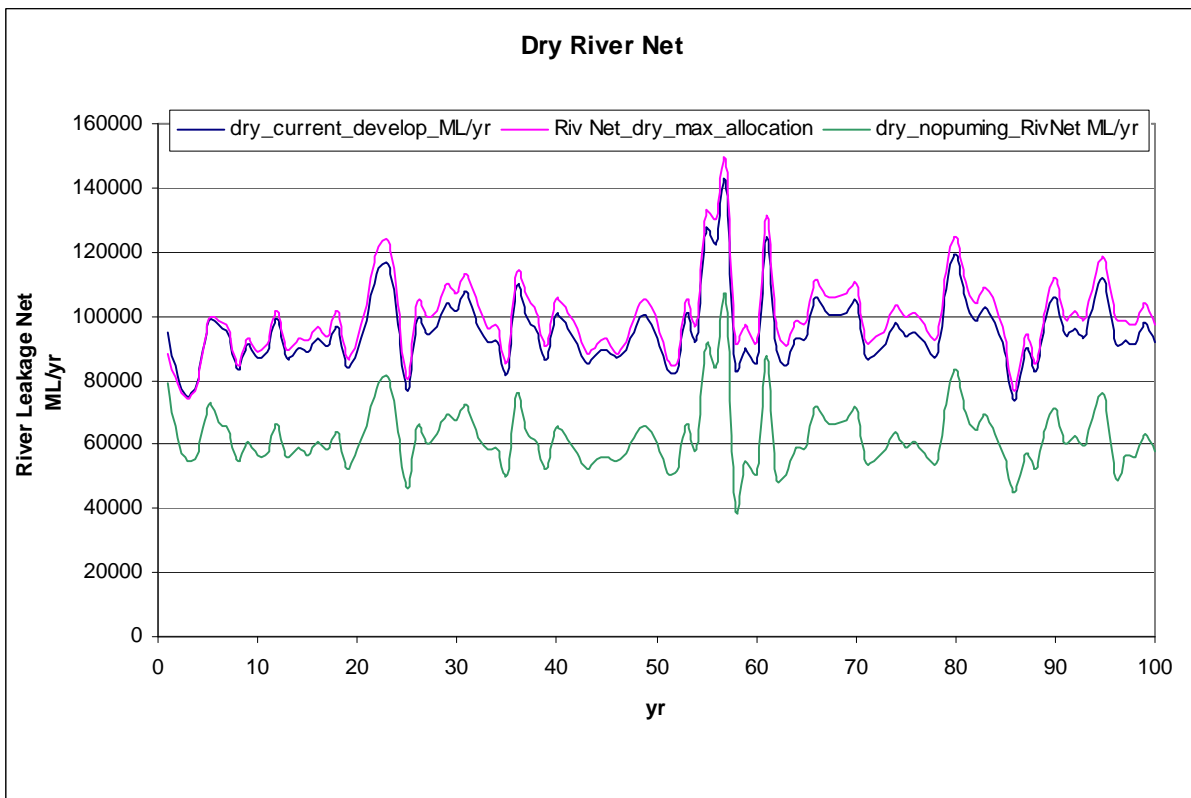


Figure 5-8 Mid Scenario yearly net river leakage over the 100 year simulation

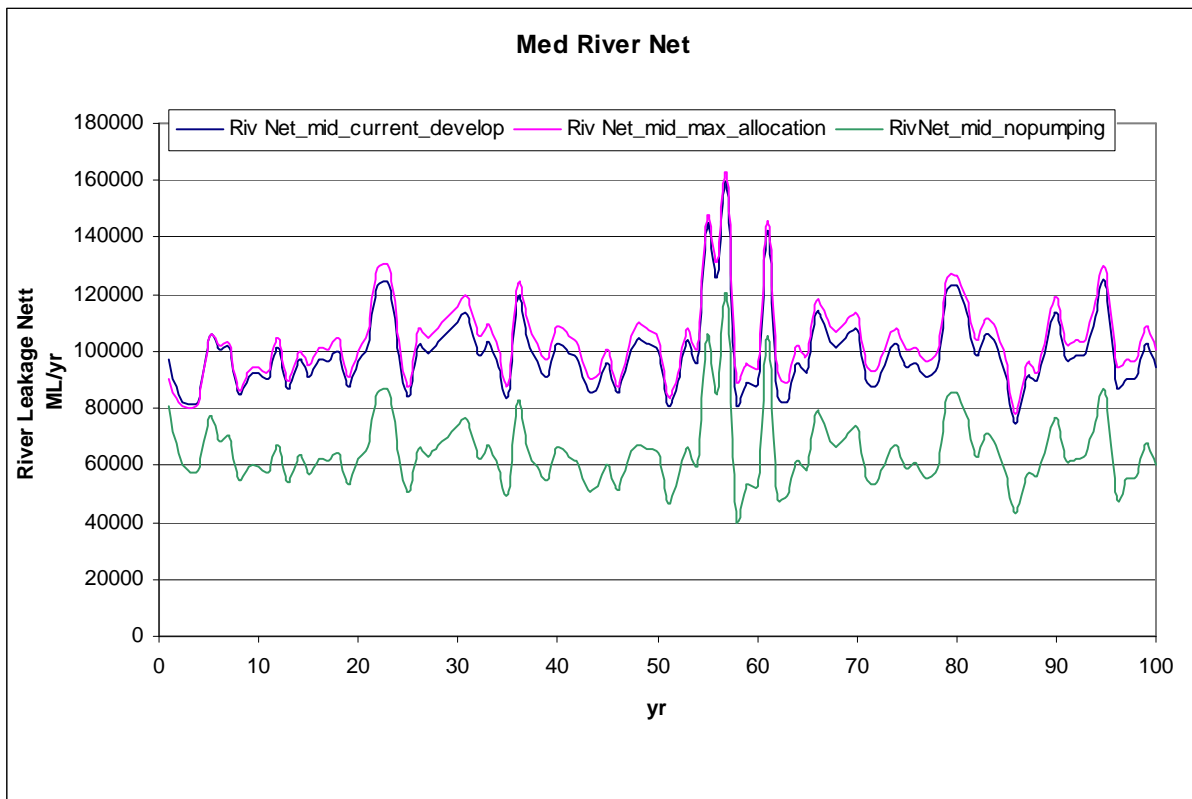
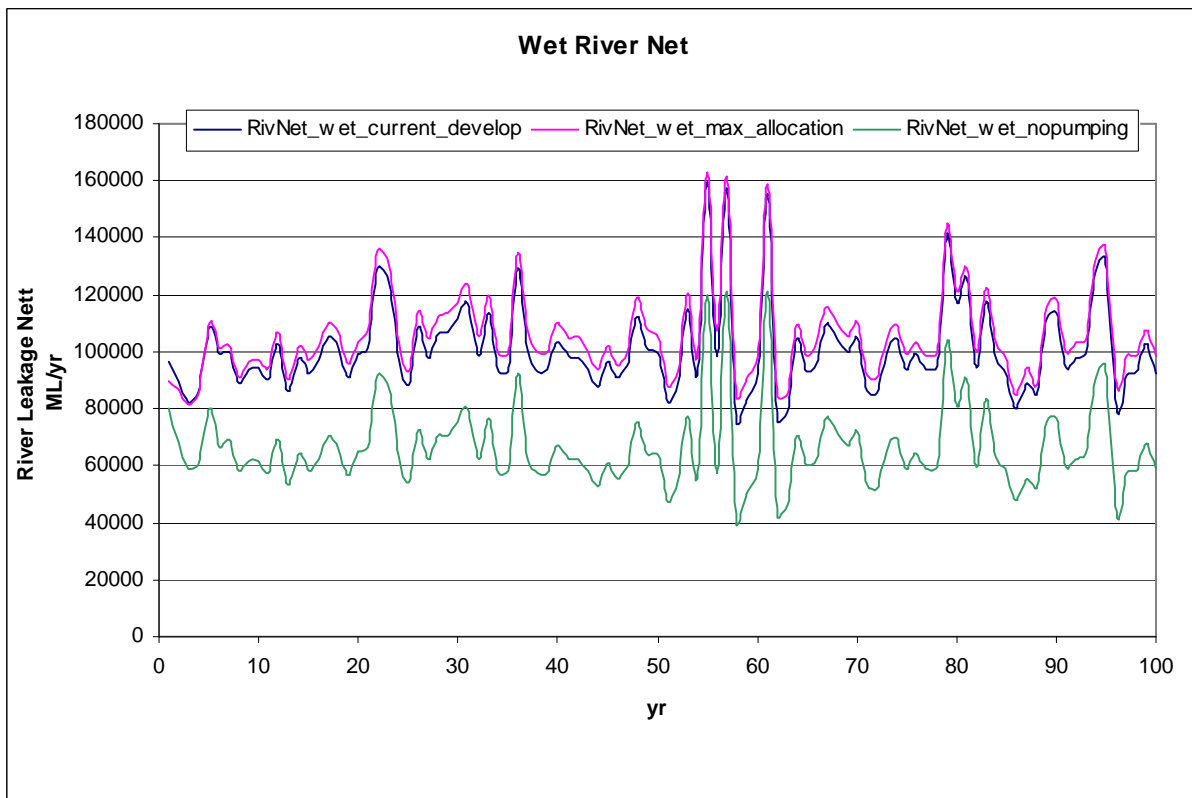


Figure 5-9 Wet Scenario yearly net river leakage over the 100 year simulation



6. Conclusions and recommendations

A groundwater flow model for the Upper Lachlan Valley has been developed to improve the understanding of the regional flow system, assess the quantity of water within the system and the amount of recharge to the aquifer and to evaluate the impact of climate change on the water balance for the regional aquifers within the valley.

The model was developed using MODFLOW (McDonald and Harbaugh, 1988) with a non uniform grid for this study. Grid cell dimensions vary from 500 m in the vicinity of the Lachlan River and increase progressively to 2000 m at distance from the river to the north and south. The model grid is rotated 20 degrees anti clockwise. The model calibration period is July 1986 to June 2008. The model consists of four layers that correspond to each of the major aquifers:

Layer 1: the unconfined Upper Cowra

Layer 2: the confined/unconfined Lower Cowra

Layer 3 the confined/unconfined Lachlan Formation

Layer 4 the confined/unconfined fractured rock (inactive layer)

The groundwater flow model identified the main recharge components as rainfall recharge, river leakage, flood recharge and irrigation recharge, whilst evapotranspiration is the major discharge component followed by groundwater usage. The aquifer outflow is to the west.

Non linear parameter estimation (PEST) was used to aid calibration of the model based on water levels from observation bores. Assessment of the model's performance, based on comparison between observed and simulated groundwater levels for the entire calibration period, indicates that, for all model layers, a good match was generally achieved except in zone 7. Low SRMS (scaled root mean square) values (less than 5%) were achieved for all three layers which confirm that the model is well calibrated.

This groundwater model simulates monthly stress periods and requires usage data at a monthly frequency. However from 1998 onwards groundwater usage data in the model have only annual frequency. There is little usage data available prior to 1998. This shortcoming in the groundwater usage data set constrained the model calibration in some cases.

The water balance summary for the 22 year period of the model (July 1986 to June 2008) shows an annual average total recharge of 186.48GL. This figure represents an average over the model spatial domain and calibration period. It is not representative of recent conditions and takes no account of spatial variability. In practice, pumping is concentrated in small areas and has increased significantly in recent years. This pattern of usage is likely to affect local water levels and may diminish local extraction potential unless sufficient recovery occurs. The model will be of value in investigate local usage scenarios. The total annual average outflow is 156.30 GL. The evapotranspiration is about 76% of this total. Therefore evapotranspiration is the dominant output over the calibration period.

Three climate scenarios (dry, wet and med) were undertaken to evaluate the aquifer's response to different levels of groundwater pumping. The 'no pumping scenario' water budget revealed the likelihood of rising water levels, reduced river leakage and increased evapotranspiration in the absence of pumping for all climatic scenarios. The increased pumping scenario showed, water level depleted causing evapotranspiration to decrease and river leakage to increase in all scenarios.

It is recommended in future attempts to revise this model the following aspects are given consideration:

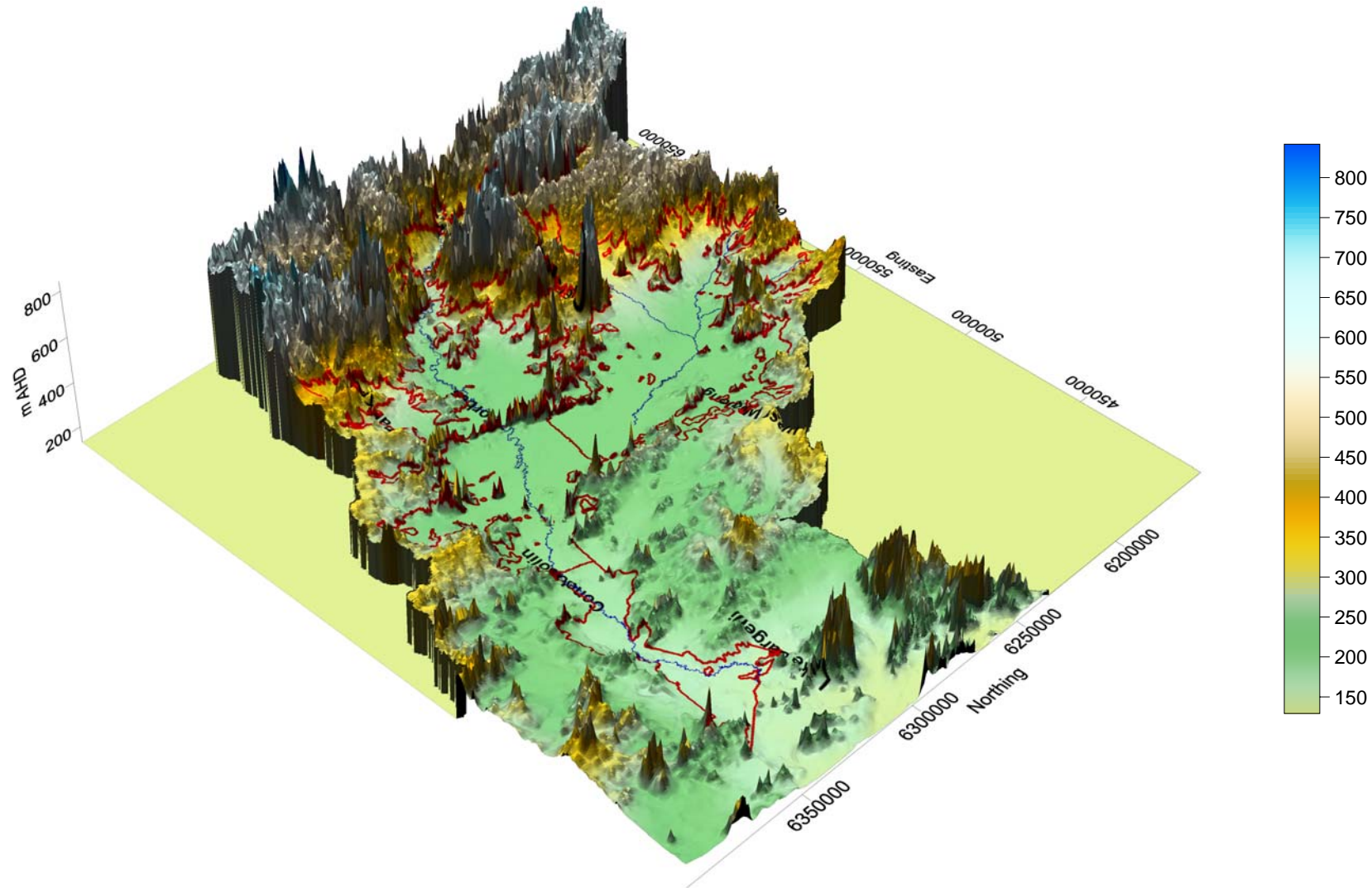
- Poor calibration of bores in Zone 7 is attributed to the complexity of the groundwater system in this area. More geological investigations are needed to obtain a proper understanding of the hydrogeological framework of the area.
- Review the hydrogeological framework of the alluvial's in zone 1 and 2.
- Independent studies of the groundwater recharge process (for example, hydrochemical characterisation) could enhance calibration of the groundwater model particularly Zone 1, 2 and 7.
- Annual monitoring of groundwater production bores constrains the integrity of groundwater usage data. The requirement for monthly usage data for groundwater modelling purposes necessitates assumptions regarding temporal distribution of production. Therefore, it is recommended that, particularly in critical areas of groundwater usage, selected landholders be requested to provide monthly meter readings of production with additional data such as pumping on/off times and a log of associated management decisions.
- Some discrepancies between observed bore data and corresponding model-simulated data are attributed to the likelihood that a few existing groundwater extraction sites are not represented in the model. Future model enhancement should seek to assess the veracity of this suspected cause.
- Improved estimate of irrigation recharge based on landuse, crop patterns and combined usage of surface and groundwater.
- Verification of this model has not been undertaken. Since almost all suitable observation data sets were used to calibrate this model, spatial verification is not possible. However, temporal verification remains an available option at a future time since over two years of observation data have accumulated since the end of the calibration period of this model.

7. References

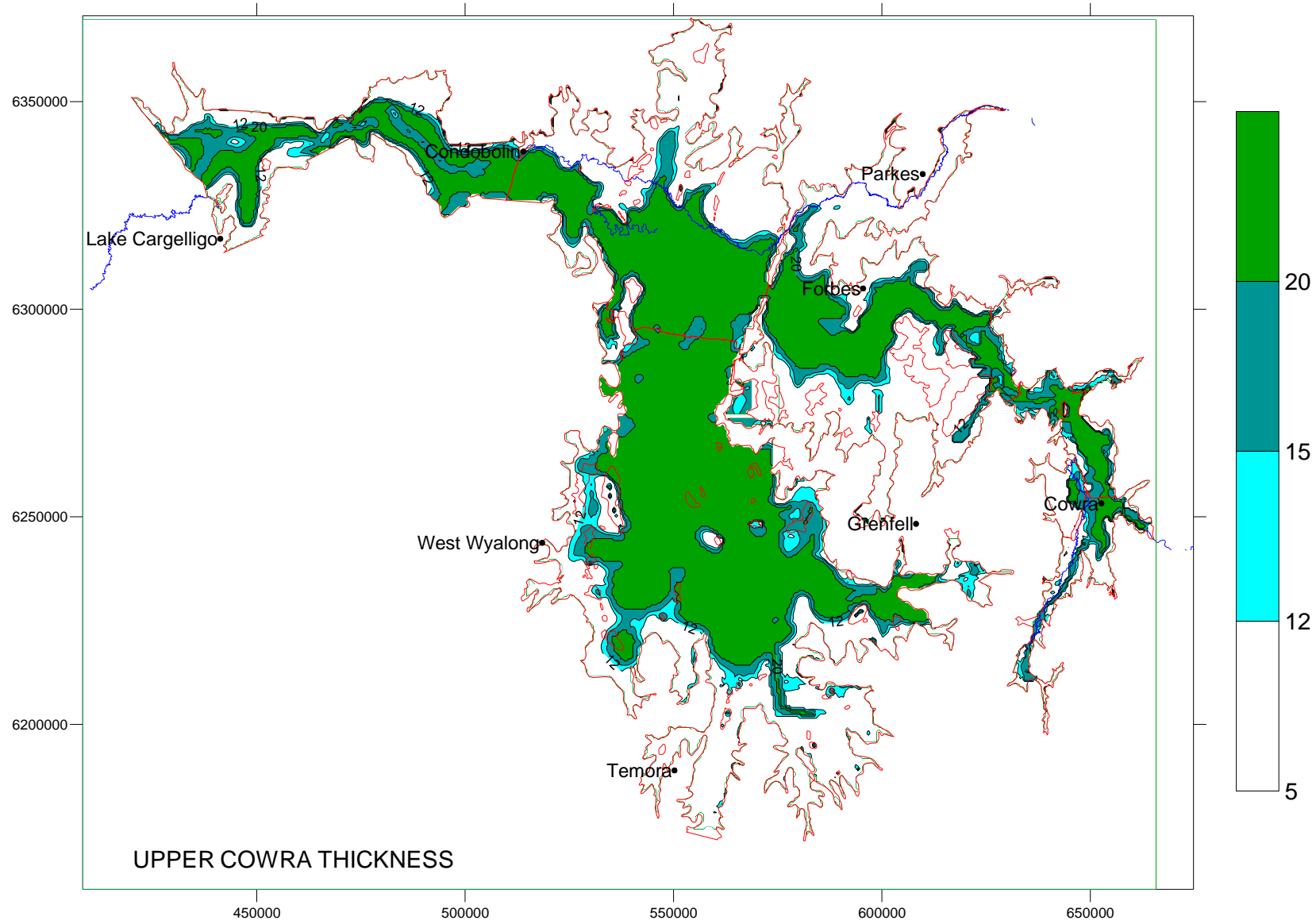
- Anderson, J., Gates, G., and Mount, T.J., 1993. Hydrogeology of the Jemalong and Wyldes Plains Irrigation Districts, NSW Department of Water Resources.
- Barnett, B.G and Muller, J., 2008. Upper Lachlan Groundwater Model calibration Report Draft, SKM
- Bilge, H., 2001, *Lower Gwydir Valley Groundwater Model*, CNR, Department of Land and Water Conservation
- Bilge, H., 2007, *Lower Macquarie Groundwater Flow Model*, Water Management Division, Department of Water and Energy
- Bish, S. and Gates, G., 1991. Groundwater reconnaissance survey: Forbes – Condobolin-Lake Cargelligo, NSW Dept. Water Resources, T.S.91.033.
- Chiang, W. H. and W. Kinzelbach. 1996. *Processing Modflow (PM)*, Pre- and postprocessors for the simulation of flow and contaminant transport in groundwater system with MODFLOW.
- Coffey 2006. Cowal Gold Mine Groundwater Supply Modelling Study Model Calibration, Coffey Geosciences Pty. Ltd. S21910/02
- Dawes WR, Stauffacher M. and Walker GR. 2000. Calibration of Modelling of groundwater process in the Liverpool Plains. CSIRO Land and Water Technical report 5/00. February
- Demetriou, C., 1995b, *Computer program VMRIVER - pre-processor for time varying river in MODFLOW Format*, CNR, Department of Land and Water Conservation.
- Doherty, J., 2005, *PEST Model-Independent Parameter Estimation User Manual (5th edition)*.
- DWR. 1994. Review of Groundwater Use and Water Level Behaviour in the Upper Lachlan Valley 1986-1994, Status Report No. 2. Department of Water Resources Technical Services Division TS 94.078 authored by S Bish and R.M Williams Hydrogeology Unit.
- Gates, G.W.B and Williams, R.M., 1988. Dryland salinity study: Changes in groundwater levels southeast NSW, NSW Dept. Water Resources, T.S. 88.010.
- McDonald, M.G and Harbaugh A.W., 1988, *A modular three- dimensional finite difference groundwater flow model*. U.S. Geological Survey, Reston, Virginia.
- Megalla, M.N and Kalf F.R.P., 1973. buried Channel of the Lachlan from Cowra to Forbes, NSW, Water Conservation and Irrigation Commission NSW
- Merrick, N.P. 1989, *Lower Namoi Valley Groundwater Model*. Department of Water Resources, Heritage Computing.
- Murray Basin Hydrogeological Map Series CARGELLIGO scale 1:250 000
- Middlemis, H., Merrick, N. P. & Ross, J. 2001, *Groundwater flow modelling guideline*, Aquaterra Consulting Pty Ltd Report for Murray Darling Basin Commission, Project no. 125, January 2001.
- Muller, R. and Lennox, G., 1999. Review of Groundwater trends in the Lachlan Valley Upstream of Lake Cargelligo, Central West Region CW GWS 99/1
- O'Rourke, M., 2007. Upper Lachlan Groundwater Source Status Report 2007.
- Salotti, D., 1997, Borambil Creek Groundwater Model. Department of Land of Water Conservation.

APPENDIX 1: Model geometry

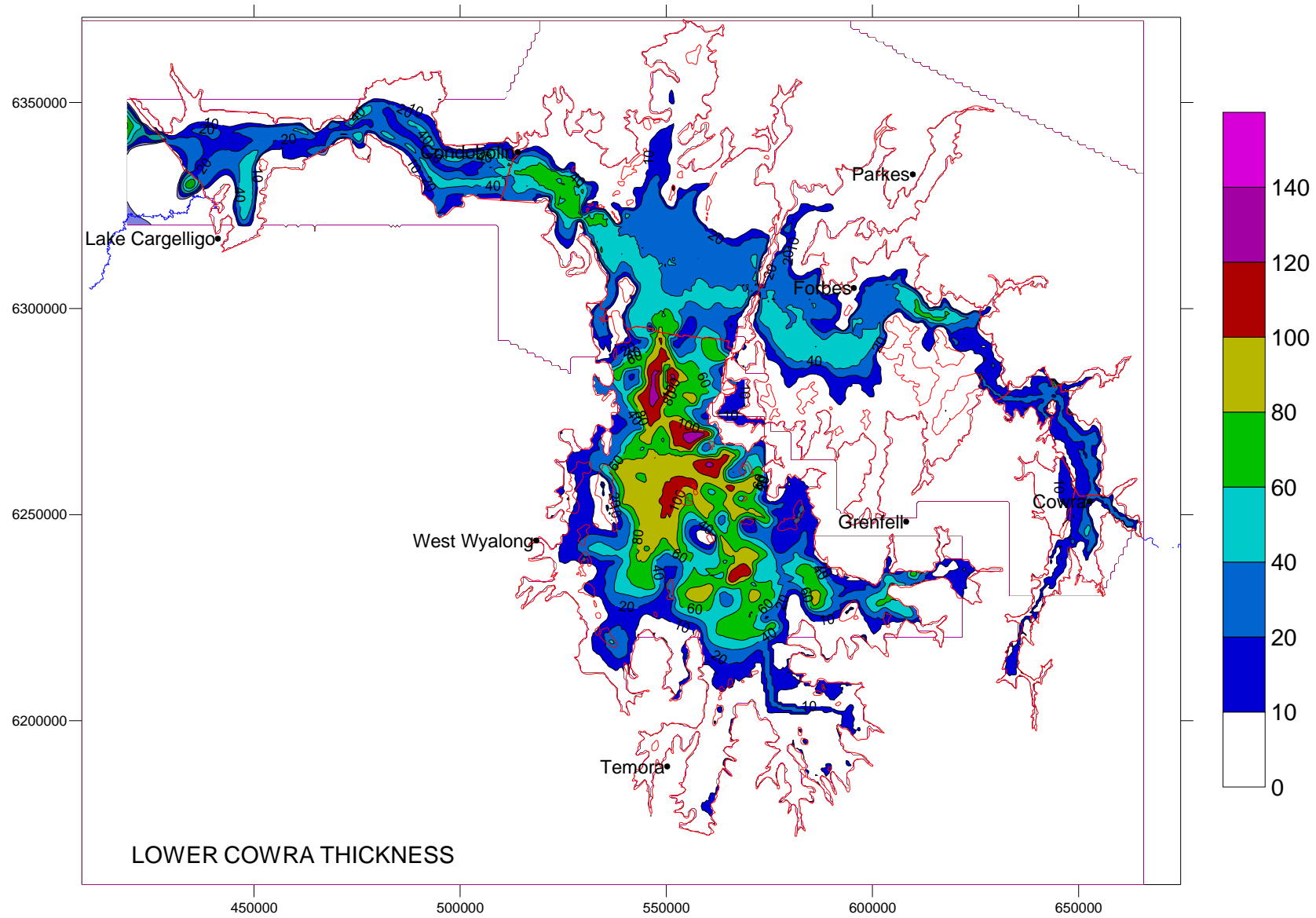
Ground Surface Elevation (m AHD)



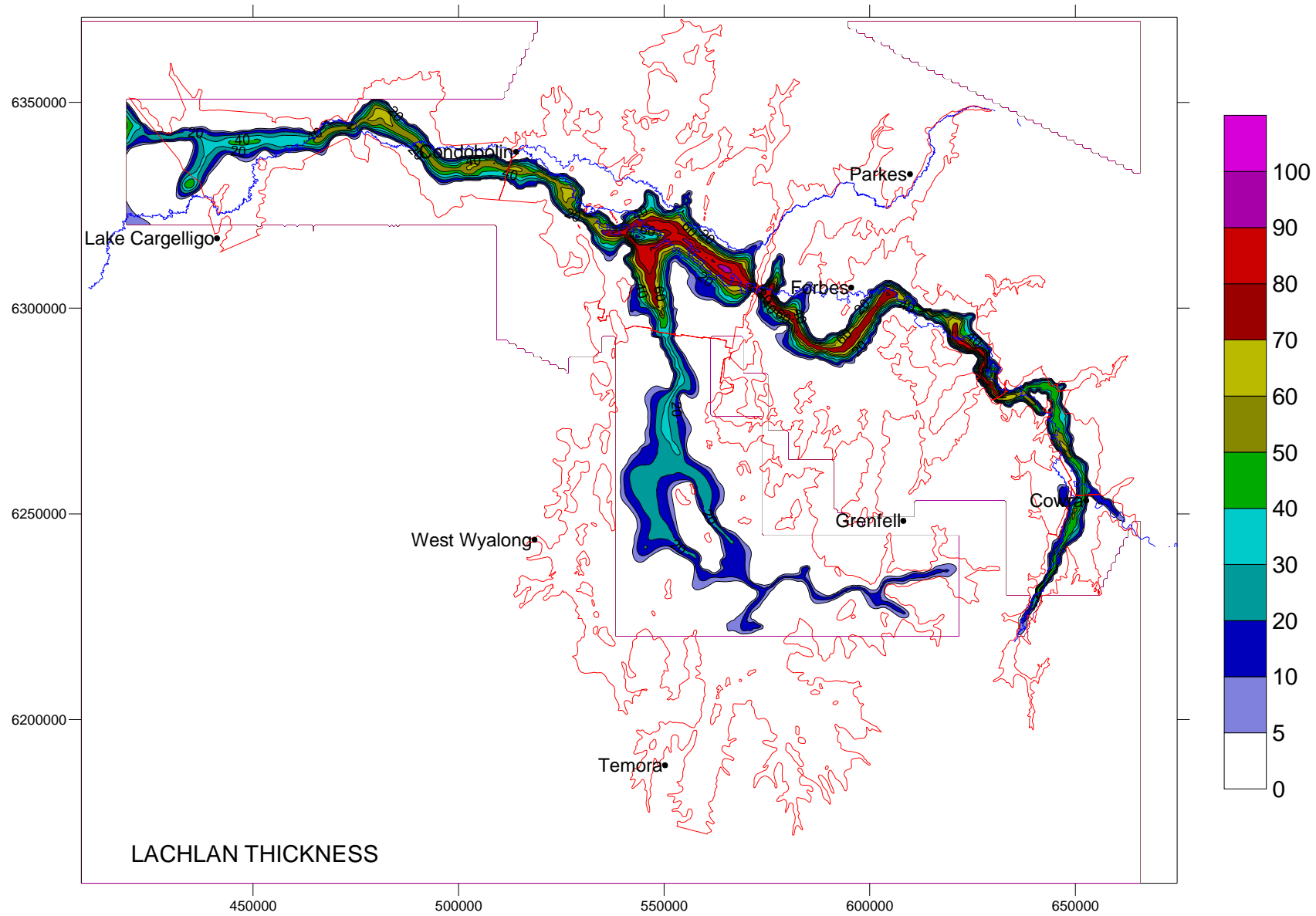
Layer1 thickness (m)



Layer 2 thickness (m)

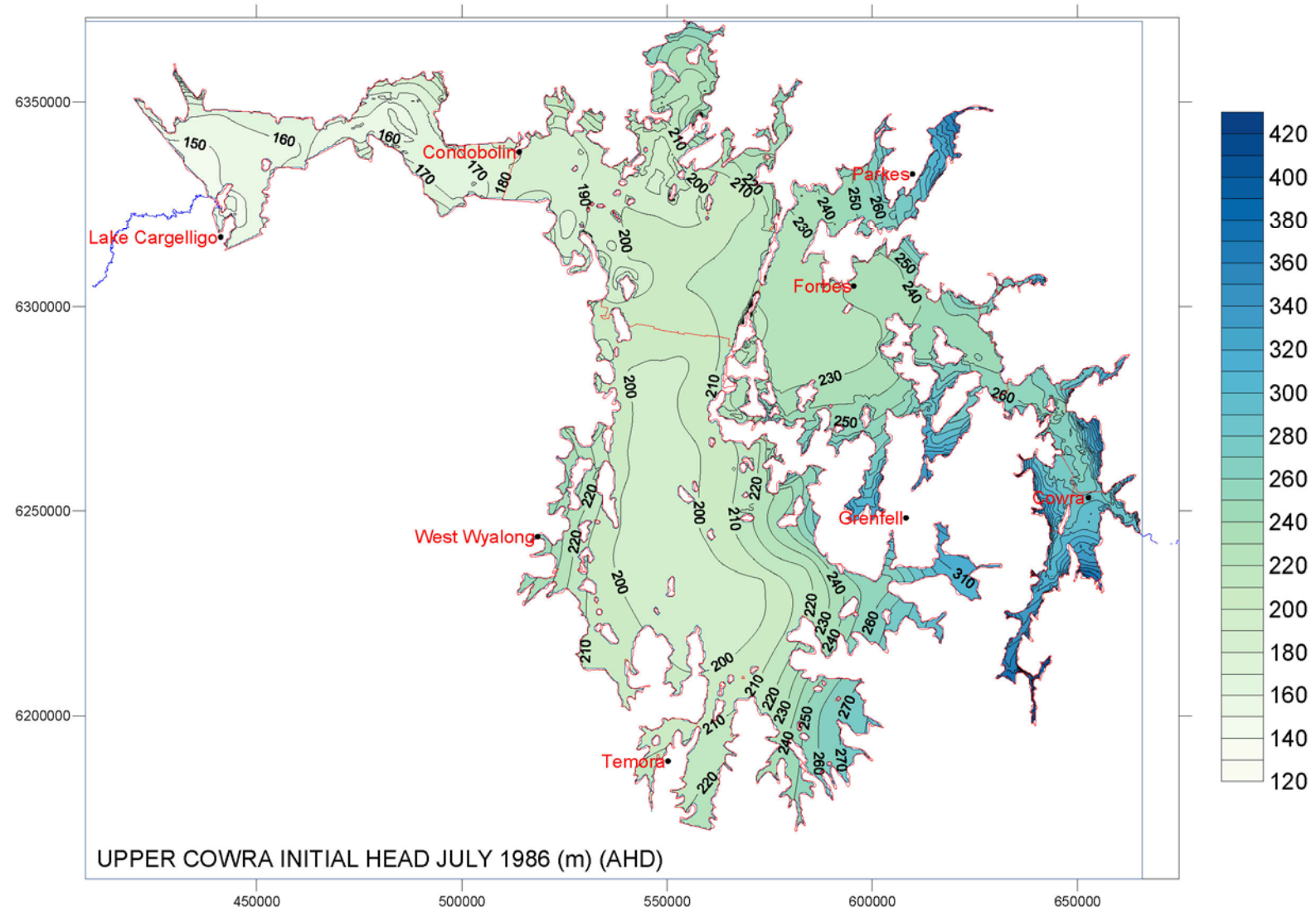


Layer 3 thickness (m)

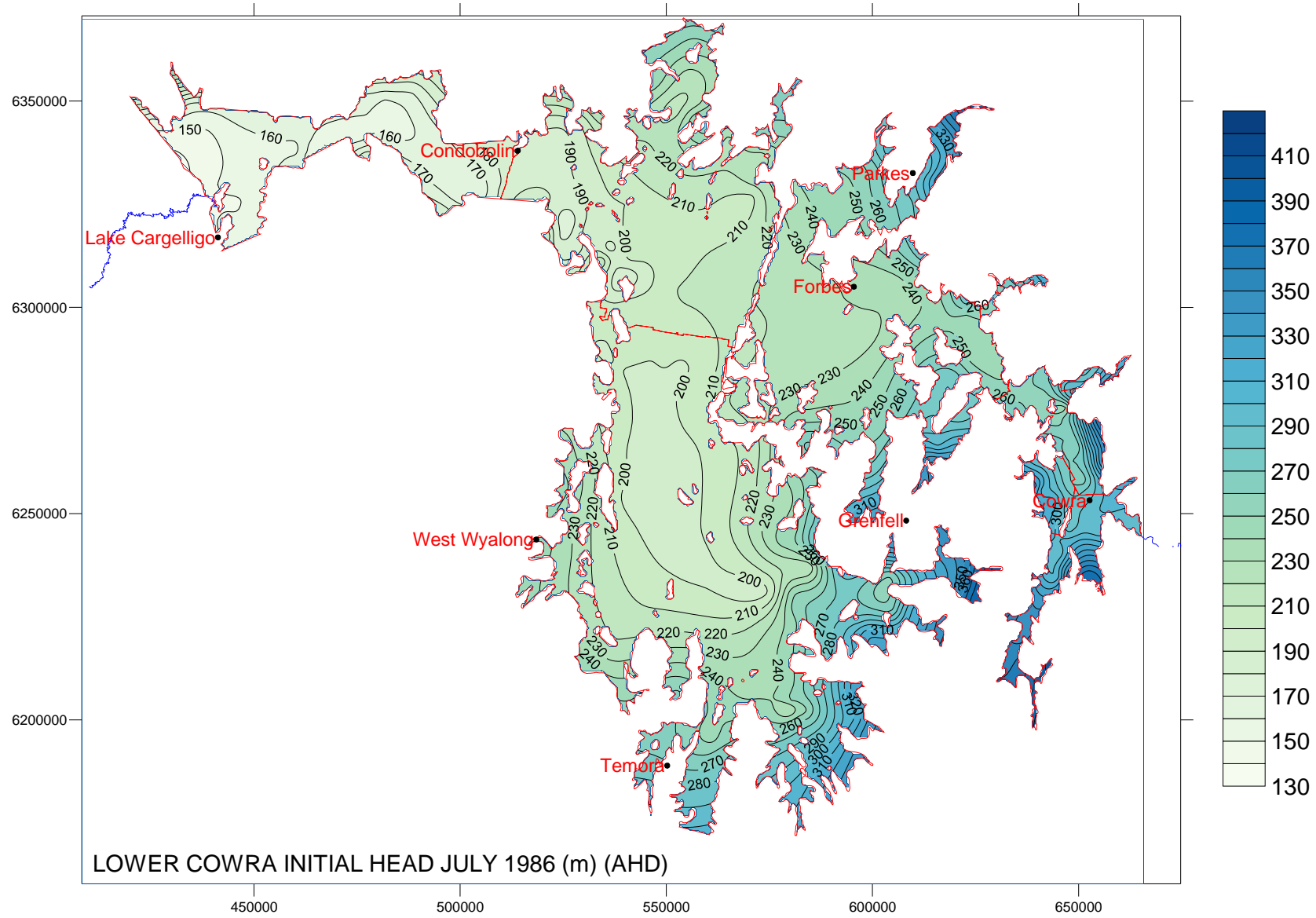


APPENDIX 2: Initial head

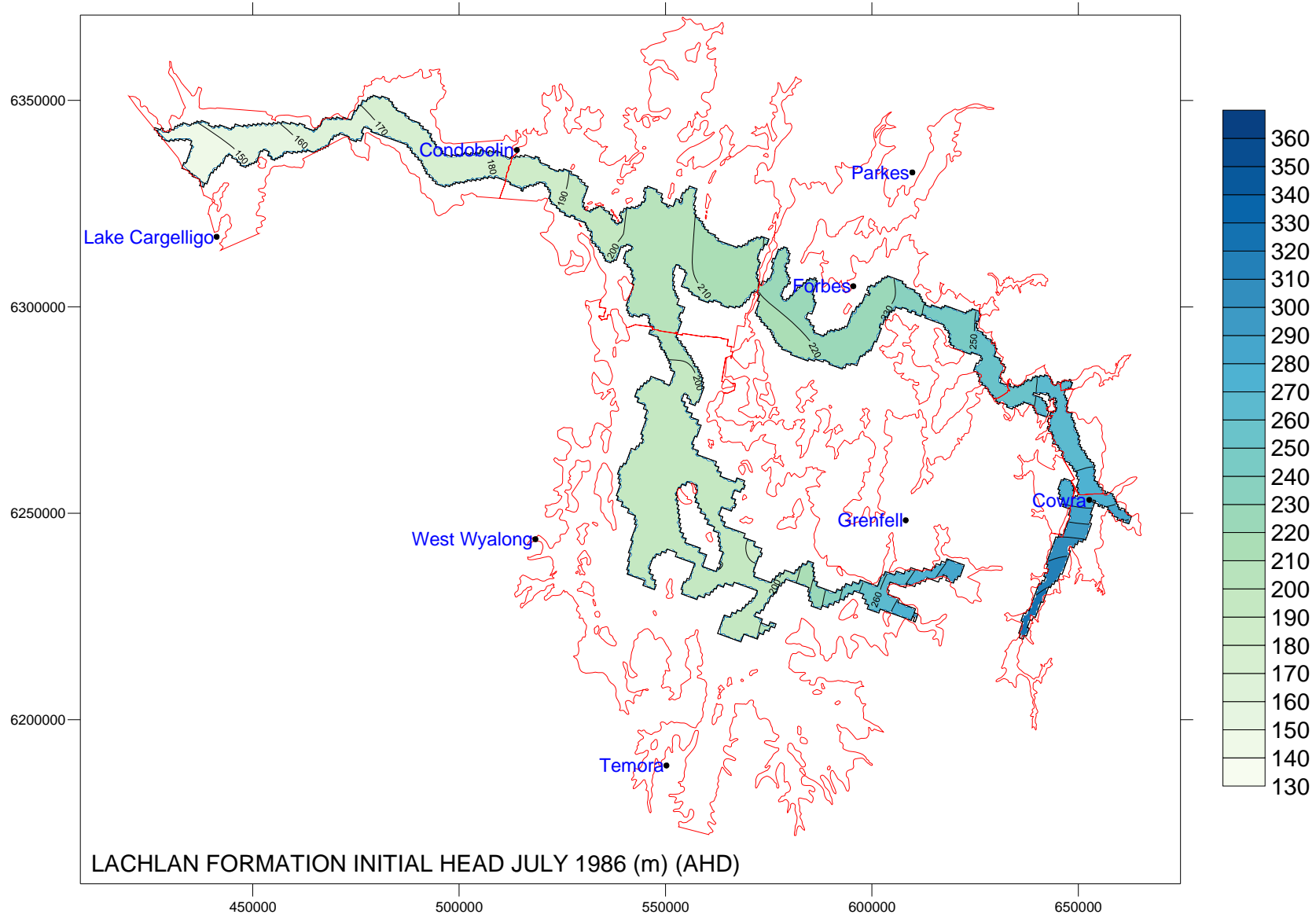
Upper Cowra Initial Heads July 1986 (m) 1986



Lower Cowra Initial Heads July 1986 (m) (AHD)



Lachlan Formation Initial Heads July 1986 (m) (AHD)



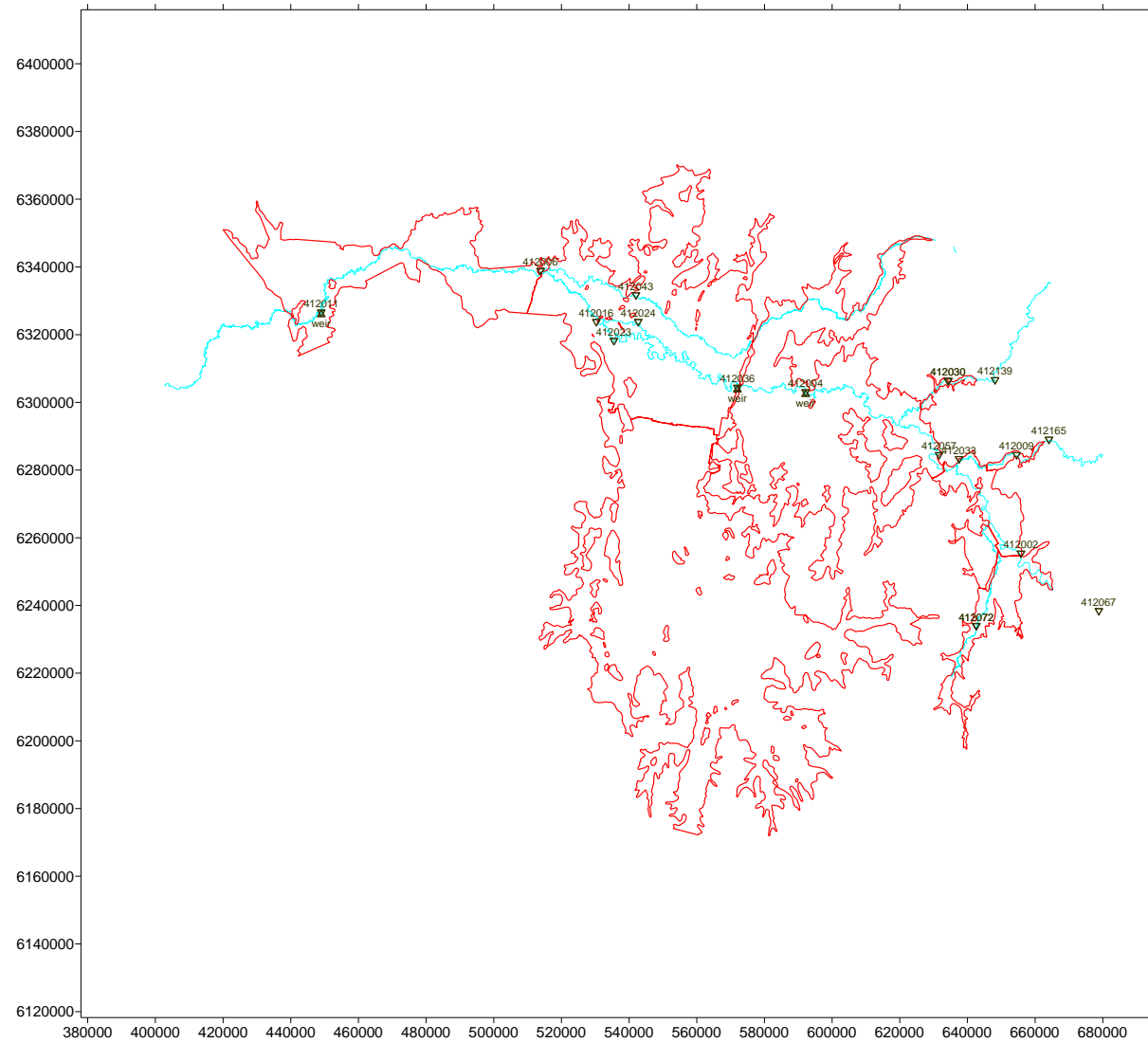
APPENDIX 3: Production bore locations

Table List of Usage Bores

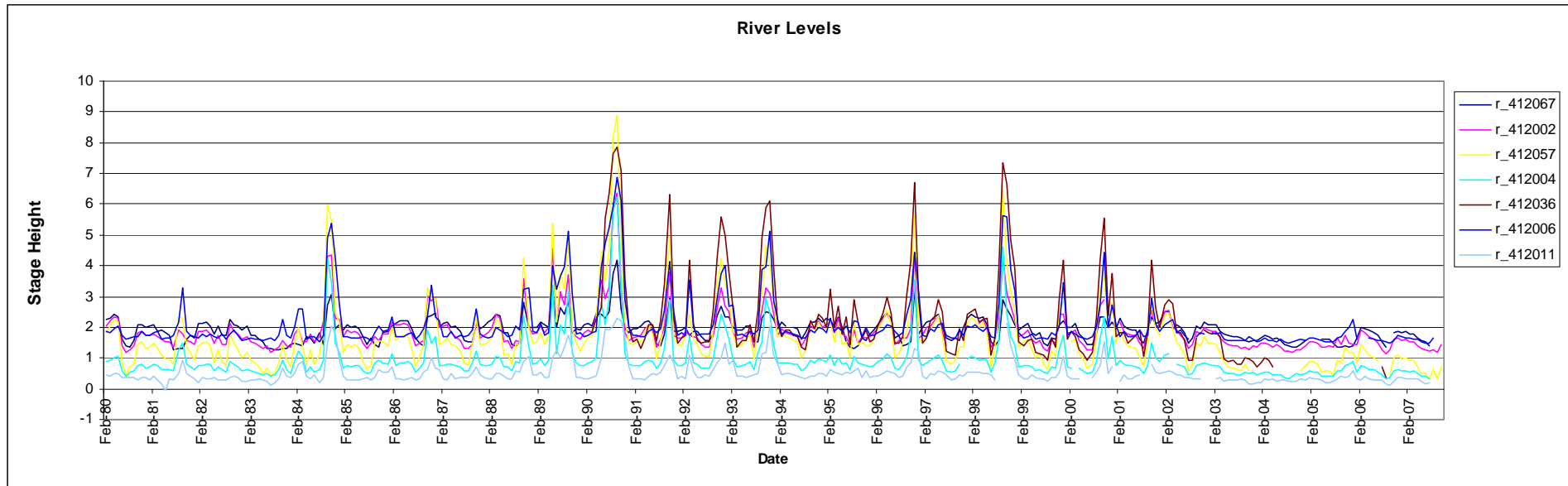
No	Licence No	Easting	Northing	No	Licence N	Easting	Northing	No	Licence No	Easting	Northing	No	Licence	Easting	Northing	No	Licence	Easting	Northing				
1	70BL003286	653152	6258438	74	70BL128649	602418	6302001	147	70BL226902	579022	6303271	220	70BL1174E	638343	6280887	293	70BL2273C	529238	6323085	366	70BL2302I	539783	6278751
2	70BL003287	650539	6257524	75	70BL128752	655062	6255696	148	70BL226940	612179	6299359	221	70BL1201E	653455	6285454	294	70BL2273Z	531313	6322685	367	70BL2302Z	539784	6278752
3	70BL003292	652985	6259273	76	70BL130274	644903	6267409	149	70BL226958	640438	6281018	222	70BL1202T	646803	6281480	295	70BL2273A	590709	6303917	368	70BL2302J	539794	6278754
4	70BL004285	652060	6256279	77	70BL130276	645105	6267191	150	70BL226959	639857	6280327	223	70BL1232T	652929	6284816	296	70BL2273B	536864	6316173	369	70BL2302K	539786	6278754
5	70BL004286	652209	6257078	78	70BL130933	640309	6267518	151	70BL227008	657260	6254453	224	70BL1240C	561863	6306314	297	70BL2273F	553145	6306233	370	70BL2302L	537234	6278351
6	70BL004294	650310	6257651	79	70BL131104	597999	6300794	152	70BL227009	650098	6253424	225	70BL1250E	648698	6281370	298	70BL2273E	517382	6335720	371	70BL2302M	537235	6278352
7	70BL005250	637980	6226943	80	70BL131459	603077	6300187	153	70BL227019	573603	6304106	226	70BL1260E	651528	6284252	299	70BL2273G	522298	6330239	372	70BL2302N	537236	6278353
8	70BL005889	653154	6257101	81	70BL133693	645155	6259586	154	70BL227046	593703	6293614	227	70BL1260F	651601	6284005	300	70BL2274A	592534	6288574	373	70BL2302O	599986	6298424
9	70BL103224	651163	6258538	82	70BL133695	648703	6263647	155	70BL227087	579703	6302854	228	70BL1264A	547190	6286821	301	70BL2274B	595581	6294266	374	70BL2302P	632206	6279828
10	70BL107674	653202	6258345	83	70BL133701	644653	6267665	156	70BL227122	647127	6265795	229	70BL1267C	646435	6281805	302	70BL2274C	599702	6296727	375	70BL2306F	575328	6224719
11	70BL103352	647971	6262710	84	70BL133702	646004	6267054	157	70BL227193	596313	6304259	230	70BL1274A	647754	6282031	303	70BL2274D	585759	6299832	376	70BL2306G	517258	6323830
12	70BL103672	645703	6275575	85	70BL133703	645486	6266815	158	70BL227194	627337	6288053	231	70BL1280E	659567	6285355	304	70BL2274E	583399	6295939	377	70BL2307B	545827	6319620
13	70BL103842	647096	6270803	86	70BL134615	633894	6277274	159	70BL227202	652903	6255264	232	70BL1285E	651168	6284320	305	70BL2274F	598208	6292782	378	70BL2308E	645975	6273631
14	70BL147074	590451	6289734	87	70BL135032	647510	6260555	160	70BL227203	650903	6255285	233	70BL1302E	654789	6284103	306	70BL2274G	594283	6303115	379	70BL2308F	587828	6302411
15	70BL105166	589192	6288606	88	70BL136431	611699	6301000	161	70BL227204	644915	6266485	234	70BL1305E	654963	6285720	307	70BL2274H	535028	6303066	380	70BL2308G	582752	6303294
16	70BL105982	595264	6297511	89	70BL136510	650162	6259598	162	70BL227235	625813	6290659	235	70BL1316C	649897	6281706	308	70BL2275C	566055	6309551	381	70BL2310A	590441	6289734
17	70BL106227	651084	6255169	90	70BL137567	572863	6304891	163	70BL227250	643145	6281900	236	70BL1329C	510969	6335271	309	70BL2275I	560749	6301580	382	70BL2311E	628294	6300530
18	70BL106471	650913	6255285	91	70BL139872	647975	6259519	164	70BL227337	660754	6251657	237	70BL1332E	649112	6281486	310	70BL2275J	566971	6306590	383	70BL2313C	606579	6298936
19	70BL106764	612239	6300387	92	70BL140178	647252	6272803	165	70BL227449	649013	6251184	238	70BL1336E	651571	6260928	311	70BL2275L	658485	6283894	384	70BL2313E	656481	6287651
20	70BL107218	645041	6274691	93	70BL141326	645276	6276384	166	70BL227476	591365	6296585	239	70BL1349E	631383	6280253	312	70BL2276C	513348	6333215	385	70BL2318E	557128	6240475
21	70BL107575	644483	6280571	94	70BL141778	639871	6284306	167	70BL227590	635187	6279474	240	70BL1362E	649173	6282102	313	70BL2276E	545469	6314259	386	70BL2320E	629155	6281758
22	70BL180177	589435	6300862	95	70BL142074	645073	6273229	168	70BL227745	620109	6296835	241	70BL1363C	648627	6281833	314	70BL2276L	647352	6273627	387	70BL2320F	545752	6308183
23	70BL18426	650757	6256242	96	70BL142332	647248	6272607	169	70BL227764	642613	6281084	242	70BL1366E	557074	6313207	315	70BL2276E	546787	6313090	388	70BL2322E	607287	6301730
24	70BL18492	634477	6279391	97	70BL142423	647248	6281709	170	70BL228186	647071	6276939	243	70BL1398E	648201	6280936	316	70BL2277Z	570229	6303291				
25	70BL18542	647483	6257110	98	70BL144990	631373	6279284	171	70BL228233	645591	6275847	244	70BL1409A	568658	6309995	317	70BL2277Z	569931	6302731				
26	70BL19024	581989	6296924	99	70BL154311	645954	6276142	172	70BL228237	646531	6258757	245	70BL1423C	627113	6299859	318	70BL2278E	643495	6278685				
27	70BL19065	645069	6280131	100	70BL154603	653935	6255991	173	70BL228239	611726	6302104	246	70BL1431E	545565	6318600	319	70BL2281E	519688	6330390				
28	70BL19113	644313	6267542	101	70BL226068	623014	6299076	174	70BL228247	650238	6255683	247	70BL1435C	566700	6303532	320	70BL2282E	628601	6282729				
29	70BL19484	644731	6279890	102	70BL226079	646581	6260918	175	70BL228248	645820	6261573	248	70BL15114	572356	6306672	321	70BL2283A	628668	6301910				
30	70BL19485	644894	6279795	103	70BL226152	597923	6293934	176	70BL228281	646580	6259413	249	70BL15114	571896	6307322	322	70BL2284E	570660	6303983				
31	70BL19676	578921	6316384	104	70BL226153	597913	6293934	177	70BL228467	647071	6276979	250	70BL15191	607539	6304052	323	70BL2285I	517372	6335720				
32	70BL20089	597284	6301723	105	70BL226208	608913	6301634	178	70BL228512	646823	6261415	251	70BL15192	608021	6303863	324	70BL2285E	609724	6225982				
33	70BL202169	597761	6306681	106	70BL226238	640000	6284273	179	70BL228847	648265	6269866	252	70BL1536E	609323	6225894	325	70BL2285Z	609313	6225894				
34	70BL202229	585381	6297016	107	70BL226271	630875	6280484	180	70BL229254	611329	6302511	253	70BL1538E	631406	6280244	326	70BL2286C	570284	6302491				
35	70BL202463	642473	6280632	108	70BL226294	627245	6283095	181	70BL229327	639959	6228940	254	70BL1545A	609734	6225982	327	70BL2286F	606608	6303802				
36	70BL202992	645864	6261734	109	70BL226330	643368	6280095	182	70BL229341	647999	6258678	255	70BL1548E	651576	6256432	328	70BL2287C	536408	6321440				
37	70BL202423	640029	6230202	110	70BL226362	613529	6298914	183	70BL229342	647473	6257110	256	70BL2260C	607103	6304264	329	70BL2289E	557158	6240472				
38	70BL227308	6295897	6289597	111	70BL226385	646592	6282173	184	70BL229451	645129	6280127	257	70BL2261E	571983	6303485	330	70BL2289A	568000	6305984				
39	70BL203104	647454	6274225	112	70BL226386	650229	6255773	185	70BL229490	645161	6259584	258	70BL2261E	553751	6314540	331	70BL2281E	514965	6337541				
40	70BL203683	596856	6306842	113	70BL226407	651466	6256101	186	70BL229528	592558	6297733	259	70BL2262E	559284	6316435	332	70BL2281E	571501	6304712				
41	70BL203791	602006	6295409	114	70BL226470	647999	6256878	187	70BL229532	640455	6283962	260	70BL2262E	564214	6309385	333	70BL2282E	552408	6282736				
42	70BL301172	593436	6297747	115	70BL226492	644903	6277868	188	70BL229627	660740	6251663	261	70BL2262E	545012	6265729	334	70BL2292A	555360	6283678				
43	70BL30536	647623	6270706	116	70BL226498	646482	6275654	189	70BL229700	611707	6300985	262	70BL2262A	571863	6308935	335	70BL2292E	553071	6285635				
44	70BL30726	602121	6300117	117	70BL226501	649310	6269854	190	70BL229813	647368	6261203	263	70BL2262A	571813	6308485	336	70BL2292E	553276	6287386				
45	70BL30780	622035	6296644	118	70BL226517	639676	6277962	191	70BL229898	654253	6255624	264	70BL2262A	571763	6308135	337	70BL2293Z	572027	6307439				
46	70BL30836	647781	6260081	119	70BL226518	646532	6258760	192	70BL229983	637212	6280244	265	70BL2262A	571713	6307685	338	70BL2293Z	568763	6305784				
47	70BL30968	640120	6231187	120	70BL226520	647499	6273454	193	70BL230075	644884	6273454	266	70BL2262A	571563	6307035	339	70BL2293Z	530744	6325317				
48	70BL301238	626406</																					

APPENDIX 4: River details

River Gauging station and weirs in the model area

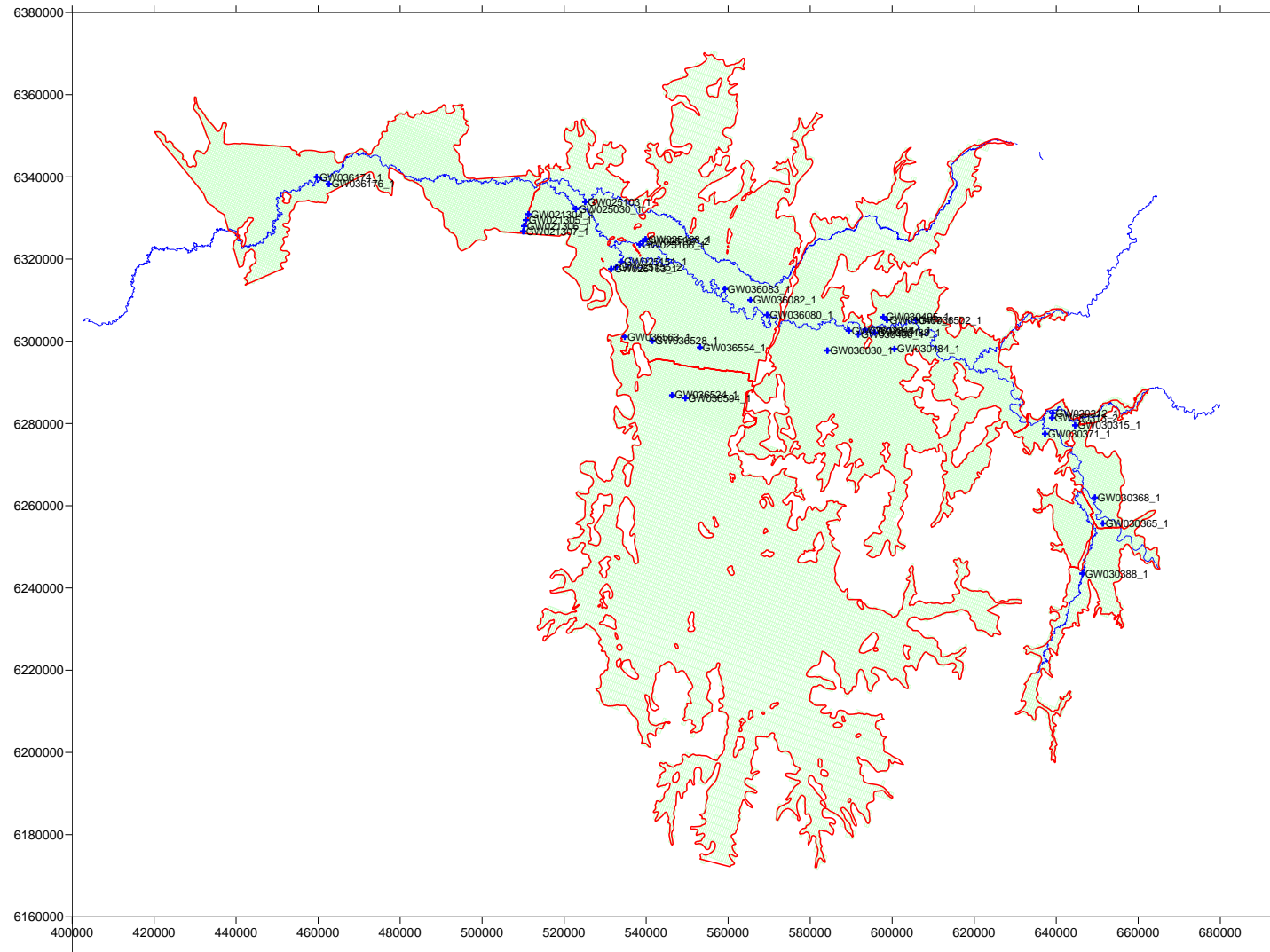


River stage data for each gauging station

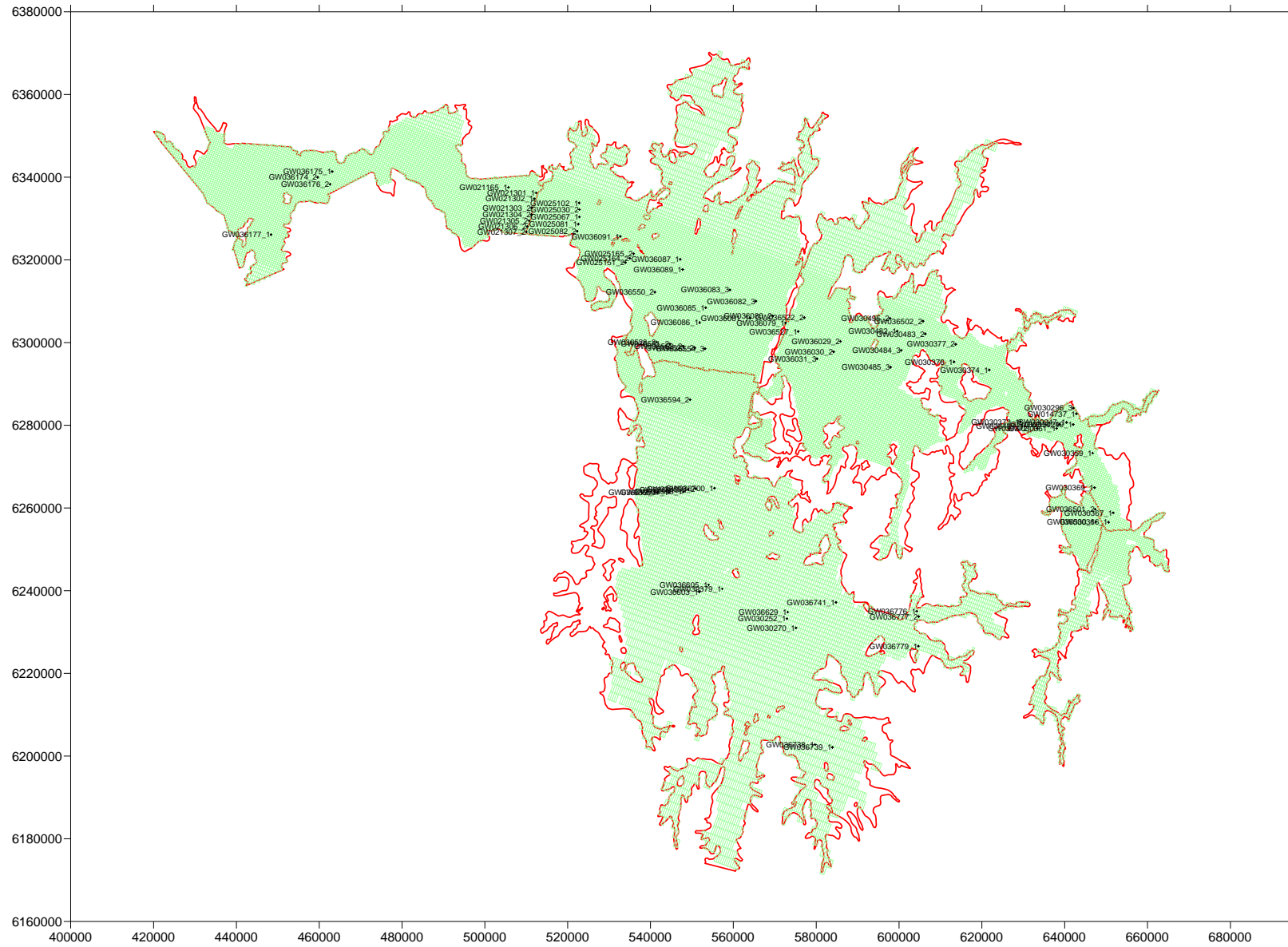


APPENDIX 5: Monitoring bore locations and model layer boundaries

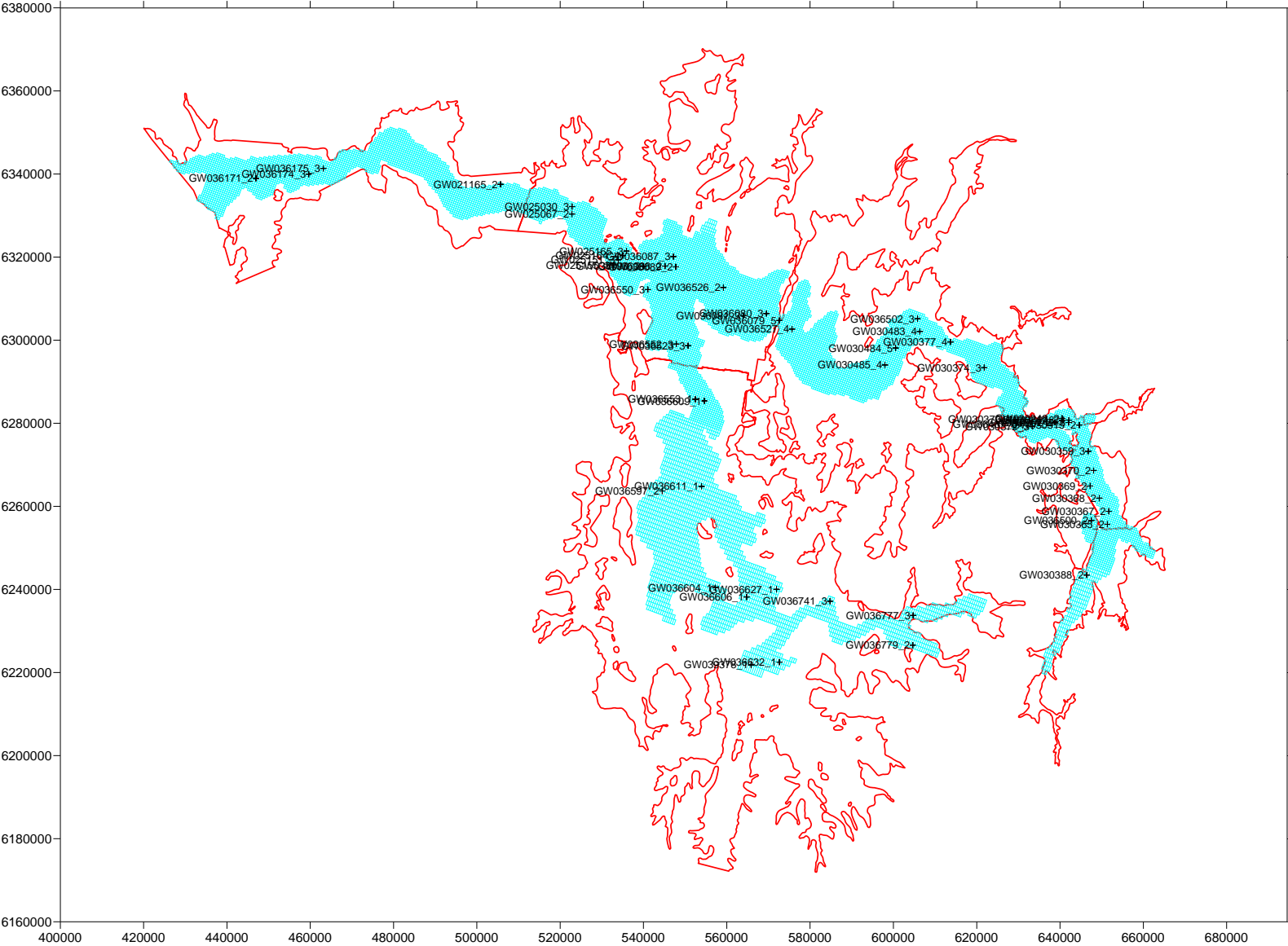
Upper Cowra model boundaries and bore locations



Lower Cowra model boundaries and bore locations



Lachlan Formation model boundaries and bore locations



APPENDIX 6: Observed and simulated water level hydrographs

Figure 6-1 Comparison between simulated and observed water levels in layer 1 in Zone 6 (m) (AHD)

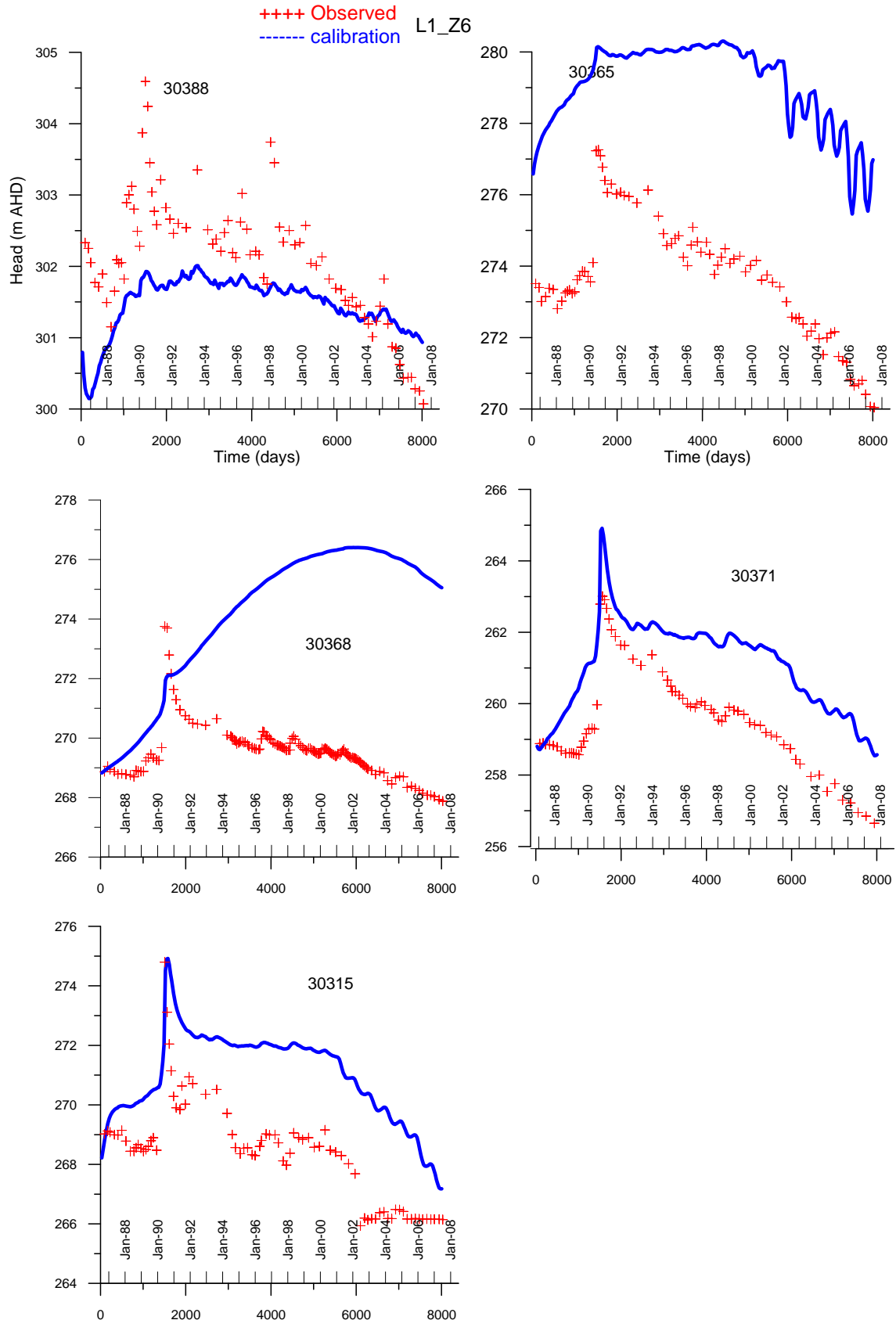


Figure 6-2 Comparison between simulated and observed water levels in layer 1 in Zone 2 & 3 (m) (AHD)

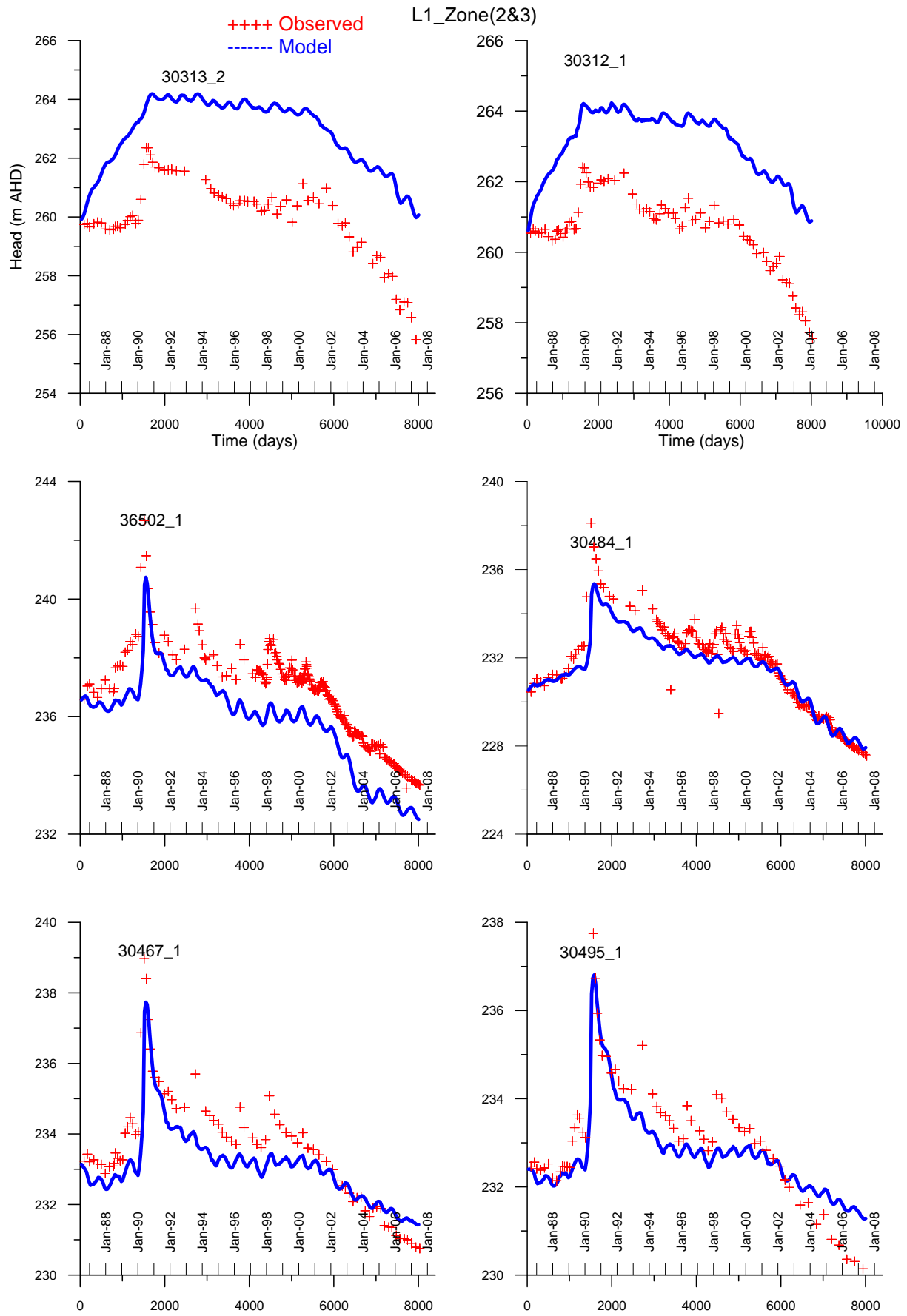


Figure 6-3 Comparison between simulated and observed water levels in layer 1 in Zone 3 (m) (AHD)

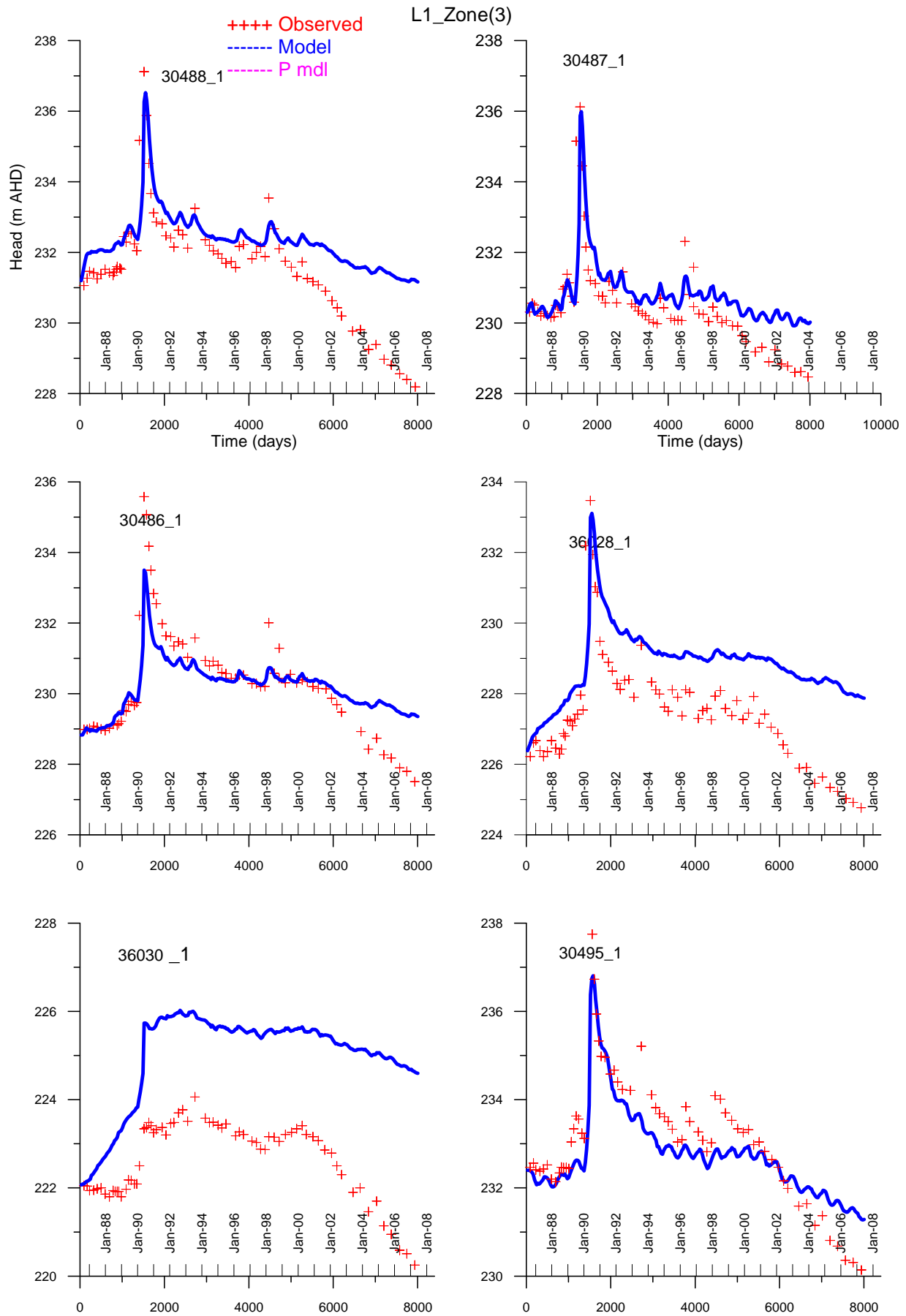


Figure 6-4 Comparison between simulated and observed water levels in layer 1 in Zone 5 (m) (AHD)

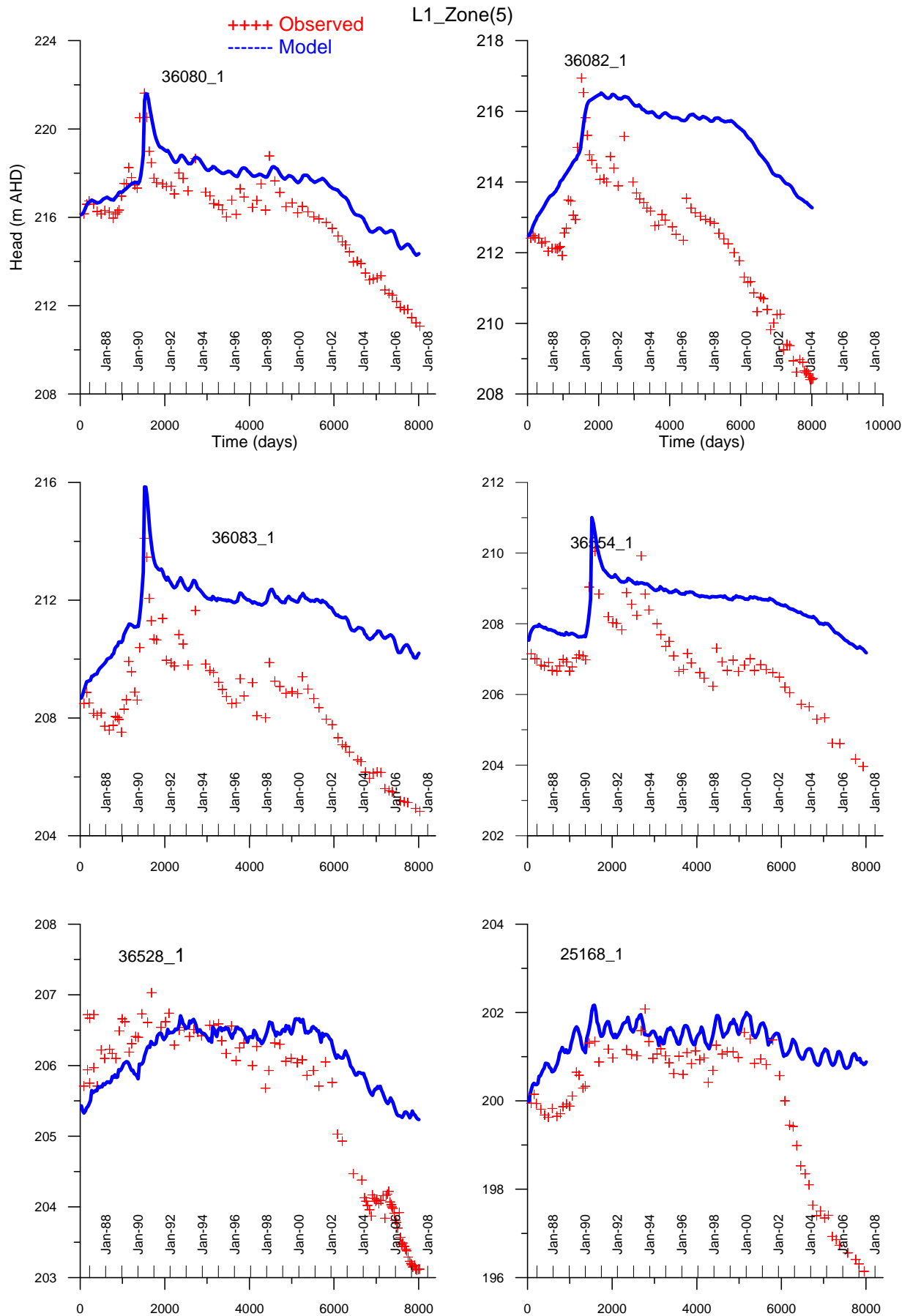


Figure 6-5 Comparison between simulated and observed water levels in layer 1 in Zone 5 (m) (AHD)

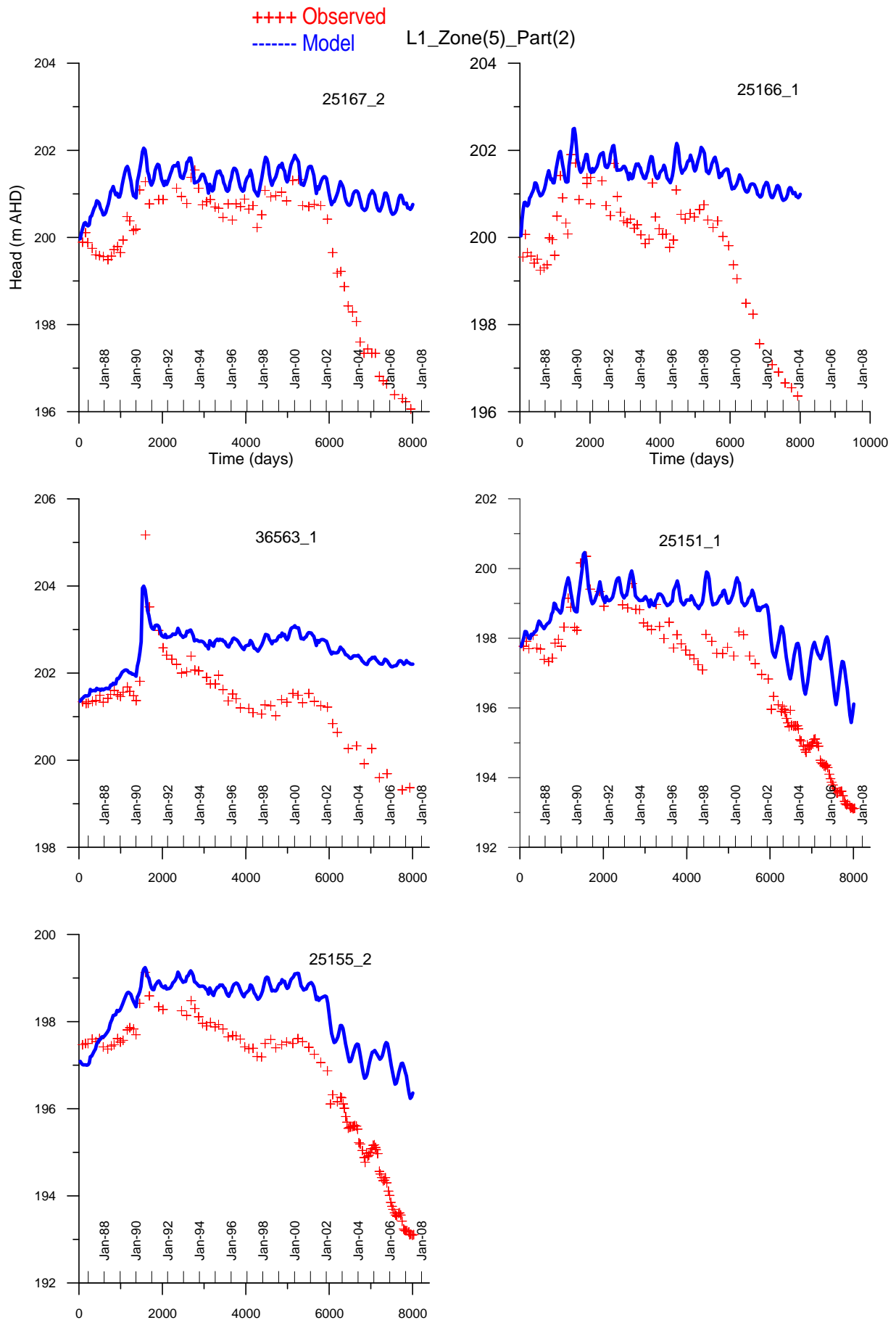


Figure 6-6 Comparison between simulated and observed water levels in layer 1 in Zone 5 (m) (AHD)

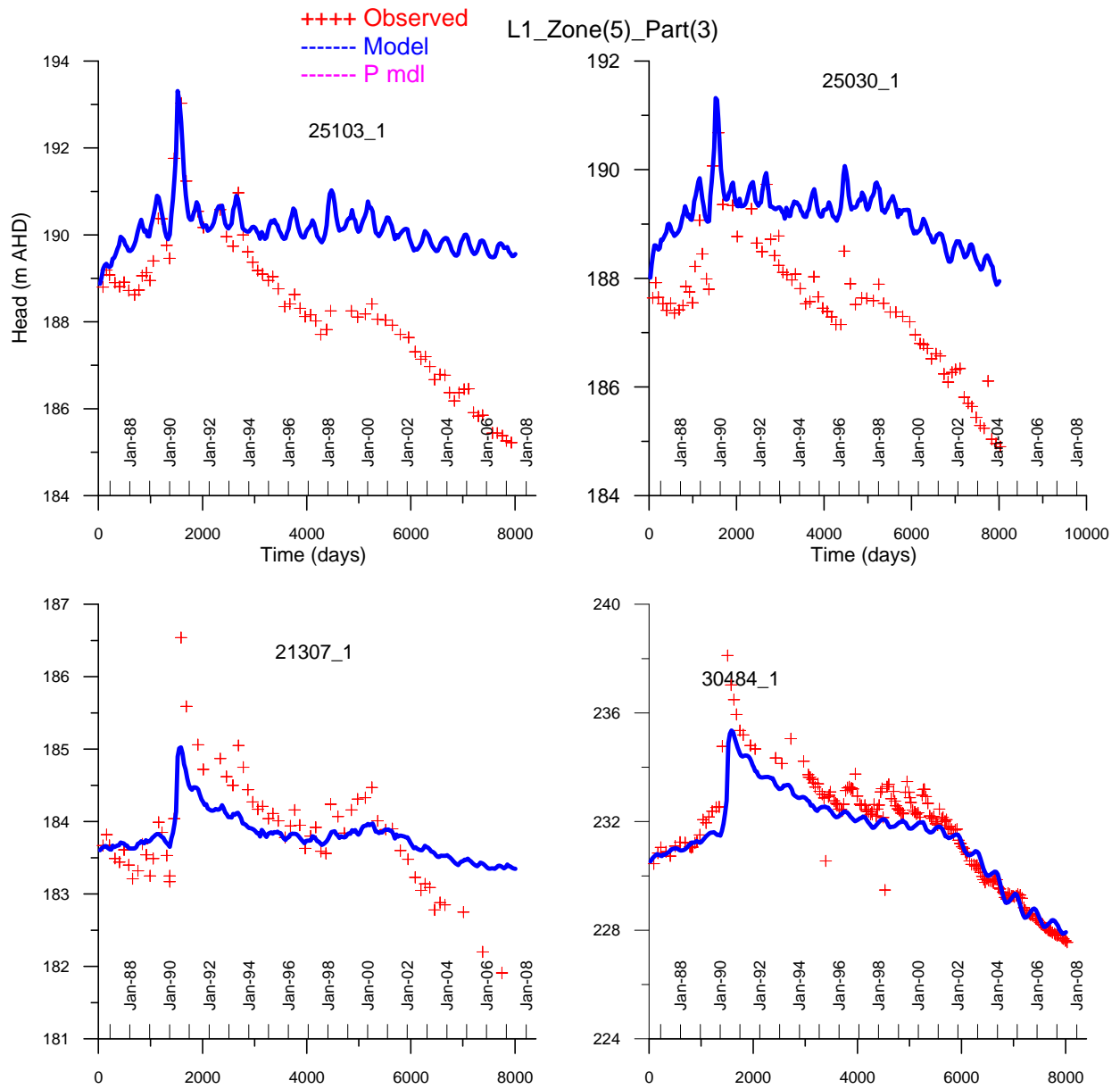


Figure 6-7 Comparison between simulated and observed water levels in layer 1 in Zone 6 (m) (AHD)

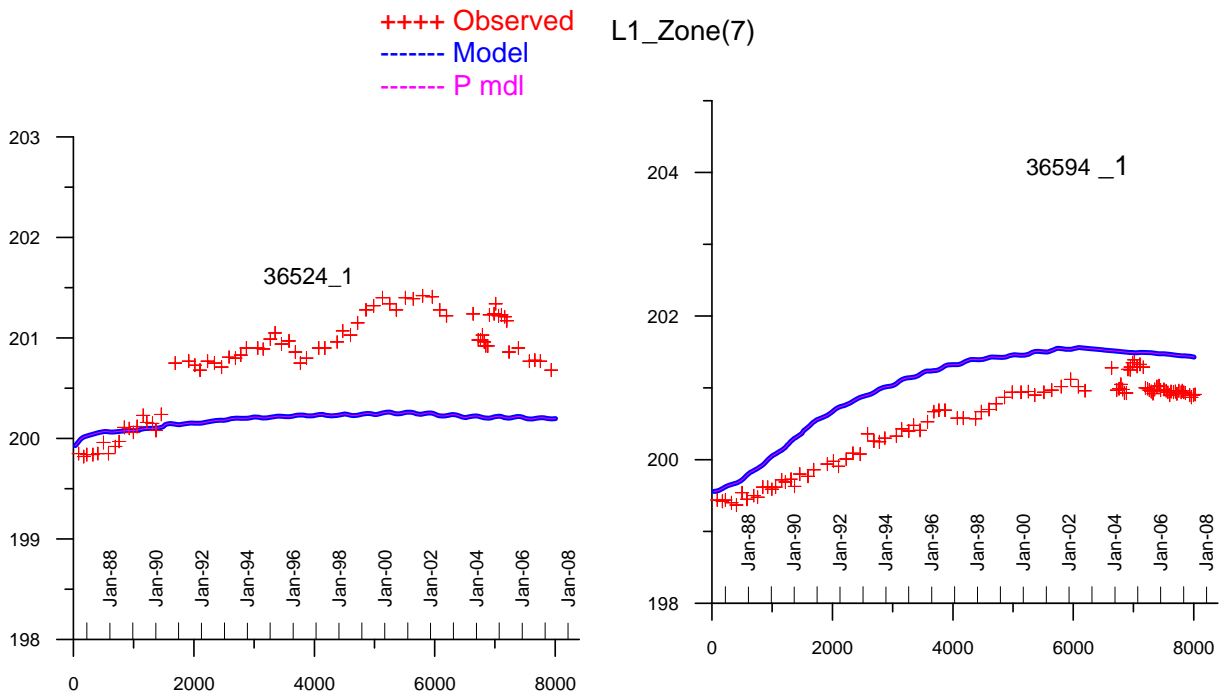


Figure 6-8 Comparison between simulated and observed water levels in layer 1 in Zone 8 (m) (AHD)

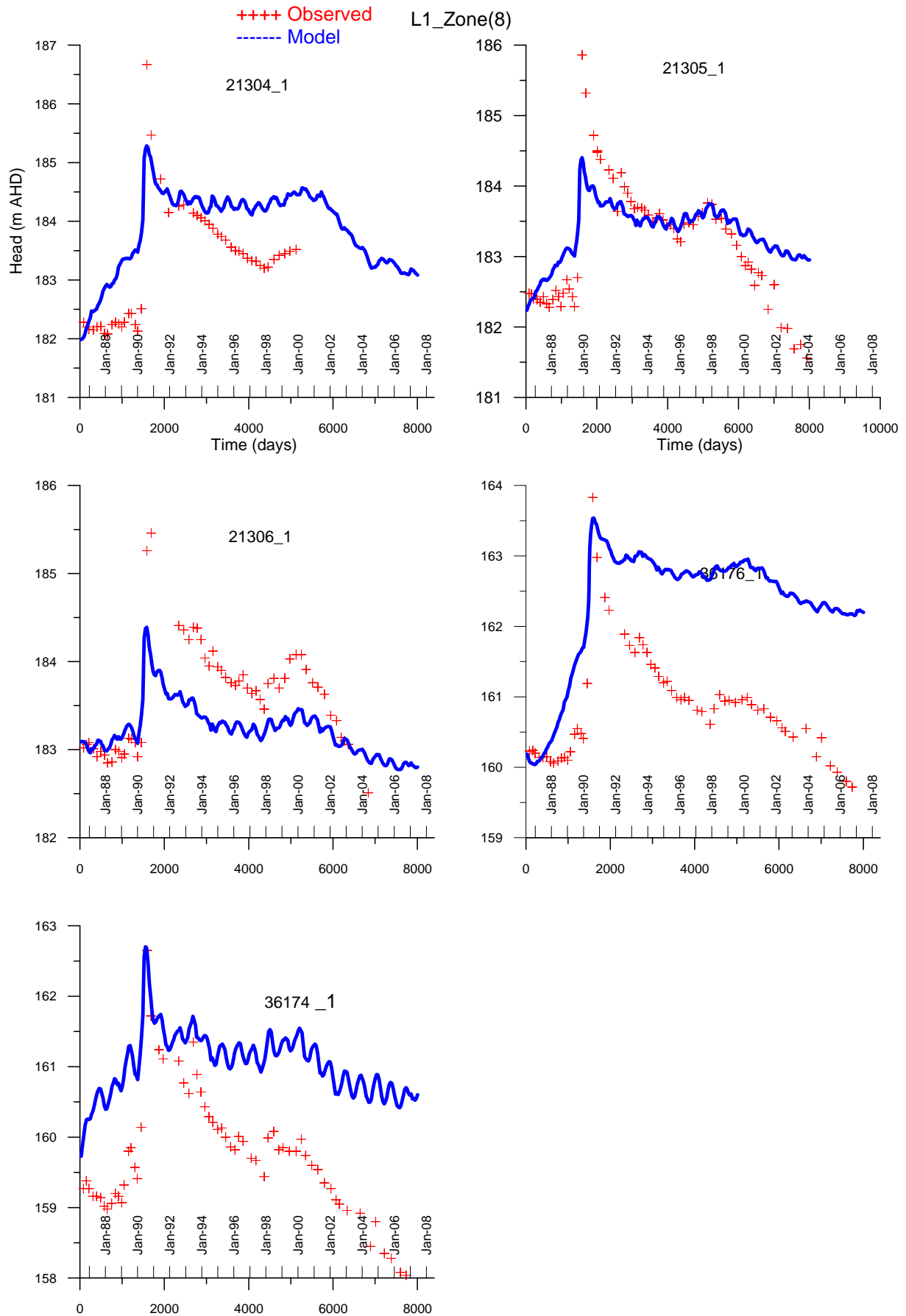


Figure 6-9 Comparison between simulated and observed water levels in layer 2 in Zone 2 (m) (AHD)

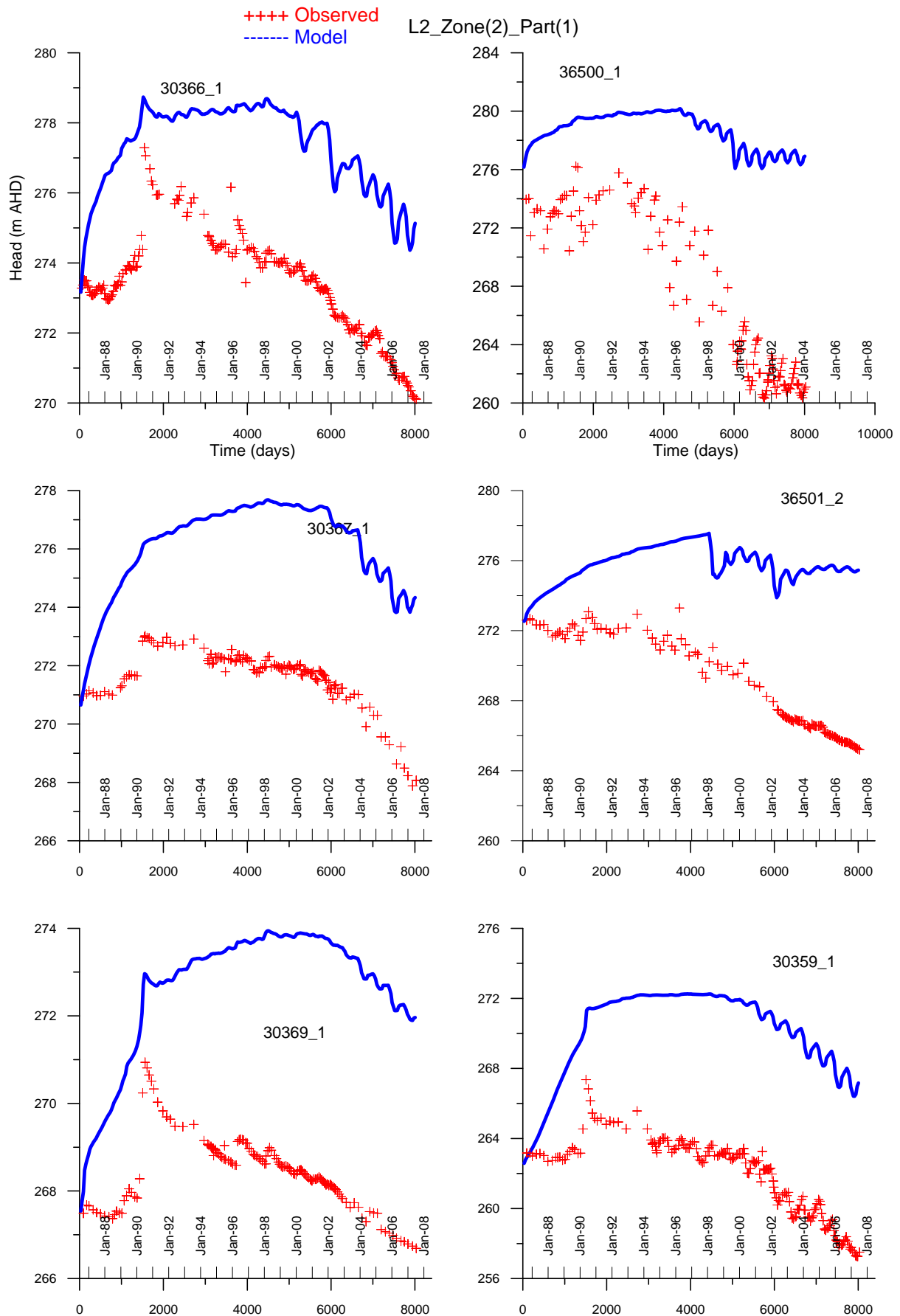


Figure 6-10 Comparison between simulated and observed water levels in layer 2 in Zone 2 (m) (AHD)

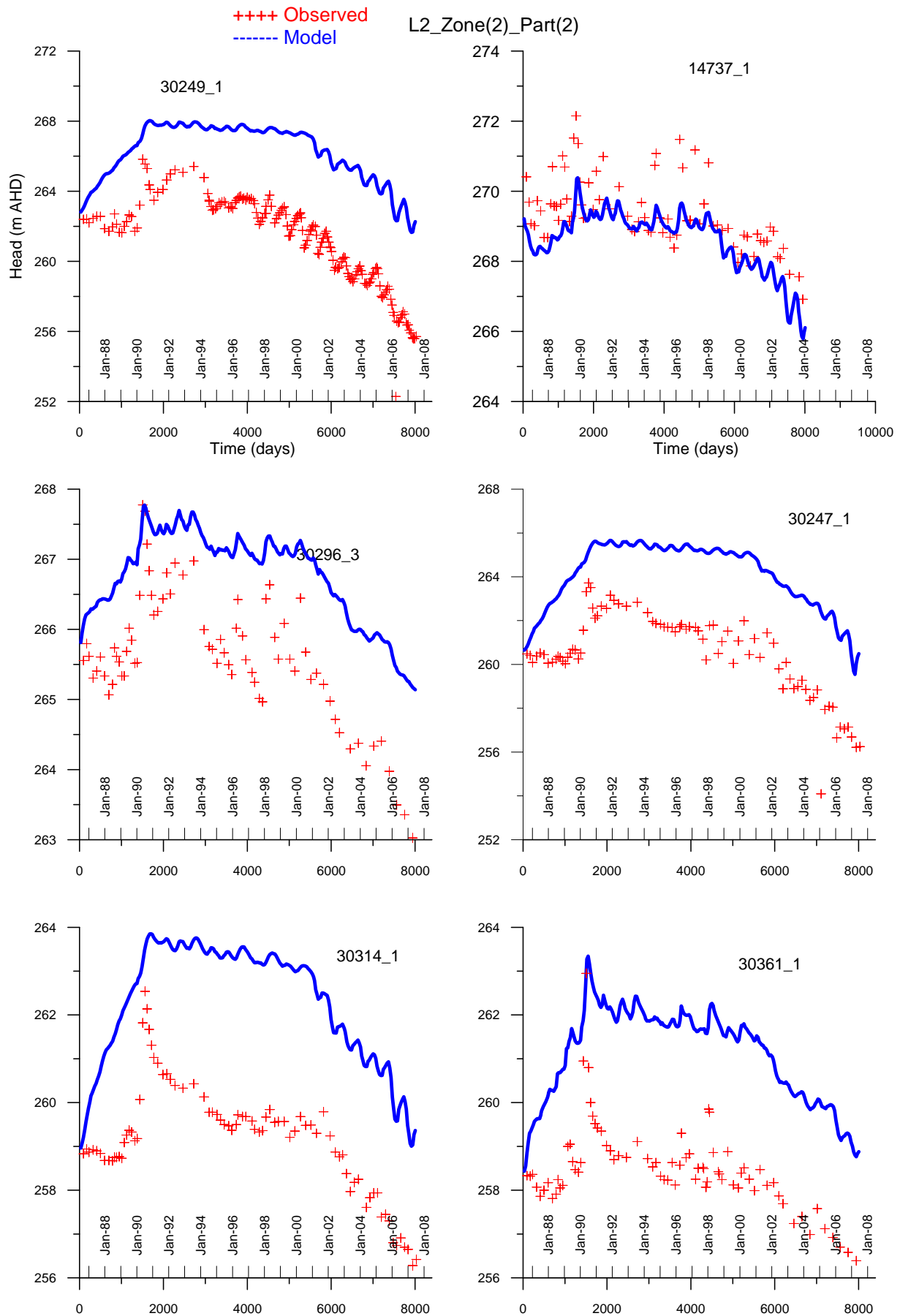


Figure 6-11 Comparison between simulated and observed water levels in layer 2 in Zone 2&3 (m) (AHD)

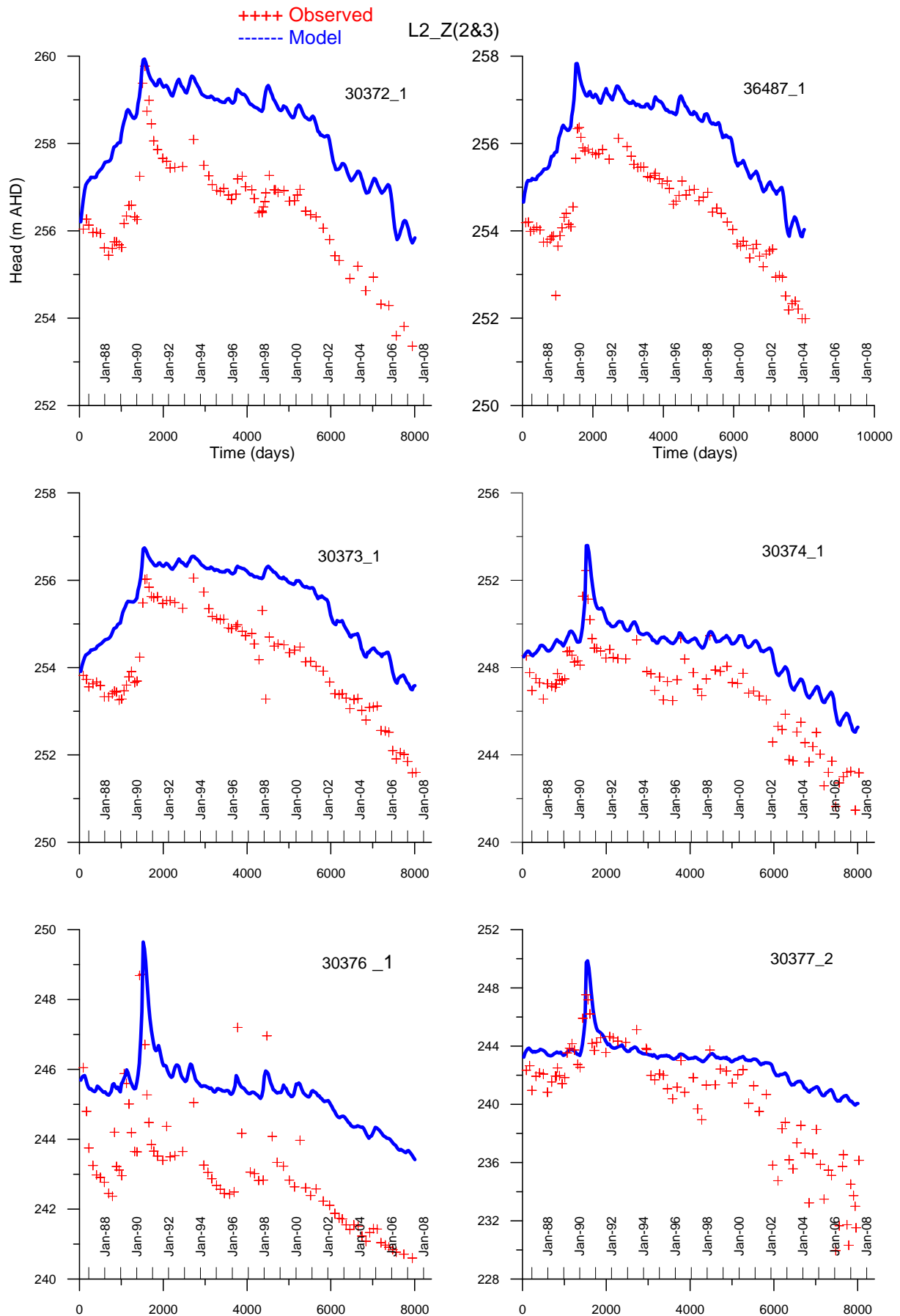


Figure 6-12 Comparison between simulated and observed water levels in layer 2 in Zone 3 (m) (AHD)

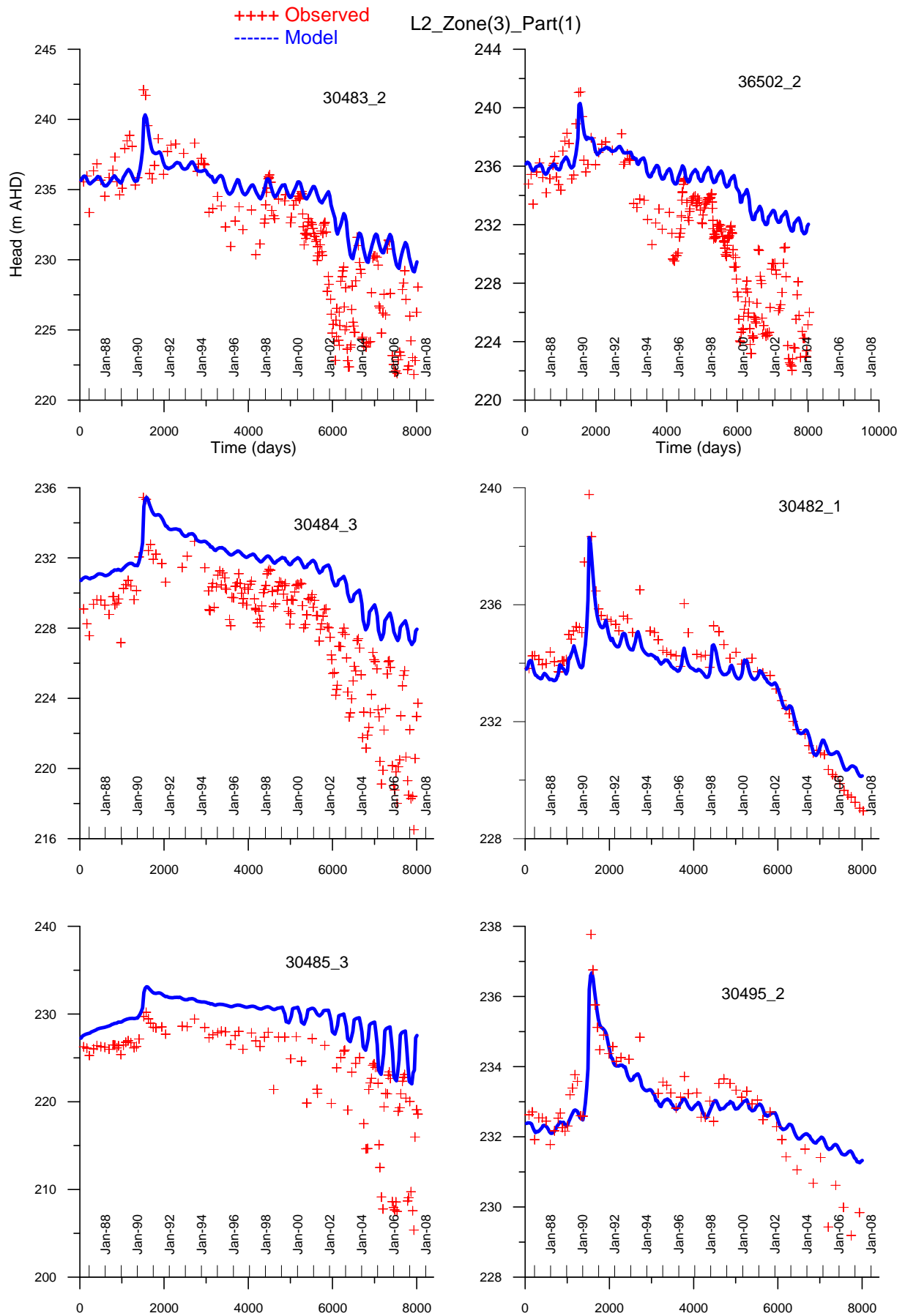


Figure 6-13 Comparison between simulated and observed water levels in layer 2 in Zone 3 (m) (AHD)

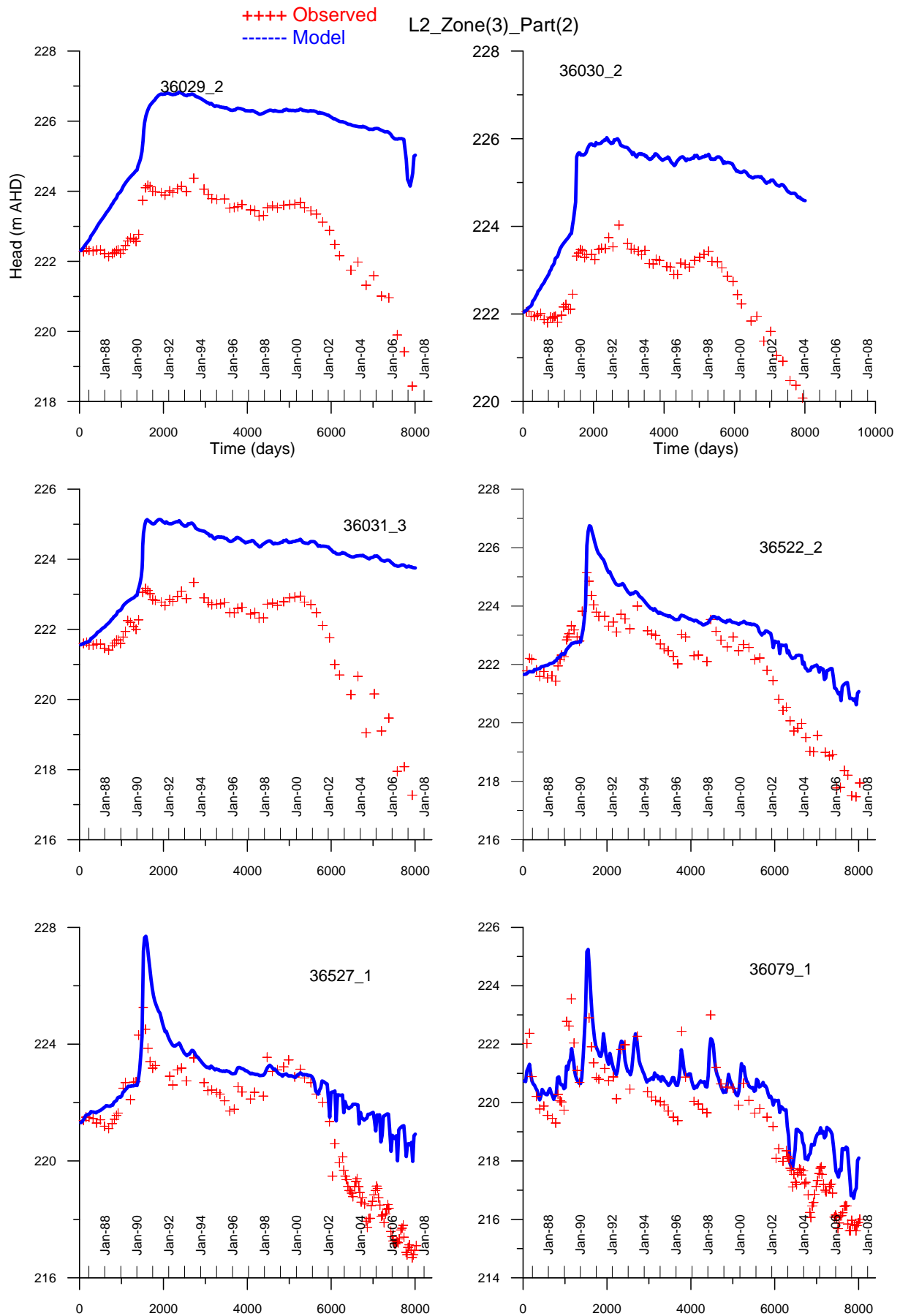


Figure 6-14 Comparison between simulated and observed water levels in layer 2 in Zone 5 (m) (AHD)

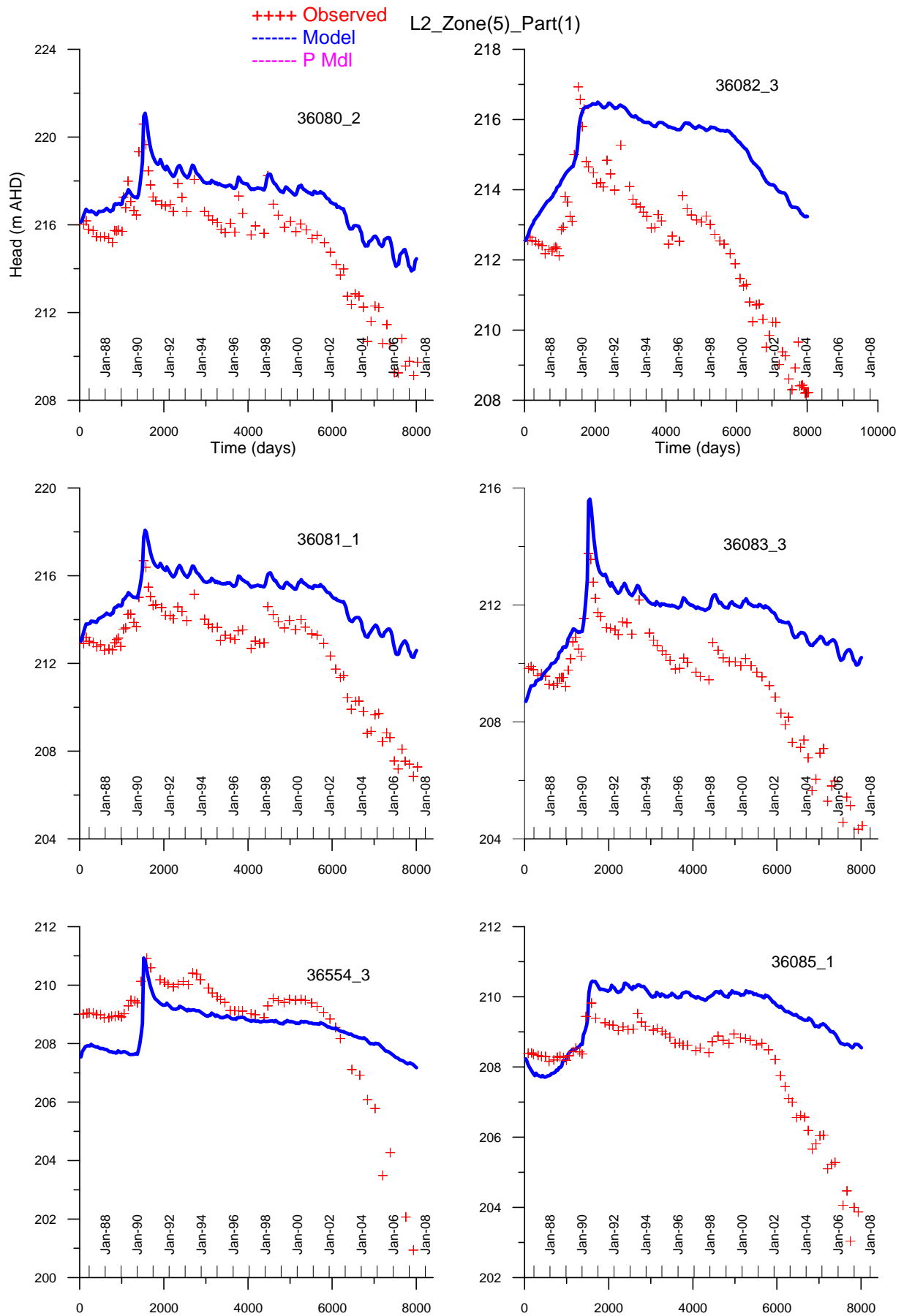


Figure 6-15 Comparison between simulated and observed water levels in layer 2 in Zone 5 (m) (AHD)

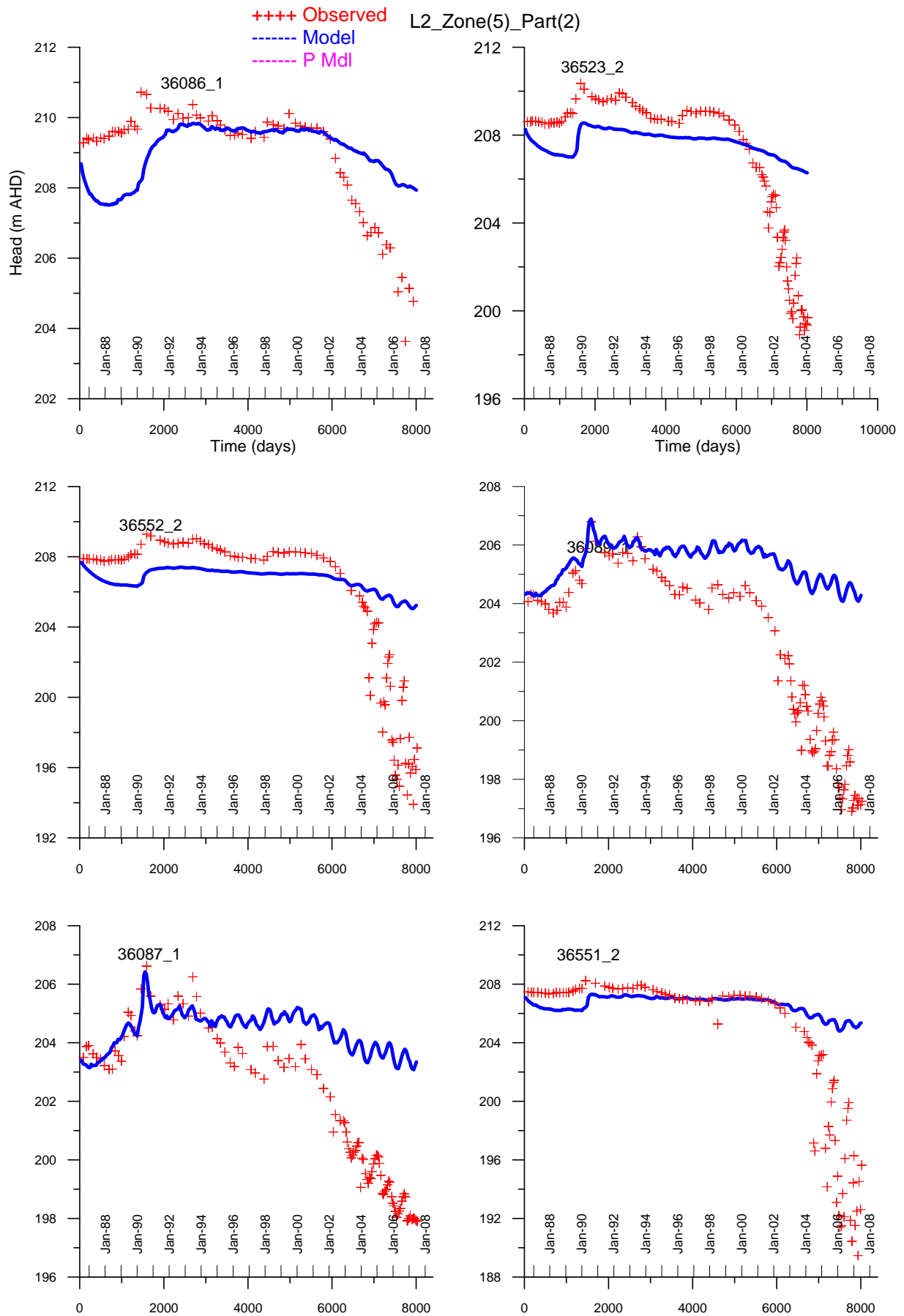


Figure 6-16 Comparison between simulated and observed water levels in layer 2 in Zone 5 (m) (AHD)

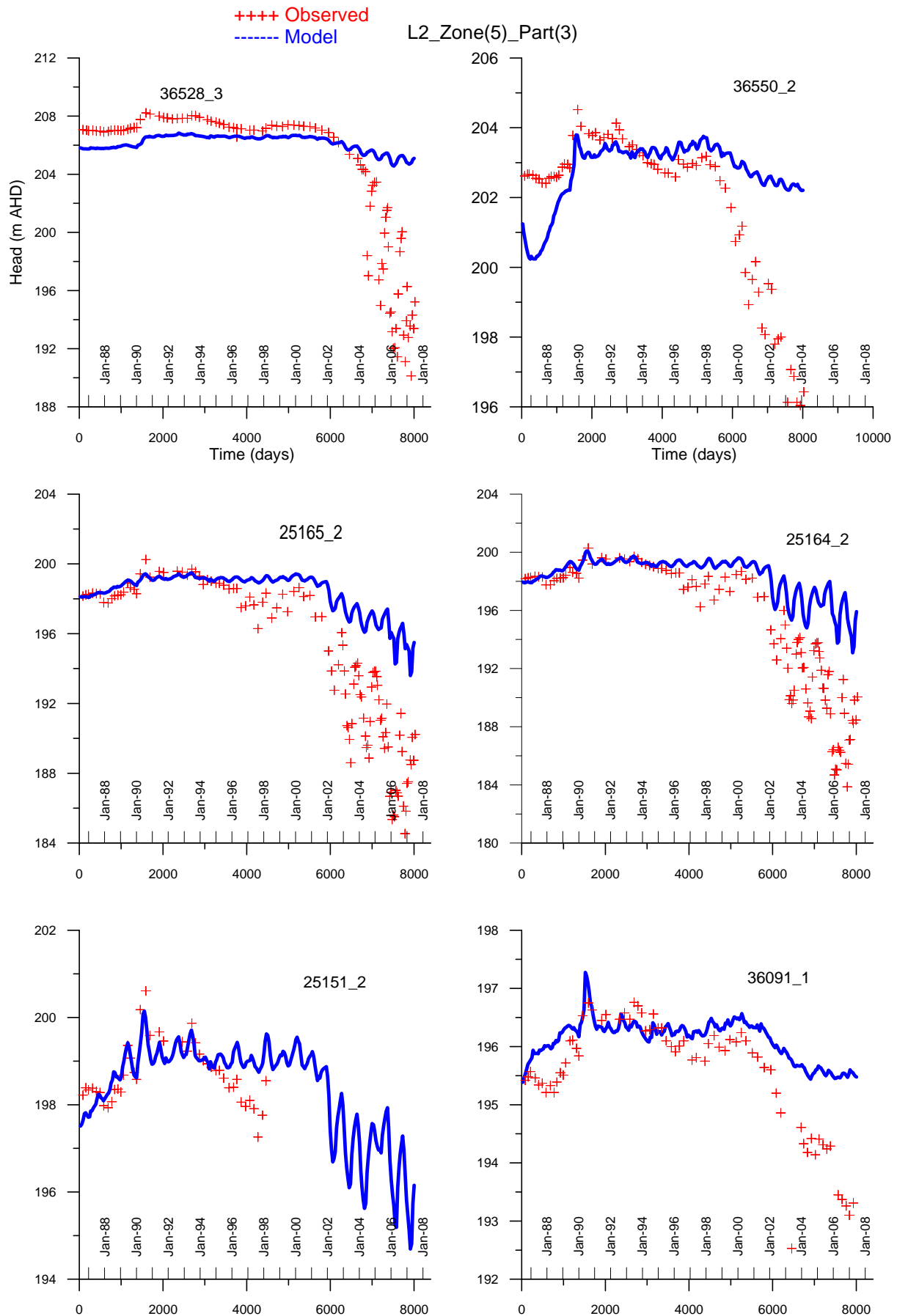


Figure 6-17 Comparison between simulated and observed water levels in layer 2 in Zone 5 (m) (AHD)

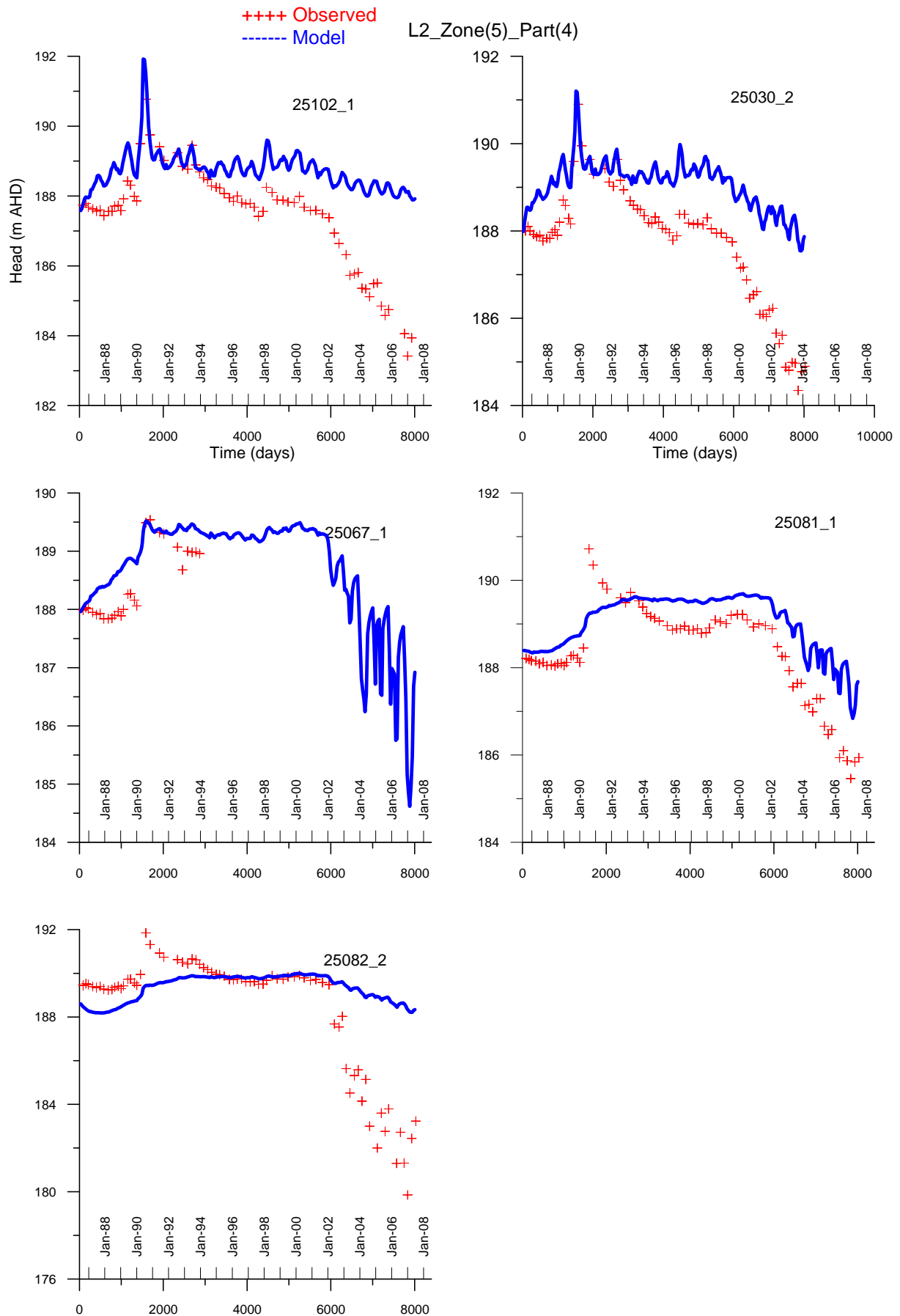


Figure 6-18 Comparison between simulated and observed water levels in layer 2 in Zone 7 (m) (AHD)

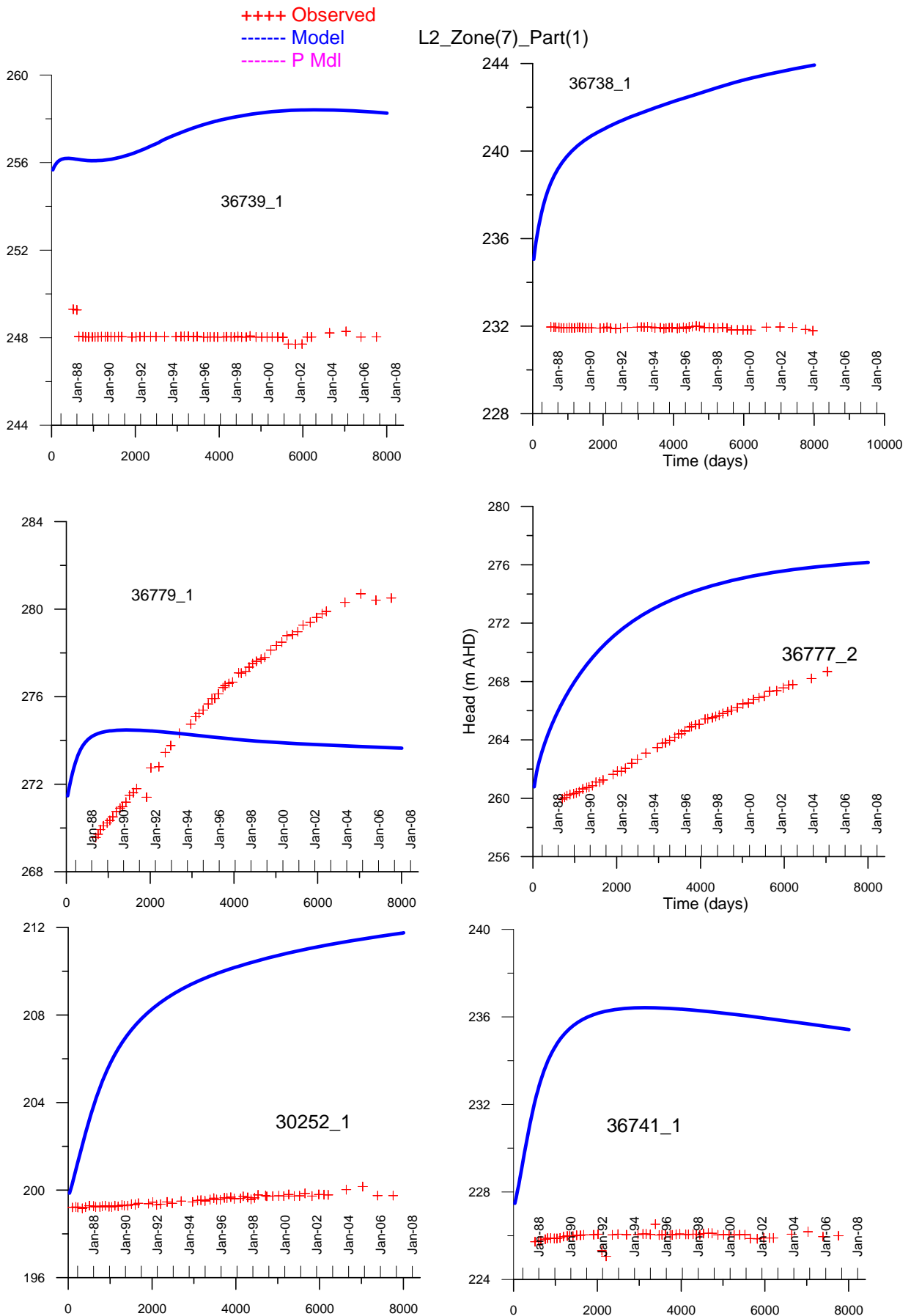


Figure 6-19 Comparison between simulated and observed water levels in layer 2 in Zone 7 (m) (AHD)

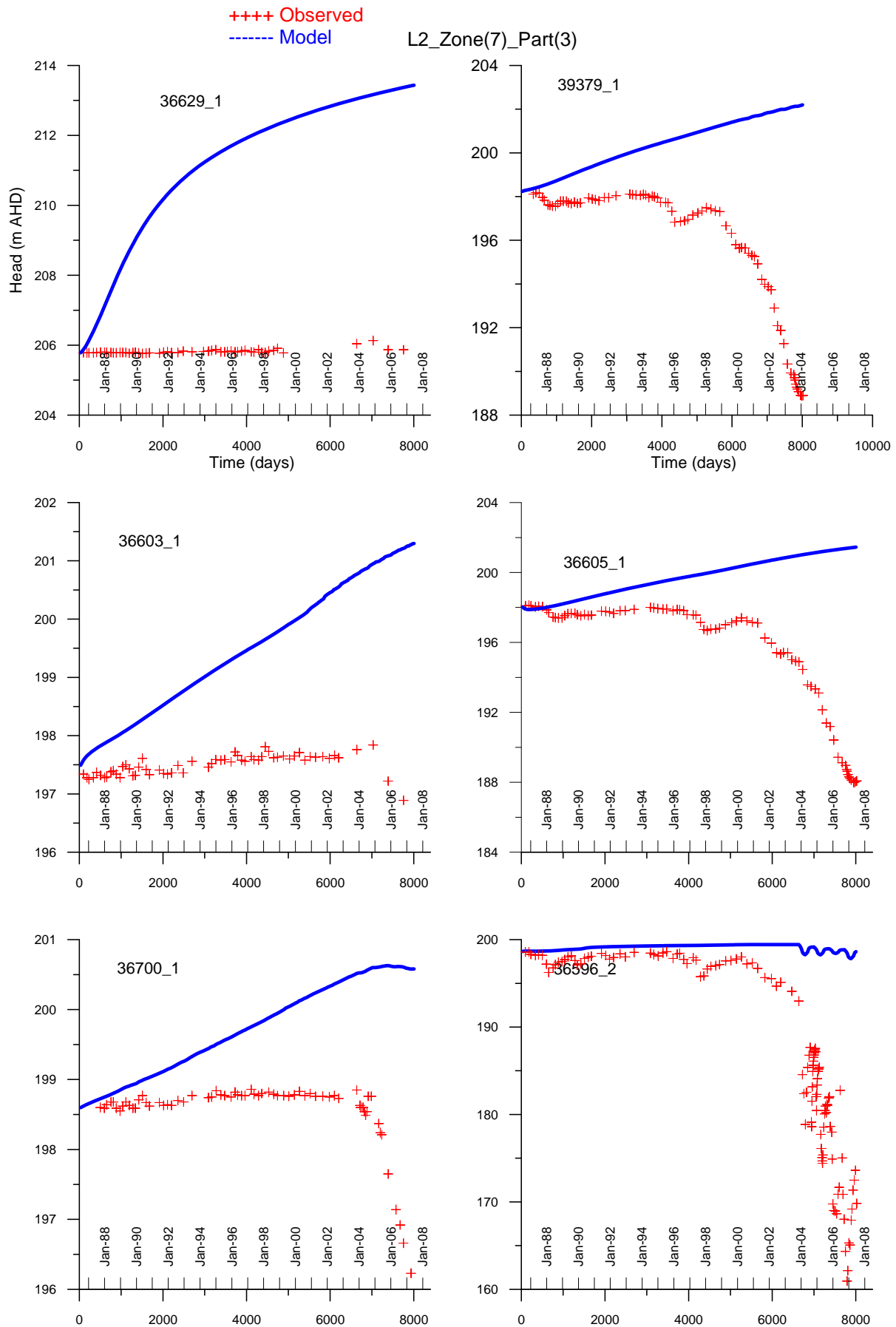


Figure 6-20 Comparison between simulated and observed water levels in layer 2 in Zone 7 (m) (AHD)

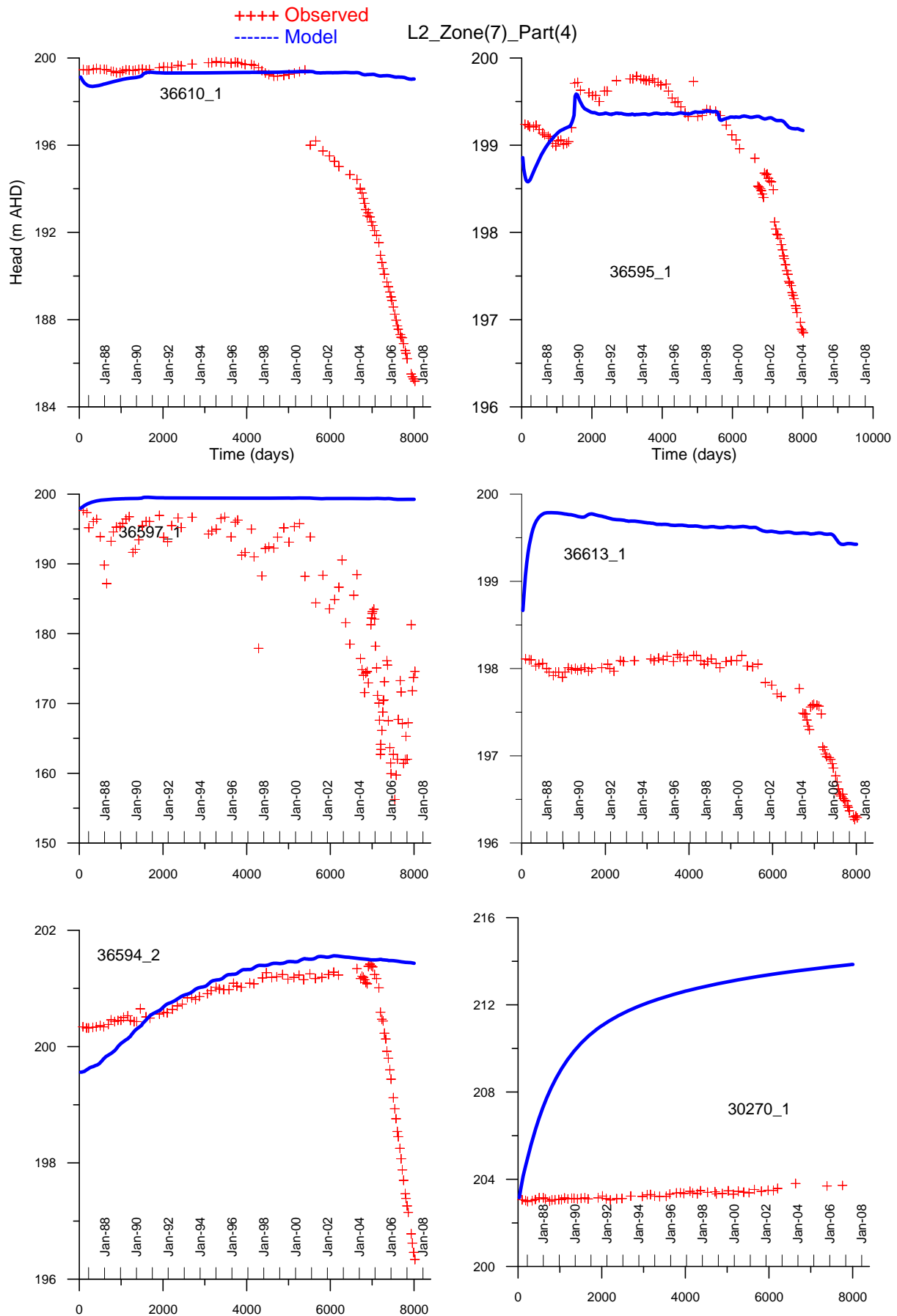


Figure 6-21 Comparison between simulated and observed water levels in layer 2 in Zone 8 (m) (AHD)

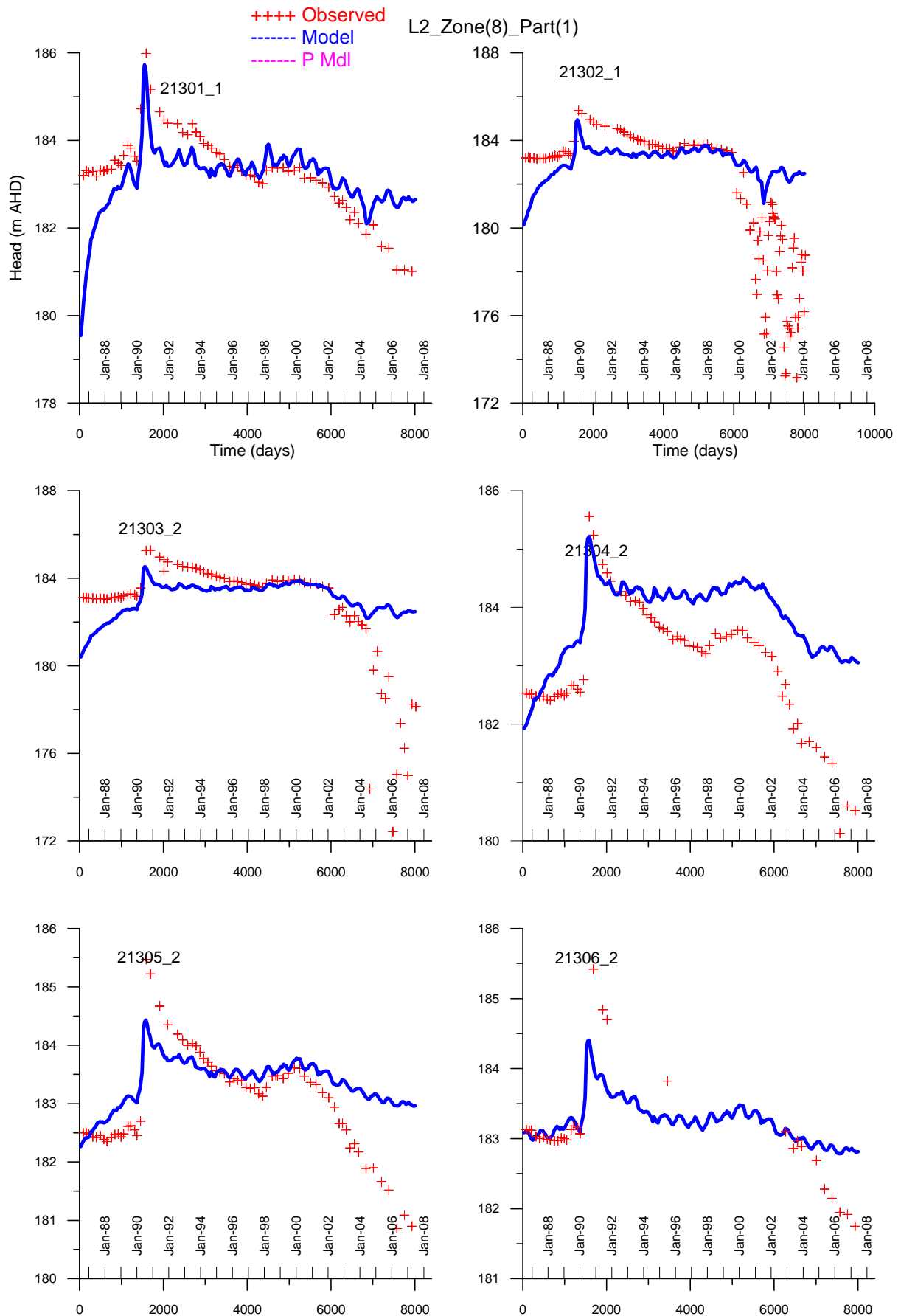


Figure 6-22 Comparison between simulated and observed water levels in layer 2 in Zone 8 (m) (AHD)

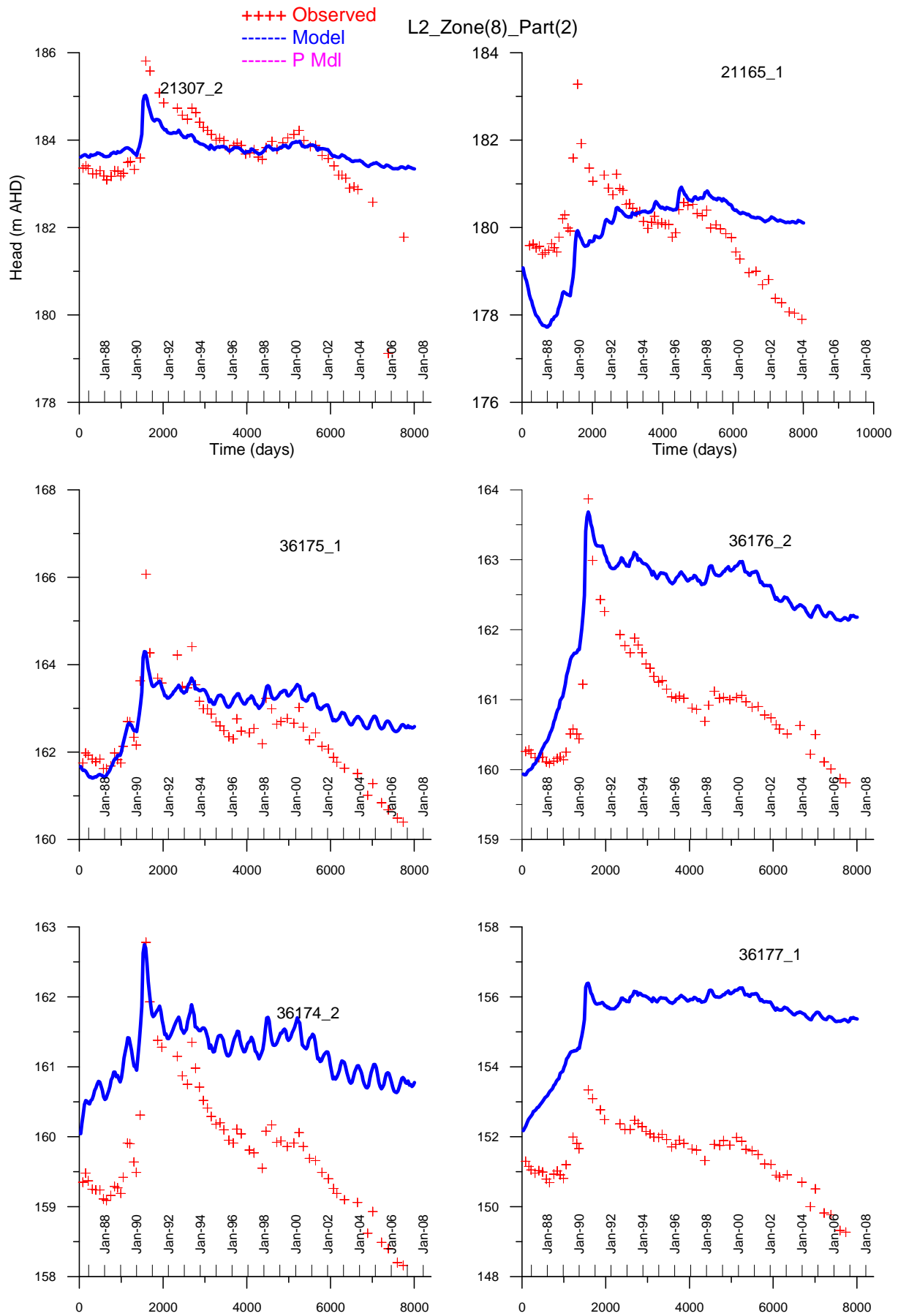


Figure 6-23 Comparison between simulated and observed water levels in layer 3 in Zone 2 (m) (AHD)

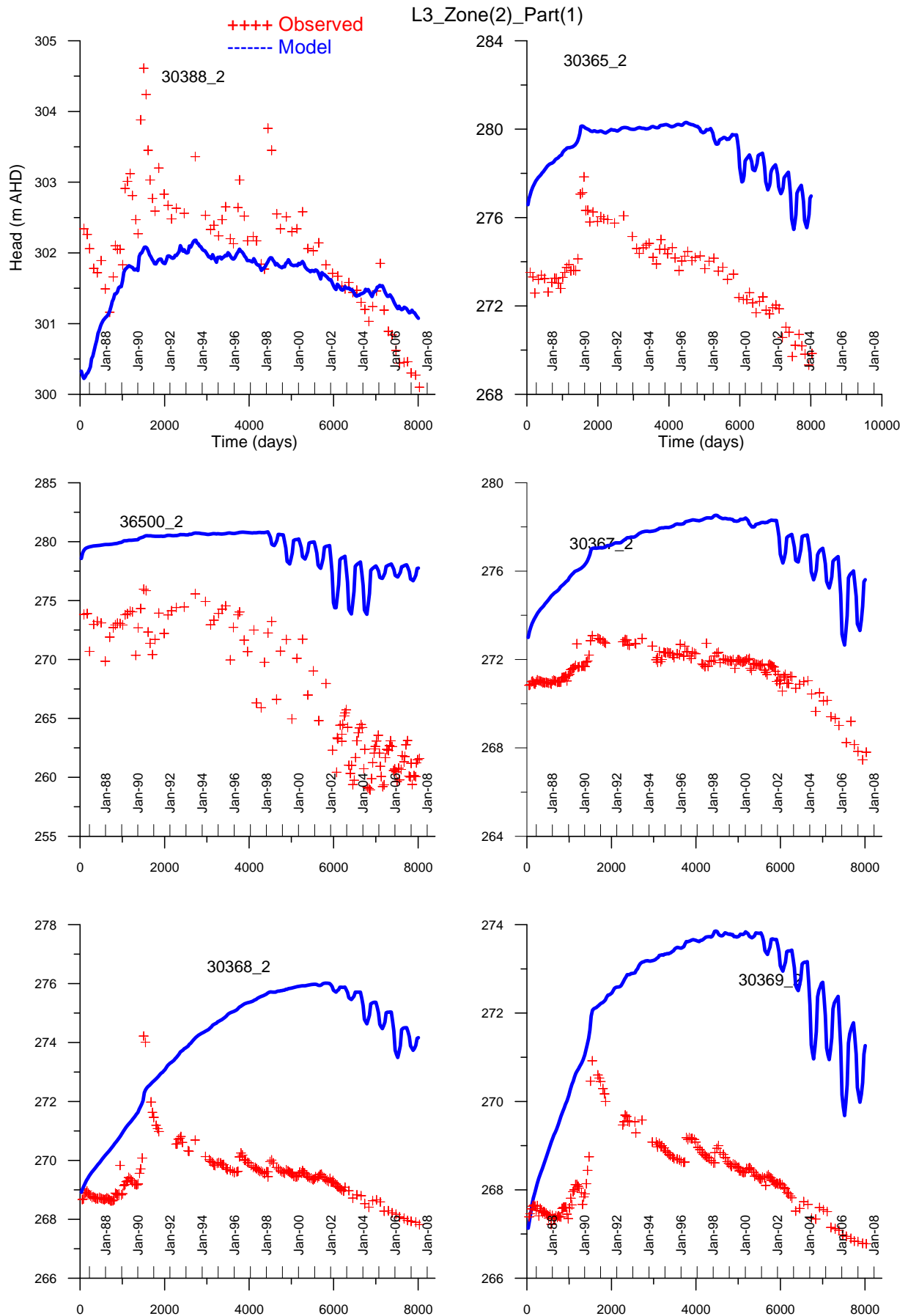


Figure 6-24 Comparison between simulated and observed water levels in layer 3 in Zone 2 (m) (AHD)

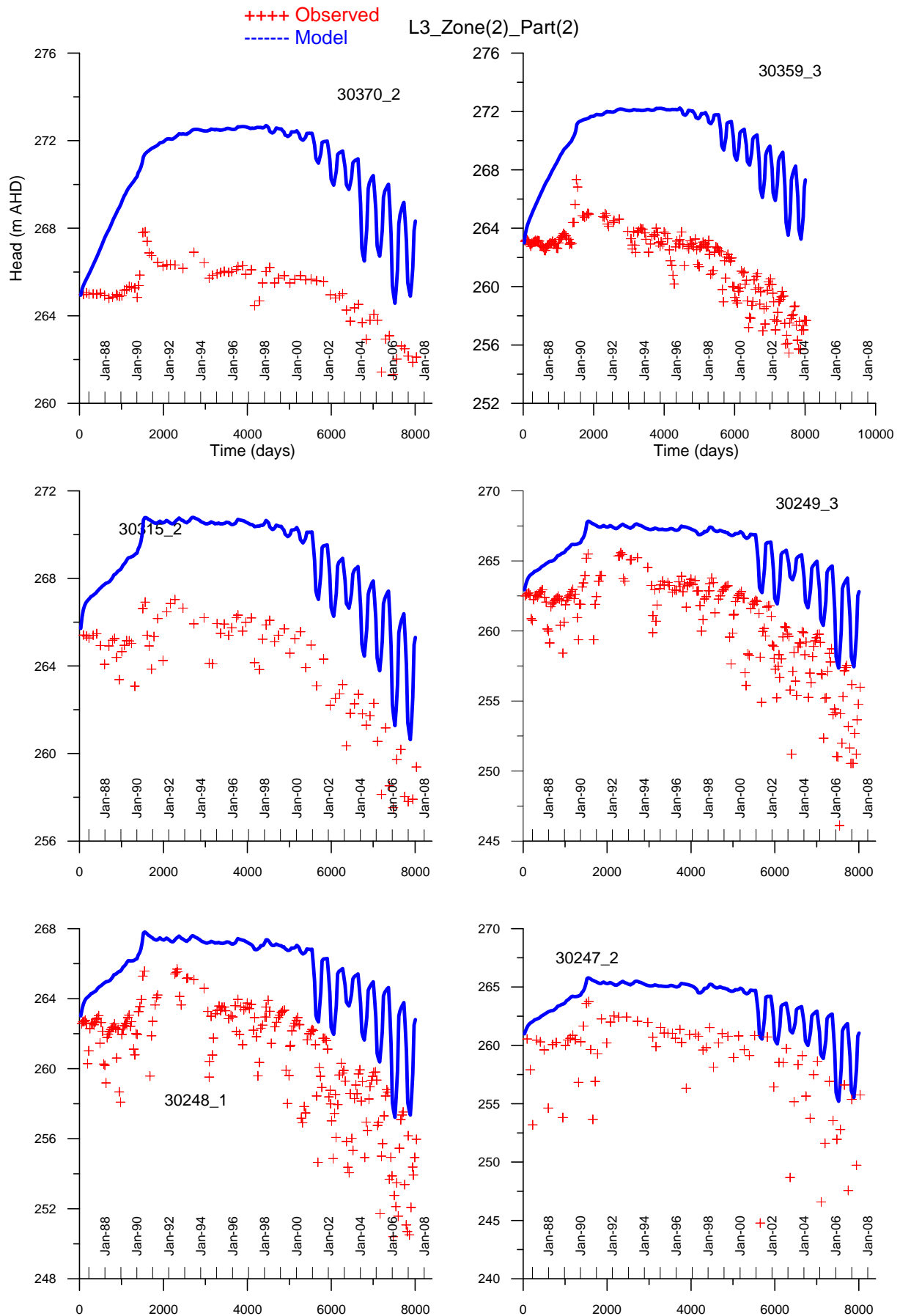


Figure 6-25 Comparison between simulated and observed water levels in layer 3 in Zone 3 (m) (AHD)

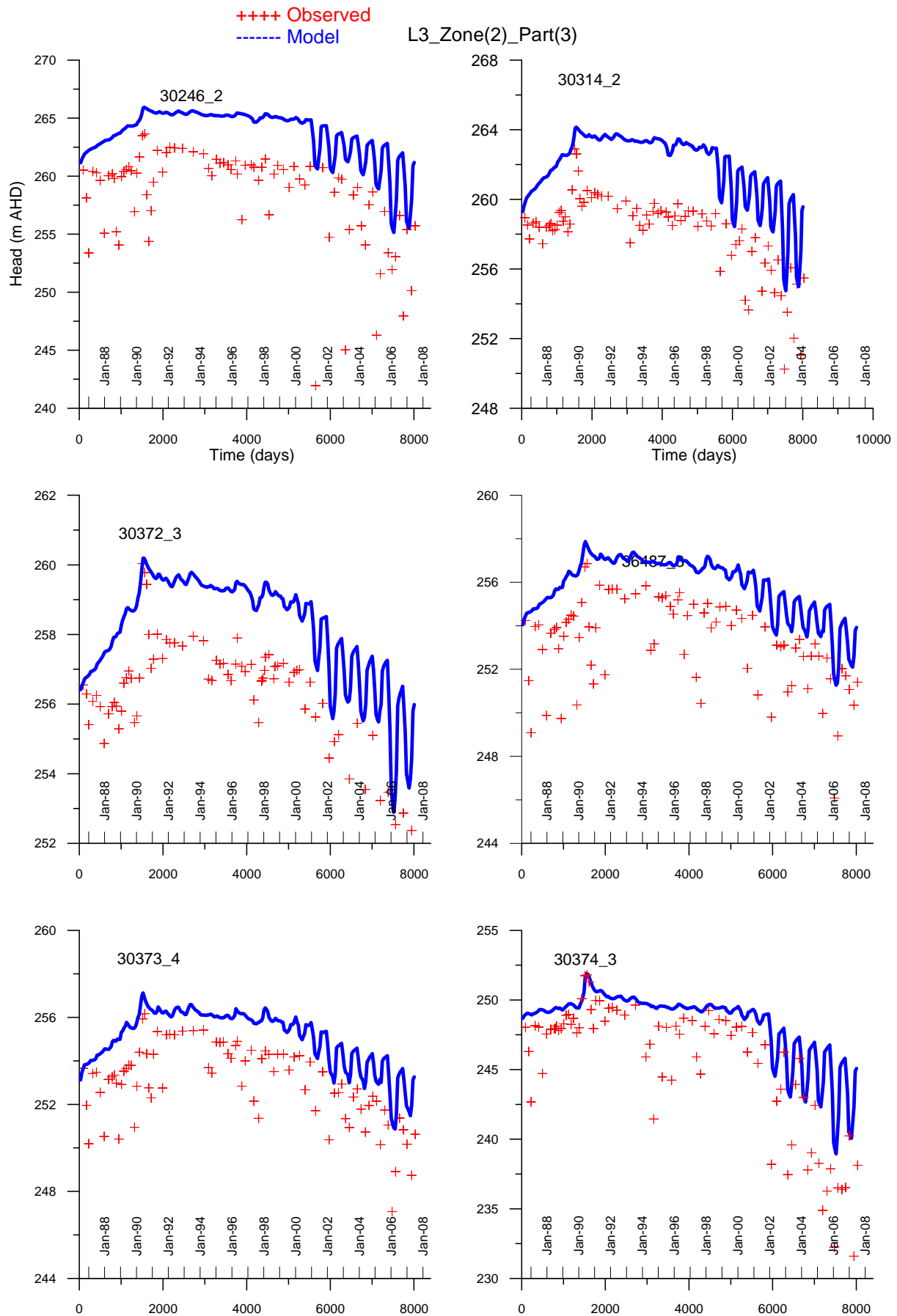


Figure 6-26 Comparison between simulated and observed water levels in layer 3 in Zone 3 (m) (AHD)

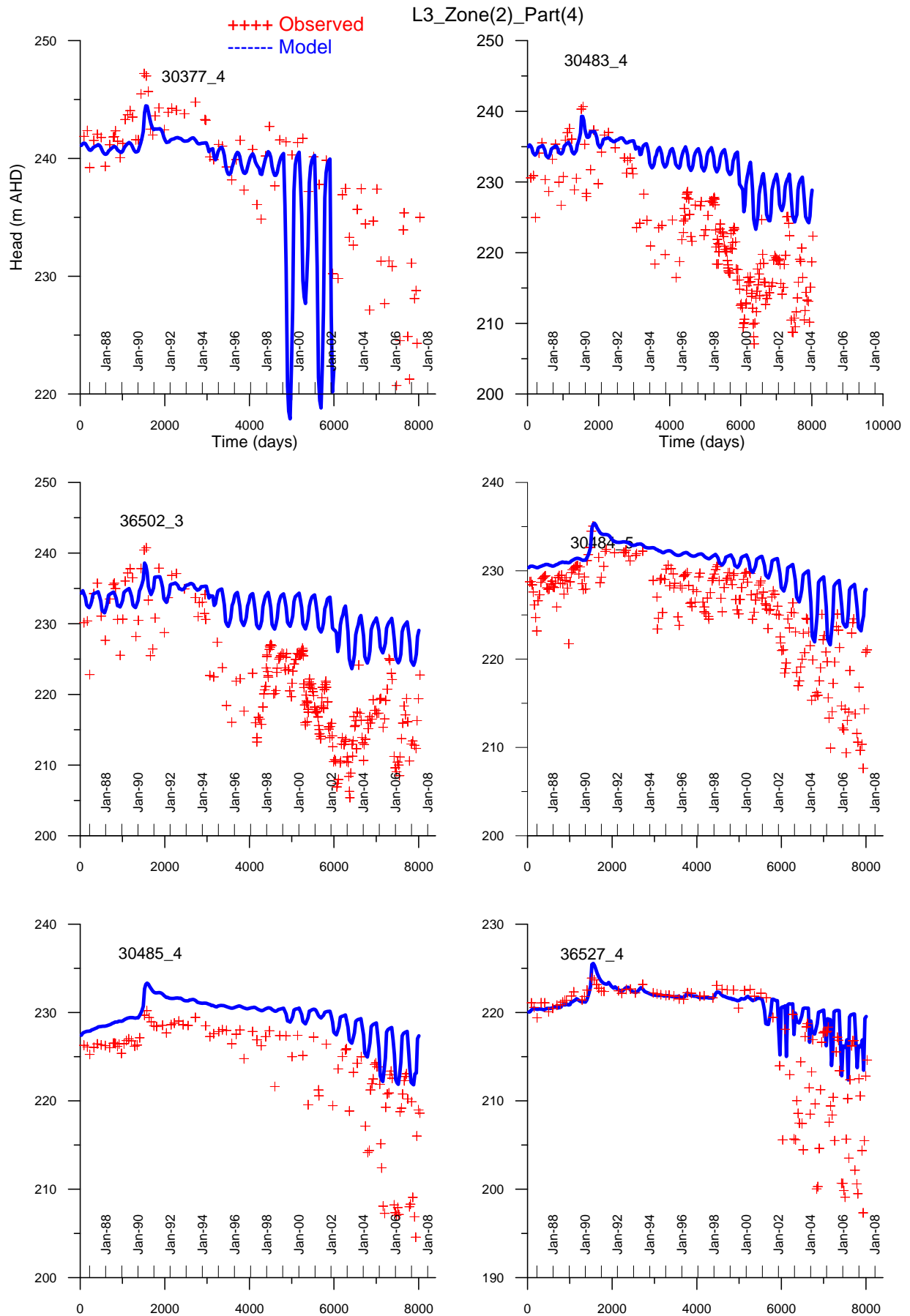


Figure 6-27 Comparison between simulated and observed water levels in layer 3 in Zone 5 (m) (AHD)

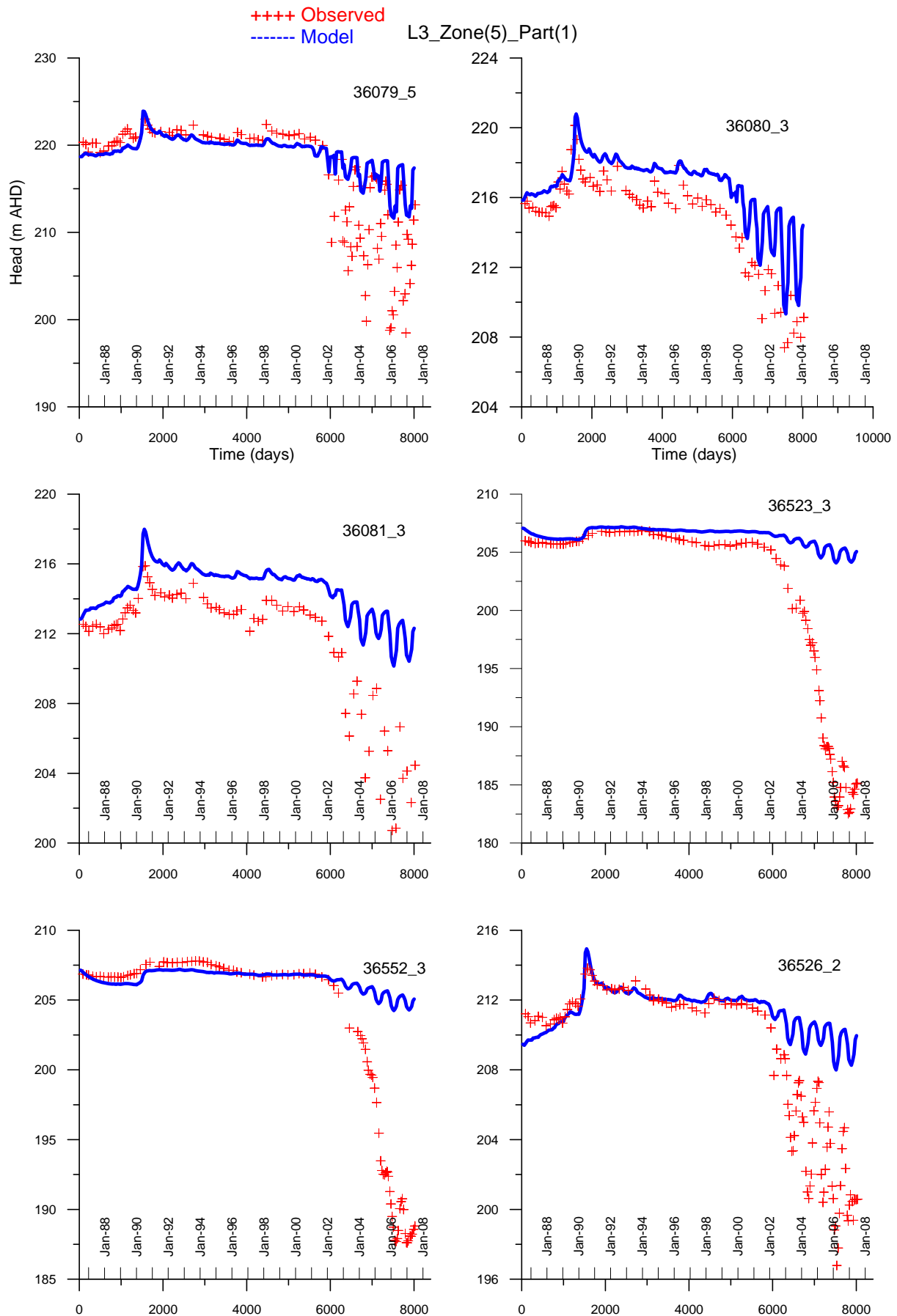


Figure 6-28 Comparison between simulated and observed water levels in layer 3 in Zone 5 (m) (AHD)

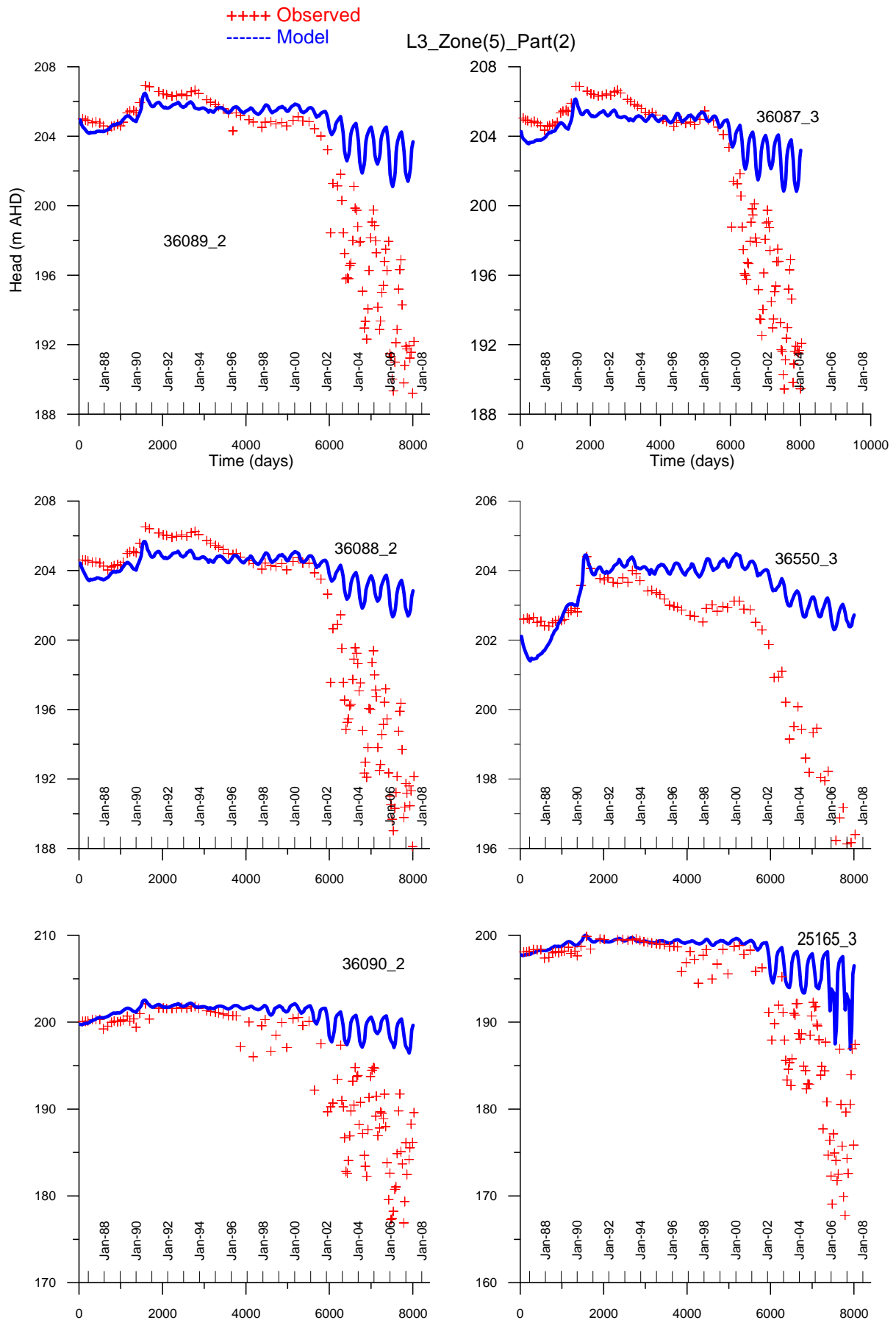


Figure 6-29 Comparison between simulated and observed water levels in layer 3 in Zone 5 (m) (AHD)

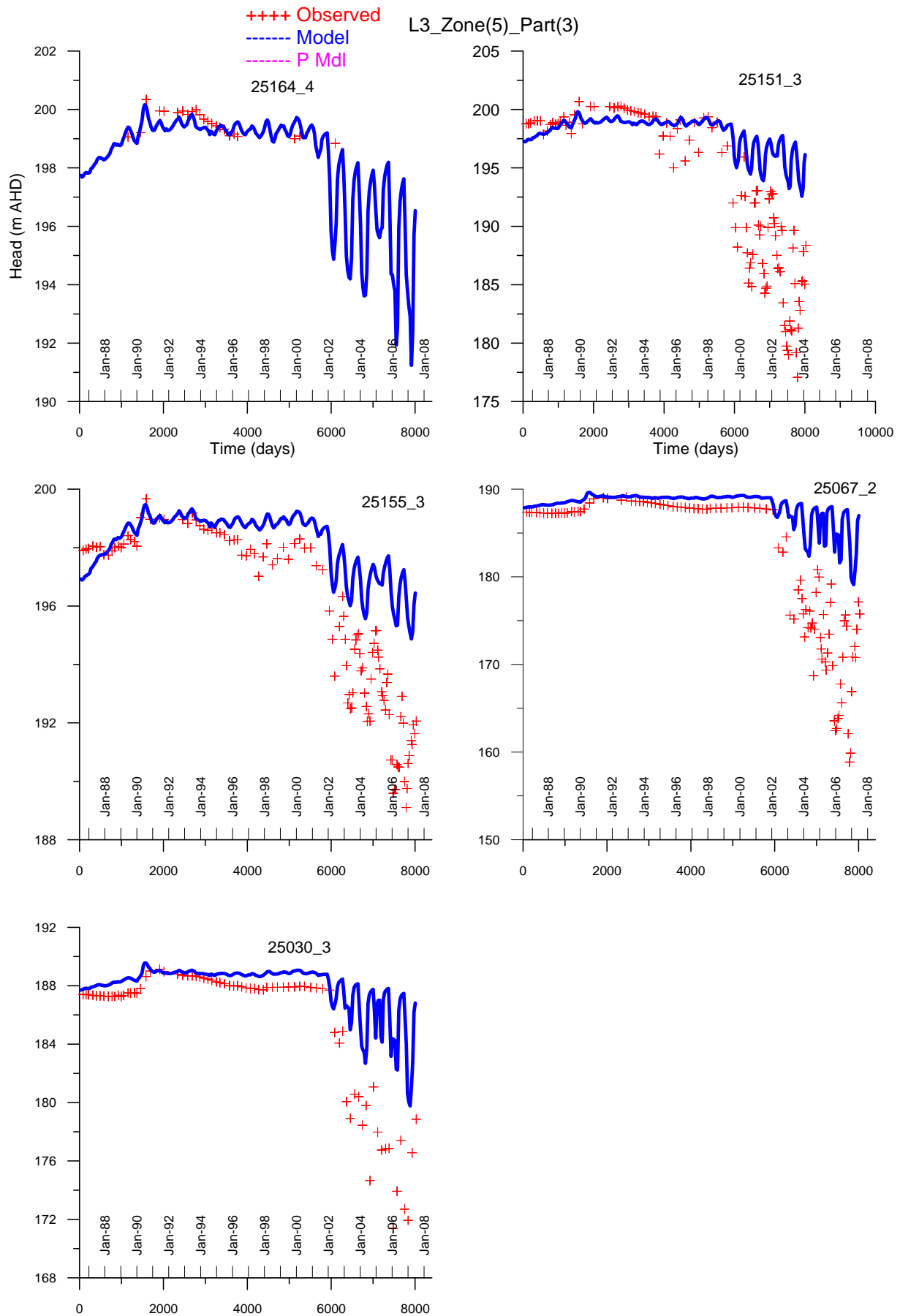


Figure 6-30 Comparison between simulated and observed water levels in layer 3 in Zone 7 (m) (AHD)

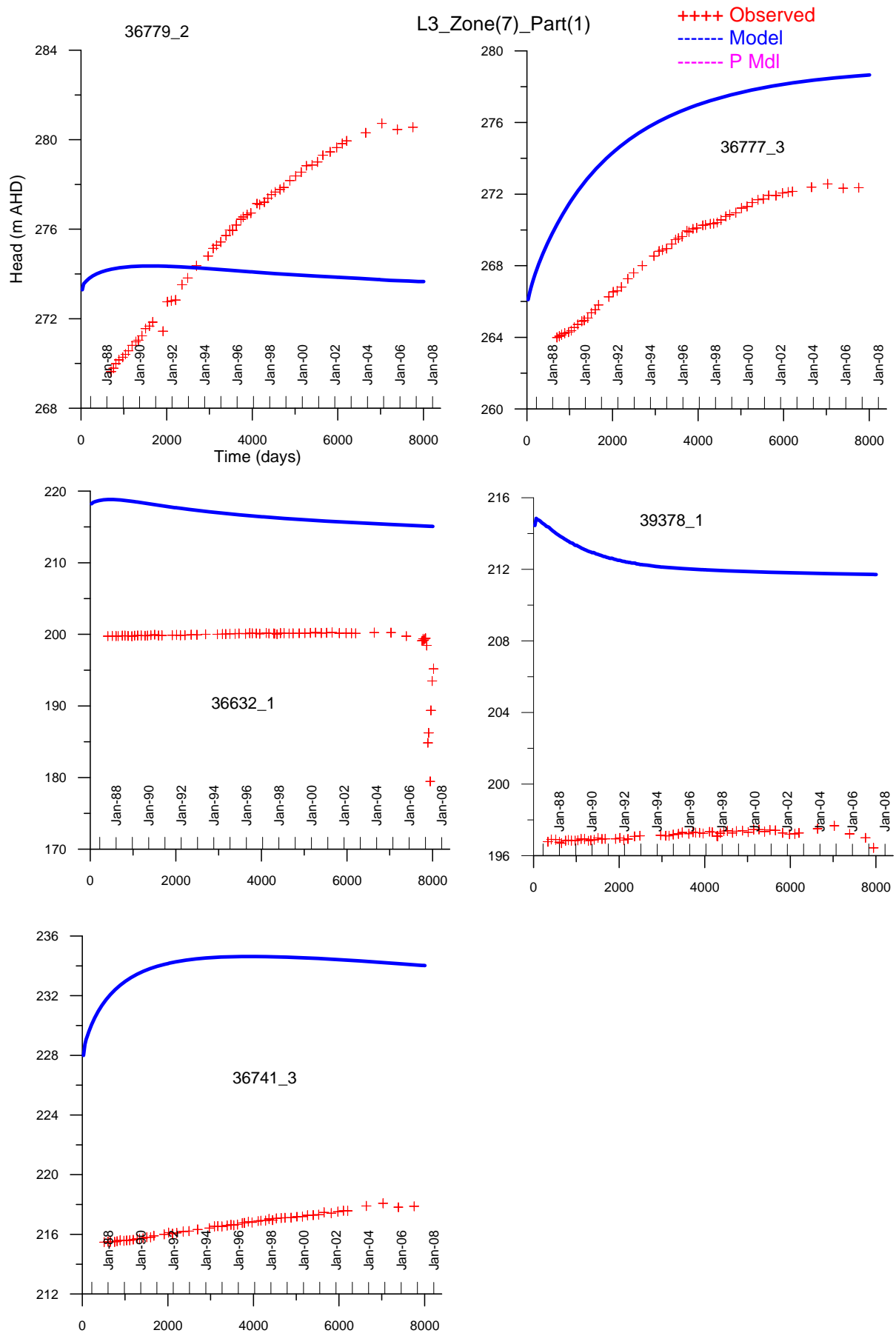


Figure 6-31 Comparison between simulated and observed water levels in layer 3 in Zone 7 (m) (AHD)

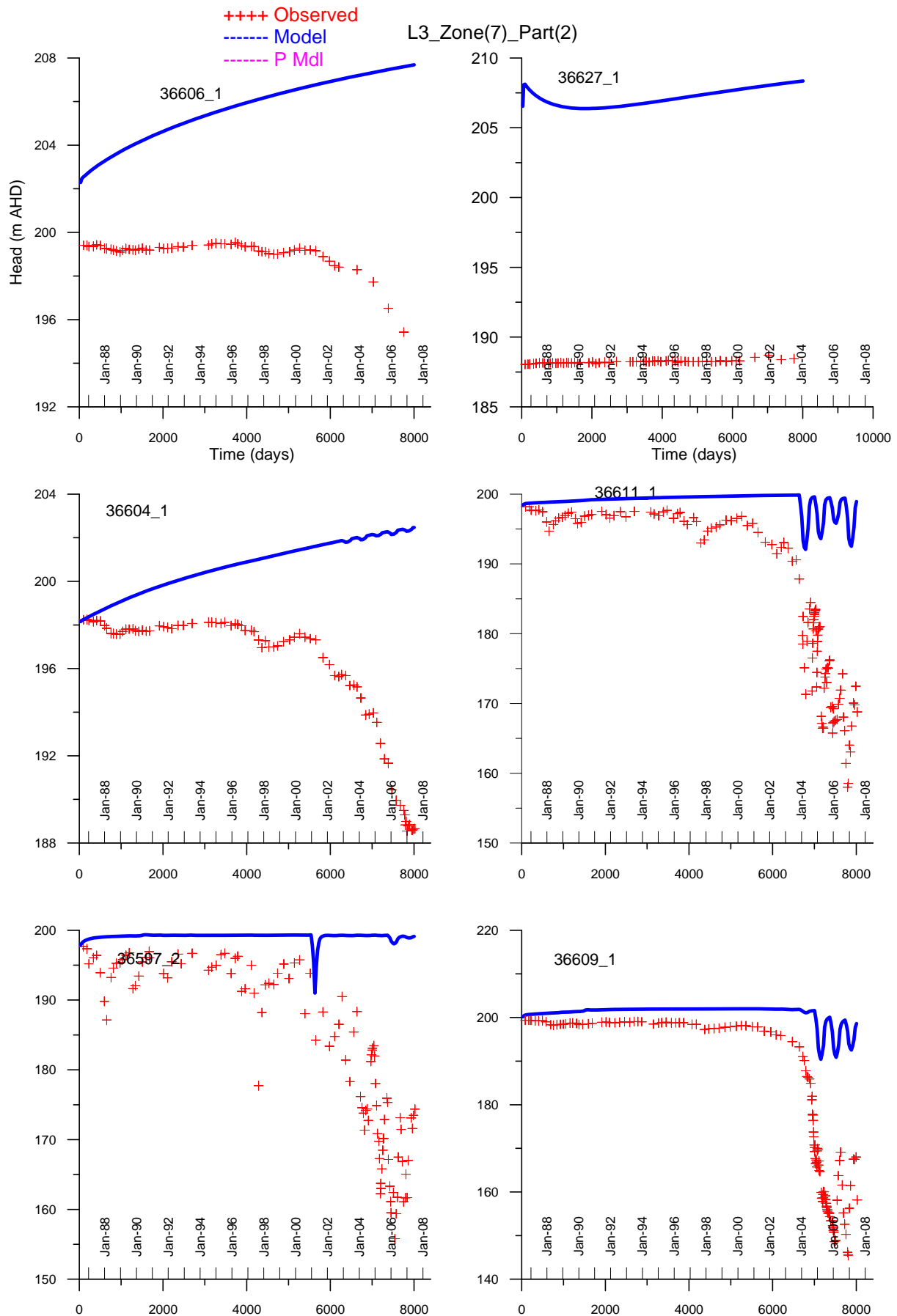


Figure 6-32 Comparison between simulated and observed water levels in layer 3 in Zone 8 (m) (AHD)

